Subglacial hydrology of the Icelandic ice caps

Outburst floods and ice dynamics

Bergur Einarsson

Faculty of Earth Science
University of Iceland
2018

Subglacial hydrology of the Icelandic ice caps

Outburst floods and ice dynamics

Bergur Einarsson

Dissertation submitted in partial fulfilment of a
Philosophiae Doctor degree in Geophysics

Advisor
Tómas Jóhannesson

PhD Committee
Helgi Björnsson
Gwenn E. Flowers

Opponents
Ian Hewitt
Halldór Pálsson

Faculty of Earth Science
School of Engineering and Natural Sciences
University of Iceland
Reykjavík, May 2018

Subglacial hydrology of the Icelandic ice caps: Outburst floods and ice dynamics
Subglacial hydrology of the Icelandic ice caps
Dissertation submitted in partial fulfilment of a *Philosophiae Doctor* degree in Geophysics

Faculty of Earth Science
School of Engineering and Natural Sciences
University of Iceland
Sturlugata 7
101, Reykjavík
Iceland

Telephone: 525-4000

Bibliographic information:
Bergur Einarsson, 2018, *Subglacial hydrology of the Icelandic ice caps: Outburst floods and ice dynamics*, PhD dissertation, Faculty of Earth Science, University of Iceland, 111 pp.

ISBN 978-9935-9306-9-9

Printing: Háskólaprent
Reykjavík, Iceland, May 2018

Abstract

Continuous GPS measurements on three broad and gently sloping temperate ice-cap outlets in southern and western Vatnajökull, southeast Iceland, and in northern Hofsjökull, central Iceland, are the subject of this thesis. The measurements show events of increased ice velocity and how jökulhlaups (glacial outburst floods) affect glacier motion. Interpretation of these events, with the aid of other available hydrological and glaciological data, such as discharge time series from proglacial rivers and runoff modelling calibrated with mass balance measurements, sheds light on the time-dependent development of the subglacial hydraulic system of the ice cap outlets, and its interaction with ice motion.

Motion events unrelated to jökulhlaups are observed: (i) during the early melt season, (ii) contemporaneous with events of increased surface melt or rain, and (iii) during the emptying of supraglacial slush ponds. Events of slower movement than late winter velocities are also observed, prior to early-melt-season motion events and in the wake of motion events during the height of the melt season. We interpret these events, with the aid of runoff modelling on the glacier and estimates of longitudinal stress-gradient coupling lengths, as being induced by hydrological forcing on basal slip. Lack of response in movement to certain runoff pulses and the characteristics of the diurnal variation in measured proglacial discharge indicate the development in the ablation zone of a fast, efficient subglacial hydraulic system early in the summer. The passing of a jökulhlaup and high subglacial groundwater flow do not disturb this development.

Three GPS campaigns to measure jökulhlaups have been carried out over known jökulhlaup paths in two outlets from Vatnajökull ice cap, Skaftárjökull and Skeiðarárjökull. Two slowly rising jökulhlaups from Grímsvötn and two rapidly rising jökulhlaups from the western and eastern Skaftá cauldrons were captured in these campaigns, with maximum discharge ranging from 240 to 3300 $\mathrm{m^3\,s^{-1}}$. Glacier surface movements measured in these campaigns are presented along with the corresponding discharge curves. The measurements are interpreted as indicating: (i) initiation of rapidly rising jökulhlaups with a propagating subglacial pressure wave, (ii) decreased glacier basal friction during jökulhlaups, (iii) subglacial accumulation of water in slowly rising jökulhlaups and (iv) lifting of the glacier caused by subglacial water pressure exceeding overburden in both rapidly and slowly rising jökulhlaups. The latter two observations are inconsistent with assumptions typically made in theoretical and numerical modelling of jökulhlaups.

Measurements of discharge and water temperature in the Skaftá river, and of the lowering of the ice shelf over the subglacial lake at the western Skaftá cauldron are, furthermore, available for a rapidly rising jökulhlaup in September 2006. Outflow from the lake, flood discharge at the glacier terminus and the transient subglacial volume of

floodwater during the jökulhlaup are derived from these data. The 40 km long initial subglacial path of the jökulhlaup was mainly formed by lifting and deformation of the overlying ice, induced by water pressure in excess of the ice overburden pressure. Melting of ice due to the heat of the floodwater from the subglacial lake and frictional heat generated by the dissipation of potential energy in the flow played a smaller role. Therefore this event, like other rapidly rising jökulhlaups, cannot be explained by the jökulhlaup theory of Nye (1976). Instead, our observations indicate that they can be explained by a coupled subglacial-sheet–conduit mechanism where essentially all of the initial flood path is formed as a sheet by the propagation of a subglacial pressure wave. Both viscous and elastic deformation of the glacier as well as turbulent hydraulic fracture at the ice/bedrock interface are important in the dynamics of the subglacial pressure wave at the front of rapidly rising jökulhlaups.

Útdráttur

Meginviðfangsefni þessarar ritgerðar eru rannsóknir á vatnskerfi jökla og áhrif þess á botnskrið, við bæði venjulegar aðstæður og aftakaaðstæður í jökulhlaupum. Vatn undir jöklum getur haft mikil áhrif á hreyfingu þeirra. Nýlegar rannsóknir á Grænlandsjökli og Suðurskautsjöklinum sýna að gerð vatnskerfisins og vatnsmagn við botn, og breytileiki í afrennsli vatns til botns, getur haft mikil áhrif á botnskrið. Hugsanlegar breytingar á þessum þáttum vegna loftslagsbreytinga á komandi áratugum gætu því mögulega valdið auknu skriði og aukinni kelfingu í sjó fram sem síðan gæti haft áhrif á sjávarborð heimshafanna. Aukið botnskrið getur einnig leitt til breytinga í lögun jöklanna sem síðan hefur áhrif á afkomu þeirra. Aukin skilningur á vatnskerfi við botn breiðra lítt hallandi skriðjökla og áhrifum þess á skrið þeirra er því mikilvægur fyrir spár um breytingar á jöklunum.

Skriðjöklar íslensku hveljöklanna, t.d. Vatnajökuls og Hofsjökuls, eru að mörgu leyti svipaðir skriðjöklum Grænlandsjökuls nema hvað þeir íslensku eru þíðjöklar en þeir grænlensku eru gaddjöklar, auk þess sem íslensku jöklarnir eru í hlýrra og votara loftslagi. Núverandi aðstæður á íslensku jöklunum eru því hugsanlega hliðstæða við framtíðaraðstæður í hlýrra loftslagi á Grænlandi. Rannsóknir á vatnskerfum þeirra geta því nýst í alþjóðlegu samhengi. Þessu til viðbótar er góð þekking á vatnafari íslenskra jökla og framtíð þeirra æskileg því jökulár, upprunnar frá þeim, leggja til um u.þ.b. 65% af raforkuframleiðslu landsins. Breytingar á vatnafari í kringum jökla geta einnig haft mikil áhrif á ýmsa innviði, svo sem brýr, rafmagnslínur, ræktarland og fleira, líkt og fjölmörg dæmi úr sögu nábýlis Íslendinga við jökla sýna. Breytingar á farvegi Skeiðarár þar sem lengsta brú landsins liggur nú yfir litla sprænu er nærtækt dæmi. Jökulhlaup geta skapað hættu fyrir fólk, raforkuframleiðslu og ýmsa innviði. Góð þekking á ferlunum sem liggja þar að baki er því mikilvæg. Samspil íslenskra jökla og jökulhlaupa getur einnig nýst sem hálfgerð tilraunastofa til þess að kanna þau ferli sem ráða hreyfingu jökla þegar vatnskerfið undir jöklinum yfirfyllist.

Þessi ritgerð byggist á mælingum á hreyfingu jökla og gögnum um rennsli jökulhlaupa og jökuláa. Því til viðbótar er notast við líkanreiknað afrennsli frá norðanverðum Hofsjökli og vestanverðum Vatnajökli vegna bráðnunar og úrkomu. Að auki eru notuð gögn frá jöklahópi Jarðvísindastofnunar Háskólans um orkubúskap á Tungnaárjökli og botnlandslag undir Skaftár- og Skeiðarárjökli. Einnig er notast við líkanreikninga á ísflæði í íshellu yfir lónum við jökulbotn sem tæmast í jökulhlaupum líkt og undir vestari Skaftárkatli, hitamælingar í lónunum undir eystri og vestari Skaftárkatli og hitamælingar á hlaupvatni í Skaftá. Hreyfing jöklanna er mæld samfellt með GPS tækjum á yfirborði jökulsins. Þrjú slík tæki voru rekin samtímis á mismunandi stöðum á leysingarsvæði Skaftárjökuls sumarið 2008, tvö sumarið 2013 og svo eitt tæki hátt á leysingasvæði Sátujökuls sumrin 2011, 2012 og 2013. Þessu til viðbótar er notast við GPS mælingar

frá Skeiðarárjökli í tveimur jökulhlaupum frá Grímsvötnum árin 2004 og 2010 og á íshellu vestari Skaftárketilsins haustið 2006. Hreyfingar á yfirborði Skaftárjökuls voru mældar í tveimur jökulhlaupum sumarið 2008. Alls eru því GPS mælingar tiltækar fyrir fjögur jökulhlaup með hámarksrennsli á bilinu 240 til 3300 $m^3 s^{-1}$. Auk þess mældist sig íshellunnar yfir vestari Skaftárkatlinum í litlu (hámarksrennsli um 100 $m^3 s^{-1}$) jökulhlaupi haustið 2006. Öll þrjú hlaupin frá Skaftárkötlunum voru með hraðrísandi rennsli en Grímsvatnahlaupin eru hægrísandi. Til viðbótar við hlaupgögnin eru svo mælingar við venjulegar aðstæður á mismunandi stöðum frá fjórum sumrum.

Mælingarnar og túlkun gagnanna frá jökulhlaupunum sýna: (i) hvernig þrýstibylgja gengur niður hlaupfarveginn undir jöklinum í hraðrísandi jökulhlaupum og myndar rými fyrir flóðvatnið með því að lyfta jöklinum, (ii) aukna hreyfingu jökulsins meðan á jökulhlaupum stendur vegna minnkaðs viðnáms við botn (iii) vatnssöfnun undir jöklinum í hægrísandi jökulhlaupum (iv) lyftingu jökulsins í bæði hæg- og hraðrísandi jökulhlaupum vegna vatnsþrýstings við botn sem er hærri en fargþrýstingur jökulsins. Seinustu tvær niðurstöðurnar stangast á við hefðbundnar kenningar um hægrísandi jökulhlaup. Mælingar á sigi íshellunnar í vestari Skaftárkatli í hlaupinu haustið 2006, ásamt ísflæðireikningum á lækkun íshellunnar, voru notaðar til þess að reikna útrennsli úr lóninu við jökulbotn í hlaupinu. Þær niðurstöður ásamt mælingum á hlauprennslinu utan jökuls og hitamælingum á hlaupvatninu í lóninu og í Skaftá, gera kleift að meta magn vatns undir jöklinum á hverjum tíma. Það er margfalt meira heldur en hægt er að búa til rými fyrir með bræðslu vegna upphafsvarma hlaupvatnsins í lóninu og varma sem myndast vegna viðnáms í farveginum undir jöklinum, líkt og gert er ráð fyrir í kenningum Nye (1976) um jökulhlaup. Skaftárhlaupið haustið 2006, líkt og önnur hraðrísandi jökulhlaup, er því ekki unnt að skýra með kenningu Nye. Mælingarnar benda til þess að hlaupfarvegurinn sé í upphafi að mestu myndaður við lyftingu og aflögun jökulsins vegna framgangs þrýstibylgju þar sem vatnsþrýstingur er hærri en fargþrýstingur.

Mælingar á hreyfingu Sátujökuls og Skaftárjökuls fyrir tímabil milli hlaupa sýna aukna hreyfingu: (i) við upphaf sumarleysingar, (ii) samtímis skarpri aukningu í afrennsli vegna bráðnunar eða rigningar og (iii) þegar krapatjarnir á yfirborði jökulsins tæmast. Mælingarnar sýna einnig að jökulinn hægir stundum á sér niður fyrir dæmigerðan vetrarskriðhraða, rétt fyrir upphaf leysingar og í kjölfar aukins hraða í hámarki leysingartímabilsins. Ætla má með samtúlkun við afrennslisreikninga, að þessar hraðabreytingar séu tilkomnar vegna áhrifa vatns á viðnám við botn. Litlar breytingar í skriðhraða vegna toppa í afrennsli þegar líður á leysingartímabilið og dægursveifla í rennsli ánna sem falla frá jöklunum benda til að vatnsrásir þróist undir jöklunum yfir sumarið. Slíkt rásakerfi leiðir vatn með skilvirkari hætti að jökuljaðrinum heldur en samtengt kerfi lítilla holrýma og vatnsæða sem er ráðandi undir jöklinum að vetri til. Þessi þróun vatnskerfisins er í samræmi við kenningar sem áður hafa verið settar fram fyrir t.d. daljökla í Ölpunum. Grunnvatnsstreymi undir jöklum í gosbeltinu, þar sem jarðlög eru gropin, og jökulhlaup hafa lítil áhrif á þessa þróun vatnskerfa við jökulbotn.

Dedication

To my beloved friend, the slayer of three dragons who now bravely fights the fourth.

Preface

The attitude of humans towards glaciers has varied through history. Glaciers have been described in literature as magnificent and beautiful but they have also often been portrayed as dragons. They are then described as formidable creatures that come tumbling down the mountains, crawling over farmland and settlements and spewing out waves of water causing destruction and devastation. I agree that glaciers can be beastly, but believe that they are like the rest of nature, neither malevolent nor evil, they just do not notice or care whether human beings are around or not. They therefore do not need to be fought and slain, but we should know them. Know their behaviour and be able to predict what they will do next, so that we or our precious belongings are not trampled on when they come rambling around, or flushed away when they spew out jökulhlaups. Thus we need to understand glaciological processes. If we do this properly we might even harness their power for both our and their benefit, i.e. harness the renewable hydropower of the glacier rivers and fight human-induced climate change that is endangering these magnificent creatures. Because of their intrinsic value we must try to ensure that they do not meet an ominous fate and literally melt away. This is all the more urgent as their fate might be interwoven with our own.

I wonder whether, and hope that, this can be the role of the glaciologist: to study these dragons, learn their ways and then bring the findings to society for the benefit of all. We might then even have to learn not to turn ourselves into beasts trampling on them and the rest of nature, as it seems that the balance of power has changed in our favour during the current Anthropocene. I hope that we may soon learn to wield our power wisely. Playing a small part in making our society more resilient to the risk of jökulhlaups and other glaciological hazards, by knowing those dangers better, is a worthwhile effort in that direction, with the hope that both glaciers and humanity may live long and prosper.

Table of Contents

List of Figures

List of Original Papers

Paper I: Einarsson B, Magnússon E, Roberts MJ, Pálsson F, Thorsteinsson Th and Jóhannesson T (2016) A spectrum of jökulhlaup dynamics revealed by GPS measurements of glacier surface motion. *Annals of Glaciology*, **57**, 47–61 (doi:10.1017/aog.2016.8)

Paper II: Einarsson B, Jóhannesson T, Thorsteinsson Th, Gaidos E and Zwinger T (2017) Subglacial flood path development during a rapidly rising jökulhlaup from the western Skaftá cauldron, Vatnajökull, Iceland. *Journal of Glaciology*, **63**(240), 670–682 (doi:10.1017/jog.2017.33)

Paper III: Einarsson B and Jóhannesson T (2018) Hydrology and dynamics of two Icelandic outlet glaciers revealed by discharge and GPS measurements. *To be submitted to the Journal of Glaciology.*

List of Symbols

Variables

t	Time [s]
x	Horizontal coordinate [m]
s	Along-subglacial-conduit horizontal coordinate [m]
z	Vertical coordinate [m]
h	Ice thickness [m]
$\mathrm{z_b}$	Elevation of glacier bed [m]
$\mathrm{z_s}$	Elevation of glacier surface [m]
$\mathrm{h_i}$	Ice thickness, $h_\mathrm{i} = z_\mathrm{s} - z_\mathrm{b}$ [m]
h_0	Average ice thickness [m]
α	Ice surface slope [–]
α_0	Average ice surface slope [–]
p	Pressure [Pa]
p_w	Subglacial water pressure [Pa]
p_i	Ice overburden pressure [Pa]
Δp	Difference between subglacial water pressure and ice overburden, $\Delta p = p_\mathrm{w} - p_\mathrm{i}$ [Pa]
σ	Stress [Pa]
τ	Deviatoric stress [Pa]
τ_b	Basal shear stress [Pa]
τ_0	Average basal shear stress [Pa]
$\dot{e}$	Strain rate [$\mathrm{s^{-1}}$]
η	Effective viscosity [Pa s]
$\bar{\eta}$	Average effective longitudinal viscosity [Pa s]
τ_M	Maxwell time [s]
S	Cross-sectional area of a subglacial conduit (in thesis introduction and paper I) [$\mathrm{m^2}$]

S_0	Initial conduit cross-sectional area [m^2]
h_w	Thickness of a subglacial water sheet [m]
h_{wave}	Water sheet thickness within a propagating subglacial pressure wave [m]
h_{sb}	Water sheet thickness behind a propagating subglacial pressure wave [m]
A_w	Cross-sectional area of a sheet-like subglacial flood path [m^2]
b_w	Effective width of a sheet-like subglacial flood path [m]
n_m	Manning's friction coefficient in a subglacial watercourse [$m^{-1/3}$ s]
$\bar{v}$	Mean flow speed of water in a subglacial watercourse [$m\,s^{-1}$]
Q	Discharge in a subglacial conduit [$m^3\,s^{-1}$]
q	The discharge per unit width in a sheet-like subglacial flood path [$m^2\,s^{-1}$]
ϕ	Hydraulic potential, $\phi = \rho_w g z_b + p_w$ [Pa]
$\frac{\partial \phi}{\partial s}$	Hydraulic gradient at the glacier bed [$Pa\,m^{-1}$]
ϕ_{wave}	Hydraulic potential in a propagating subglacial pressure wave [Pa]
$\frac{\partial \phi_{wave}}{\partial s}$	Hydraulic gradient in a propagating subglacial pressure wave [$Pa\,m^{-1}$]
ϕ_{sb}	Hydraulic potential behind a propagating subglacial pressure wave [Pa]
$\frac{\partial \phi_{sb}}{\partial s}$	Hydraulic gradient behind a propagating subglacial pressure wave [$Pa\,m^{-1}$]
ϕ_s	Hydraulic potential in a subglacial water sheet, $\phi_s = \rho_w g z_b + \rho_w g h_w + p_w$ [Pa]
m_i	Melt rate of the walls in a subglacial conduit [$kg\,m^{-1}\,s^{-1}$]
μ	Melt-rate ability in a subglacial watercourse [$Pa\,m^{-1}$]
$\bar{u}_0$	Vertically averaged ice-flow velocity [$m\,s^{-1}$]
u_b	Bed-parallel basal sliding velocity [$m\,s^{-1}$]
$\frac{d\bar{u}}{dx}$	Longitudinal strain rate [s^{-1}]
l	Longitudinal ice-flow coupling length [m]
w_i	Weight on runoff from a grid point, based on longitudinal ice-flow coupling length [–]
w_v	Rate of viscous lifting over a propagating subglacial pressure wave [$m\,s^{-1}$]
ε_e	Elastic lifting over a propagating subglacial pressure wave [m]
a	Horizontal dimension of the area affected by overpressure in a propagating subglacial pressure wave [m]
R	Flexure rigidity of a plate, $R = E h_i^3/(12(1-\nu^2))$ [$Pa\,m^3$]
$L_{\Delta p}$	Distance of the inflow location from the tip of a propagating crack at the ice–bedrock interface [m]
U_{tip}	Propagating velocity of a crack tip at the ice–bedrock interface [$m\,s^{-1}$]

k	Nikuradse roughness height [m]
$\hat{w}$	Time-varying spatial average of non-dimensional opening of a propagating crack at the ice–bedrock interface, $\hat{w}_{\mathrm{avg}} \approx 1.72 + 0.89(L_{\Delta \mathrm{p}}/h_{\mathrm{i}})^2$ [–]
V_{melt}	Volume of the part of the subglacial system created by melting [m^3]
V_{in}	Volume of water input into the subglacial system [m^3]
V_{s}	Volume of water released from the subglacial system at a glacier snout [m^3]
V_{l}	Volume of water input into the subglacial system, from a subglacial lake [m^3]
T_{in}	Temperature of water input into the subglacial system [°C]
T_{s}	Temperature of water released from the subglacial system at a glacier snout [°C]
ΔH	The elevation difference between an input location of water into the subglacial system and the glacier snout [m]
r	Radius of a subglacial lake [m]
V_{w}	Volume of water in a subglacial lake and surrounding waterways [m^3]
z_{w}	Piezometric water level in a subglacial lake [m]
M	Glacier surface melt [$\mathrm{m_{w.e.}\ d^{-1}}$]
T	Daily-mean temperature [°C]

Physical parameters and constants

g	Acceleration of gravity [$9.82\,\mathrm{m\,s^{-2}}$]
ρ_{i}	Density of ice [$910\,\mathrm{kg\,m^{-3}}$]
ρ_{w}	Density of water [$1000\,\mathrm{kg\,m^{-3}}$]
c_{w}	Heat capacity of water [$4.22 \times 10^3\,\mathrm{J\,kg^{-1}\,K^{-1}}$]
c_{t}	Pressure melting coefficient of water [$7.4 \times 10^{-8}\,\mathrm{K\,Pa^{-1}}$]
L	Latent heat of fusion [$3.34 \times 10^5\,\mathrm{J\,kg^{-1}}$]
A	Parameter in Glen's flow law, $\dot{\epsilon}_{\mathrm{ij}} = A\tau_{\mathrm{ij}}^n$ [$2.4{\cdot}10^{-24}\,\mathrm{s^{-1}\,Pa^{-3}}$ for temperate ice]
B	Glen's ice rheology flow-law rate factor, $B = A^{-1/3}$ [$7.5 \times 10^7\,\mathrm{Pa\,s^{1/3}}$ for temperate ice]
n	Exponent in Glen's flow law [3]
C	Parameter in Weertman's sliding law, $u_b = C\,\tau_{\mathrm{b}}^{m-1}\,\tau_{\mathrm{b}}$ [$2.3{\cdot}10^{-21}\,\mathrm{s^{1/3}\,m^{-1/3}\,Pa}$]
m	Exponent in Weertman's sliding law [3]
E	Young's modulus for ice [$8.7{\cdot}10^9\,\mathrm{Pa}$]

ν Poisson's ratio of ice [0.319]

G Shear modulus for ice [$3.7{\cdot}10^9$ Pa]

f Channel shape factor in estimation of longitudinal ice-flow coupling length [1]

c Constant in calculations of elastic deformation over a propagating subglacial pressure wave [$c = 384$ if the shortest horizontal dimension of the area is much smaller than the longest horizontal dimension, but $c = 1024$ if the area is circular]

θ Non-dimensional multiplicative factor in calculation of the propagating velocity of a crack tip at the ice–bedrock interface, $\theta \approx 5.13 + 0.64(L_{\Delta p}/h_i) + 0.94(L_{\Delta p}/h_i)^2$ [–]

Observed and estimated parameters

Modelling of the emptying of an idealized cylindrically symmetric subglacial lake, paper II

z_d Ice divide elevation [500 m]

r_d Radius to the ice divide at the boundary of the cauldron ice flow basin with the surrounding ice cap [2.52 km]

A_i Area of ice flow basin [20 km^2]

r_g Radius of the geothermal area forming the subglacial lake [1 km]

A_g Area of geothermal melting [π km^2]

r_l The initial radius to the grounding line [700 m]

b_s Surface mass balance [2.22 $m_{w.e.}\ a^{-1}$]

d_s Sum of rain and (absolute value of the) surface ablation [0.4 $m_{w.e.}\ a^{-1}$]

m_g Melting of ice at bottom of the ice shelf or glacier within radius r_g [17.8 $m_{w.e.}\ a^{-1}$]

q_s Discharge corresponding to rain and surface ablation [0.21 $m^3\ s^{-1}$]

q_f Discharge corresponding to inflow of geothermal fluid [0.40 $m^3\ s^{-1}$]

q_g Discharge corresponding to geothermal melting [1.8 $m^3\ s^{-1}$]

q_k Discharge during a jökulhlaup (maximum value after initial rise and final fall) [100 $m^3\ s^{-1}$]

z_1 Piezometric water level in the lake at the start of a jökulhlaup [400 m]

z_2 Piezometric water level in the lake at the termination of a jökulhlaup [320 m]

t_r Time period for the rise of discharge at the start of a jökulhlaup [12 hours]

t_f Time period for the fall of discharge at the end of a jökulhlaup [12 hours]

S "Storage coefficient" effective area of an assumed hydraulic connection of the subglacial lake with the atmosphere [0.1 km^2]

Melt calculations, paper III

DDF_{snow}	Degree–day factor for snow [$4.57 \cdot 10^{-3}$ $m_{w.e.}$ $°C^{-1}$ d^{-1}]
DDF_{firn}	Degree–day factor for firn [$6.47 \cdot 10^{-3}$ $m_{w.e.}$ $°C^{-1}$ d^{-1}]
DDF_{ice}	Degree–day factor for ice [$7.45 \cdot 10^{-3}$ $m_{w.e.}$ $°C^{-1}$ d^{-1}]
T_{m}	Threshold temperature for melt [0.3 °C]
$T_{\text{s/r}}$	Transition temperature for snow–rain [1.3 °C]
S_{pre}	Precipitation scaling factor [0.88]

Acknowledgements

This PhD project was part of the Nordic Centre of Excellence SVALI, 'Stability and Variations of Arctic Land Ice', funded by the Nordic Top-level Research Initiative (TRI). Part of this study is based on data gathered as part of a research project on the Skaftá cauldrons that was supported by the Icelandic Research Fund, the Landsvirkjun (National Power Company of Iceland) Research Fund, the Icelandic Road Administration and the Kvískerja fund. The Iceland Glaciological Society also provided field support which made this study possible.

Spending a long time doing a PhD means that in the end one has the pleasure of having many people to thank. First and foremost I want to thank my supervisor Tómas Jóhannesson. His supervision, guidance and support has been invaluable during my studies. Tómas has also been a constructive exemplar with his energy, enthusiasm and knowledge of fundamental physics. It is an honour to be allowed to grab the back of such persons so that they are not ridden over by buses when crossing streets thinking about glaciology during conferences in foreign cities, and to be able to find the way back down from the glacier when wrong turns have been made in field expeditions. I thank Helgi Björnsson for guidance through my studies, and for creating a fruitful path for glaciology in Iceland so that we who follow have the possibility to see further by having a giant's shoulders to stand on. Gwenn E. Flowers has also given me good advice during my studies.

I thank Þorsteinn Þorsteinsson for directing me into glaciology by hiring me as an assistant for an exciting ice core drilling early in my undergraduate studies. I also thank Þorsteinn for excellent cooperation through the years and for leading the Skaftá cauldrons project that provided a large amount of interesting data that are used in this thesis. I thank Vilhjálmur for support, important contributions during field trips and practical advice on motorized glacier travels and set-up of GPS stations. I thank Eyjólfur and Matthew for discussion on glacial hydrology and enjoyable cooperation. Eyjólfur, Matthew and Benedikt have all also been of great assistance with the GPS measurements and their processing. I thank the Glaciology group at the University of Iceland: Tollý, Finnur, Eyjólfur, Alex, Ági, Mona, Joaquin, Louise, Becca and the others for discussions and for including me in their weekly lunch meeting which made me feel a part of academia. Special thanks go to Tollý and Finnur for encouragement and gentle pressure to focus on this project and finish it.

The hydrologists, currently or formerly at the Met Office, Tinna, Gunnar Sig, Philippe and the others, have helped me in many ways with the melt calculations and data processing. Being in part a member of the hydrology team has been enjoyable. I thank my co-workers at the Met Office, Oddur, Jón Gunnar, Trausti and Snorri, for discussion on Iceland's glaciers, rivers and climate. They also made the afternoon coffee

breaks enlightening and interesting with discussions on the faults of capitalism, the death of unsustainable consumption, the hypocrisy of the Paris Agreement, outdoor adventures, the classic beauty of Gelandewagen and other important aspects of life. My temporary office mate Ásdís I thank for practical advice on how to navigate the journey towards a PhD.

Being part of the large PhD and postdoc group of SVALI has been pleasant. I thank Jon Ove Hagen, Tómas, Thomas Zwinger, Droplaug and all the others for making SVALI a reality and running it smoothly. I also thank Thomas Zwinger for Elmer/Ice assistance and for organizing the SVALI summer school on Earth System Models and Ice Models in 2011. All the SVALI PhDs, postdocs and associated SVALI students made meetings and conferences enjoyable events. I thank my fellow SVALI PhD students in subglacial hydrology, PiM and Alex for support, interesting discussions and enjoyable time together. Dorothee and Sergey I thank likewise for interesting discussions. I thank Solveig for friendship and discussions on the joys and sorrows of life when that was needed. I thank Katrin for making me realize that sometimes things that come to pass, good or bad, are just life and should be enjoyed or accepted. I also thank Katrin for her friendship and hospitality.

I thank Ken Moxham for help with the English language in the papers and in the thesis.

I thank Óli Magg, Ági, Heiða, Matteo, Þórdís and Steini, and all the others for backcountry ski tours and ice climbing when a sharp approach to snow and ice, with the edges of skis or the picks of ice axes, instead of geophysics, was needed to regain a calm mind. Special thanks go to Grettir, Símon and Jökull for biking, skiing, beer drinking and keeping my feet on the ground by reminding me of the pointlessness and absurdity of my university studies. The same goes to Siggi Guðjóns for his good friendship, advice, discussion, showing me how unprofitable science is compared to engineering and, furthermore, for providing me with normal activity, to rest the mind, such as moving large amounts of boxes and painting walls. Kolbeinn, Símon and Ásgeir also get special thanks for support, enjoyable travels, and undertakings and discussions on all the other aspects of life than geophysics. I also want to thank my companions in the ICE-SAR team of Hafnarfjörður for sharing undertakings, some enjoyable and others hard, which give life a deeper meaning. Special thanks to Snorri Magnússon for teaching me about the many things in life that, in his words, are not solved by finding the roots of a cubic polynomial.

Ástu heitinni og Bigga þakka ég innilega fyrir allan stuðninginn og skilyrðislausa umhyggju á þeirri löngu vegferð sem háskólanám mitt í heild hefur verið. Gyðu þakka ég allar góðu stundirnar.

My dear friend Bjarnheiður I thank for her support during these years and everything that she has taught me about life.

1 Introduction

Throughout the history of Iceland, glacier rivers have posed a threat to lives, farmland, and infrastructure, but they also provide abundant potential for hydroelectric power. There is therefore an urgent need in Iceland for hydrological measurements of glacier rivers for the design and operation of hydroelectric power plants and bridges. This has resulted in many long series of discharge measurements in glacier rivers and quantification of extreme hydrological events (Þórarinsson, 1974; Rist, 1990; Sigurðsson and Einarsson, 2005; Snorrason and others, 2012). These long-term hydrological measurements provide a unique opportunity for research on glacier hydrology, and have led to descriptive and theoretical models for jökulhlaups (Björnsson, 1974, 1975, 2010; Nye, 1976).

Subglacial water flow and variations in basal water pressure have attracted increased attention in recent years as a likely cause of large variations in ice-flow velocity that have been observed on the main outlet glaciers of the Greenland ice sheet (e.g. Rignot and Kanagaratnam, 2006; Doyle and others, 2015). Better understanding of the role of the subglacial hydraulic system in glacier dynamics, including the dynamics of the large polar ice sheets, is therefore necessary to model the future contribution of glaciers to global sea-level rise (Bell, 2008). Broad and wide Icelandic temperate ice-cap outlets resemble many of the land-terminating ice sheet outlets in southwest Greenland and might be an analogue for polar glaciers' wetter and warmer future (Björnsson, 2017). Understanding the hydrology of such ice cap outlets and its interaction with the ice motion is, thus, important.

Understanding the hydrology and the dynamics of Iceland's glaciers is also of local interest. Climate change is predicted to cause large changes in glacial runoff (Flowers and others, 2005; Jóhannesson and others, 2007; Jónsdóttir, 2008; Einarsson and Jónsson, 2010). Flowers and others (2005), furthermore, show that changes in hydraulic catchments on Vatnajökull can be expected to follow the glaciers' predicted retreat and thinning. Determining the possible effects of runoff changes on the dynamics of the glacier and possible feedbacks of the dynamics on runoff is therefore important as well.

This PhD study was initiated at the Icelandic Meteorological Office (IMO) in 2011, based on this need and availability of glaciological and hydrological data. The study was organized as part of a larger research project, the Nordic Centre of Excellence SVALI, 'Stability and Variations of Arctic Land Ice', funded by the Nordic Top-level Research Initiative (TRI).

Data from continuous GPS measurements on different kinds of interaction of subglacial hydrology with glacier dynamics during three jökulhlaups are available at IMO. These data were incorporated into the study as jökulhlaups provide one of the best

opportunities to study the response of the subglacial hydraulic system to large and sudden variations of water inflow. The lessons learned from studies of jökulhlaups may therefore be useful for understanding variations in basal sliding and ice flow in glaciers and ice sheets in general (Bell, 2008).

A sound understanding of jökulhlaups is also essential for hazard mitigation as they may endanger people and livestock. Jökulhlaups can also damage infrastructure, power supply systems, communication lines, hydropower plants, vegetation and even alter landscape to great extent (Björnsson, 2002). This necessitates research on the physical processes in jökulhlaups, in addition to the glacier dynamics aspect.

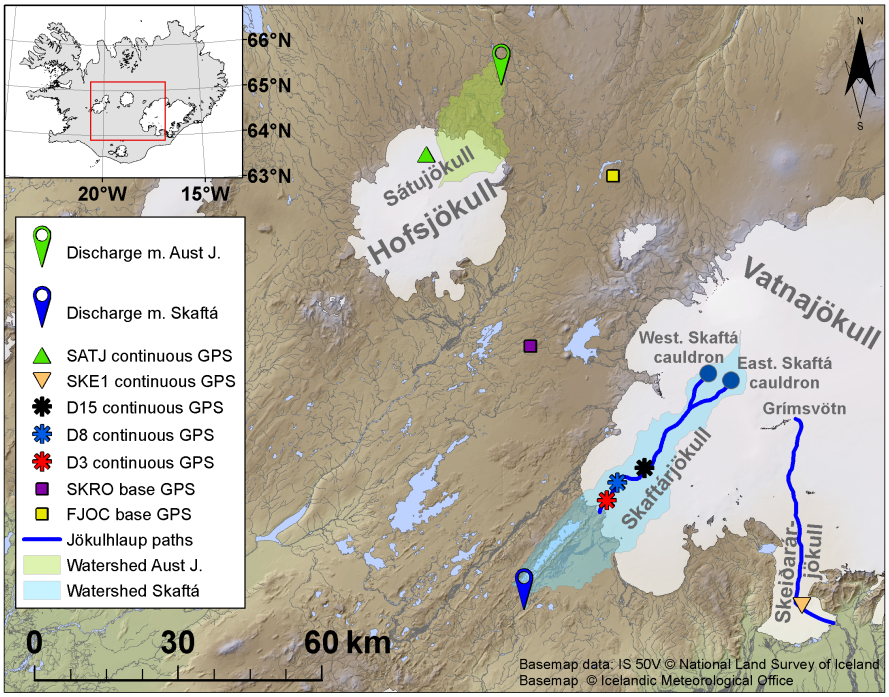

Figure 1.1. Location of Hofsjökull and Vatnajökull ice caps and the subglacial lakes at Grímsvötn and the Skaftá cauldrons. Estimated flood paths, based on the gradient of the hydraulic potential. The locations of hydrometric stations, continuous GPS measurements and GPS base stations. The watersheds of the highest up-river hydrometric stations in Austari-Jökulsá and Skaftá rivers are indicated with coloured shadings.

The available jökulhlaup data are derived largely from a research project on the subglacial lakes below the two Skaftá cauldrons (Fig. 1.1). The main focus of the project was the biology and the thermodynamics of the subglacial lakes (Jóhannesson and others, 2007; Gaidos and others, 2009), new instrumentation (Gaidos and others, 2007; Thorsteinsson and others, 2007) and jökulhlaup dynamics (Einarsson, 2009). I took part in this research project and have already processed and published part of

the jökulhlaup data in my MS thesis (Einarsson, 2009). The MS thesis deals with a small jökulhlaup from the western Skaftá cauldron in 2006. Some of the same data are used in Paper II in this thesis. They have been reprocessed with the aid of a lidar digital elevation model (DEM) acquired in 2010 and modelling of the subsidence of the ice shelf, overlying the subglacial lake below the western cauldron, with the full-Stokes ice-dynamic model Elmer/Ice (Gagliardini and others, 2013). The focus has also been moved from modelling the event with a coupled sheet–conduit jökulhlaup model (Flowers and others, 2004), presented in Einarsson (2009), to the geometry of the subglacial lake and how the ice shelf covering the lake is lowered as the lake is drained by a jökulhlaup. Better estimates of outflow and new findings from Paper I also allowed further interpretation of the processes taking place during the formation of the subglacial flood path. The approach and discussion on the 2006 jökulhlaup, presented in this thesis, is thus substantially different from the approach and discussion in the MS thesis. The estimated travel speed of the subglacial flood front, temperature measurements in Skaftá during jökulhlaups, and calculation of energy available for melt given in the MS thesis are still valid and are presented in both publications.

Paper I is based on data from two jökulhlaups from the western and eastern Skaftá cauldrons in April and October 2008, respectively, obtained in the above-mentioned research project. My collaborators, Eyjólfur Magnússon and Finnur Pálsson at the Institute of Earth Sciences, University of Iceland, and Matthew J. Roberts at the IMO, had available similar data on the dynamic response of Skeiðarárjökull, an outlet glacier from Vatnajökull ice cap, induced by jökulhlaups in 2004 and 2010 from the subglacial lake Grímsvötn (Fig. 1.1). As co-interpretation of these two datasets would add further value to each of them, data from all four jökulhlaups from Skeiðarárjökull and Skaftárjökull were included in the joint study on jökulhlaup dynamics presented in Paper I.

In addition to the GPS measurements on Skaftárjökull during jökulhlaups, the instruments provided months of data in between jökulhlaups, which are discrete and short-lived events. These data were used to study the hydraulics and dynamics of the glacier under normal conditions, which are the main subjects of Paper III. As part of the PhD project, a GPS station was also run during the 2011, 2012 and 2013 melt seasons, high in the ablation area of Sátujökull, which is an outlet glacier from Hofsjökull ice cap (Fig. 1.1). Results from this location add further information to the study and allow a comparison of two different glaciers, strengthening the generality of findings.

1.1 Research objectives

This PhD was carried out as part of SVALI work package 2.1, the aims of which were to improve understanding of the physical processes in water flow at the base of glaciers and its feedback with ice dynamics. These aims are in line with the broader aims of the TRI sub-programme “Interaction between Climate Change and the Cryosphere” (ICCC), of which SVALI was one of three subprogrammes. The aims of ICCC were to improve understanding of the stability, variations and dynamics of the cryosphere.

In order to achieve these aims, the research objectives of this study were to use discharge time series from glacier rivers, available at IMO, and continuous GPS mea-

surements of the surface motion of the glacier feeding them to gain understanding of the time-dependent development of the subglacial hydraulic system and its interaction with ice motion. The main focus is on the effects of hydrologically induced forcing on the dynamics of broad and gently sloping ice-cap outlets, under normal conditions during the melt season and extreme conditions in jökulhlaups.

Research questions

- How is the hydraulic system of broad and gently sloping ice-cap outlets in Iceland affected by seasonal variation in runoff?
- Is an effective channelized fast hydrological system formed during the melt season at the base of broad and gently sloping ice-cap outlets in Iceland, and if so how does it develop and propagate up-glacier as the melt season progresses?
- How do broad and gently sloping ice-cap outlets respond to a wide range of hydrologically induced forcing on basal slip?
- To what extent are the hydraulics of glaciers in the highly permeable active volcanic zones of Iceland affected by groundwater flow?
- What are the main processes in the formation of the subglacial flood path and how does the subglacial flood front propagate in rapidly rising jökulhlaups from the Skaftá cauldrons?
- Does a propagating subglacial pressure wave form the initial flood path in rapidly rising jökulhlaups, and if so where and how is such a wave formed?
- What effect do jökulhlaups from the Skaftá cauldrons and the subglacial lake Grímsvötn have on the dynamics of Skaftárjökull and Skeiðarárjökull glaciers?
- Is jökulhlaup behaviour more of a spectrum between rapidly and slowly rising jökulhlaups than two distinct categories?
- Which processes should be included in a conceptual model of jökulhlaups?
- How do the dynamics of an ice shelf covering a subglacial lake interact with the outflow from the lake during jökulhlaups?

1.2 Outline of the dissertation

This dissertation is based on three papers:

Paper I Einarsson B, Magnússon E, Roberts MJ, Pálsson F, Thorsteinsson Th and Jóhannesson T (2016) A spectrum of jökulhlaup dynamics revealed by GPS measurements of glacier surface motion. *Annals of Glaciology*, **57**, 47–61 (doi:10.1017/aog.2016.8)

Paper II Einarsson B, Jóhannesson T, Thorsteinsson Th, Gaidos E and Zwinger T (2017) Subglacial flood path development during a rapidly rising jökulhlaup from the western Skaftá cauldron, Vatnajökull, Iceland. *Journal of Glaciology*, **63**(240), 670–682 (doi:10.1017/jog.2017.33)

Paper III Einarsson B and Jóhannesson T (2018) Hydrology and dynamics of two Icelandic outlet glaciers revealed by discharge and GPS measurements. *To be submitted to the Journal of Glaciology.*

Each paper is presented as a chapter at the end of the thesis. An overview of the hydrology of Iceland's glaciers, a description of the main methods used in this research, a summary of each paper and general conclusions are presented before the papers.

2 Hydrological processes in Iceland's glaciers

Glaciers are important modulators of hydrology and affect the hydrological regime of a watershed in many ways. Major influencing factors are the orographic intensification of precipitation because of the higher altitude of the glacier surface compared with the subglacial terrain and the effect of the glacier geometry on watershed boundaries. The glaciers furthermore store precipitation for seasons, years and decades as snow and ice, which affects the timing and magnitude of surface runoff. Glacier hydrology also modulates runoff from melting and precipitation on shorter timescales, in particular the diurnal variation.

Runoff from glaciers contributed approximately 19% of Iceland's total runoff during the period 1961 to 1990 (Jónsdóttir, 2008). Glacier runoff is defined following Radić and Hock (2014) as "the portion of all water inputs to the glacier through melt, rain or other inflow at the surface, laterally or subglacially that drains from the glacier at its terminus" except that water draining from the glacier as groundwater is also included. In recent years, the ratio of glacier runoff to total runoff has increased because of a strong negative mass balance trend since about 1995 (Björnsson and Pálsson, 2008; Björnsson and others, 2013).

Glaciers in Iceland receive more precipitation than ice-free areas or about 20% of the total precipitation (Crochet and others, 2007), which is considerably higher than the proportion of Iceland's area that is glacier-covered (10.7%). The glaciers are located at high elevations and many are near the coast facing the predominant storm track direction. Furthermore, glaciers create their own microclimate by enhancing orographic precipitation, because the glacier ice superimposed on the underlying landscape increases the surface elevation. Increased surface elevation allows glaciers to reach into colder air, leading to more precipitation falling as snow since air temperature decreases with elevation.

Accumulation and ablation rates are high in the mild and humid maritime climate of Iceland, producing substantial glacier meltwater runoff. Melting caused by geothermal activity at the glacier bed is also unusually high in Iceland because of the large geothermal heat flux. It is estimated that about 5% of total runoff from Vatnajökull is geothermally derived basal melt (Flowers and others, 2003).

In Iceland, weather-related variations in discharge are not observed to be dampened on glacier-covered watersheds, compared to ice-free watersheds. This is in contrast to many glacierized regions in the world where discharge from ice-free areas is low during warm, dry summers but high during cold, wet summers so that glacier melt which is high during warm summers but low during cold summers compensates these variations. Dry, cold periods as well as wet, warm periods have been observed in Iceland (Jónsson, 1991),

where this compensating effect appears to be less pronounced. Discharge variations from glacier-covered watersheds in Iceland in fact tend to be amplified compared to ice-free watersheds (Crochet, 2013) as glacier melt is high during wet, warm periods and low during dry, cold periods.

A portion of the surface melt and rain that falls on the glacier surface flows through the englacial hydrological network and into the subglacial hydrological system that directs water towards the glacier margin. Part of the subglacial water percolates into the groundwater system below the ice and may appear as discharge in springs far from the glacier. Runoff from a glacier thus involves hydrological processes in surficial, englacial (within the glacier), subglacial (at the base of the glacier) and groundwater environments. A brief description of each of these hydrological systems in Iceland and the effects of glaciers on watershed boundaries is given below.

2.1 Effect of glacier surface geometry on watershed boundaries

Watershed boundaries on Icelandic ice caps have been observed to be in accordance with subglacial water pressure approximately equal to the ice-overburden pressure (Björnsson, 1988). This causes nine-tenths of the hydrological potential at the glacier bed to be controlled by the surface topography of the glacier while only about one-tenth is controlled by the subglacial topography (Shreve, 1972). Watersheds in glacier-covered areas are therefore not the same as they would be without the glacier. Radio-echo sounding of bedrock topography and ice surface maps have been used to delineate watershed boundaries on all of Iceland's major ice caps (Björnsson, 1998; Magnússon and others, 2004). The effect of glacier surface geometry on the hydrological potential, furthermore, affects where jökulhlaups are released at the glacier terminus. For example, jökulhlaups from the Skaftá cauldrons are released into the western branch of the Skaftá river, and not the eastern branch as the bedrock topography dictates, because the hydrological potential arising from the ice surface geometry drives subglacial water flow westwards over a pass in a subglacial ridge (Björnsson, 1998). This observation has been used to infer that subglacial water pressure at this location is at least 96% of ice-overburden pressure (Björnsson, 1998). This westward flow is not restricted to conditions during jökulhlaups, but might be sensitive to temporal changes in the drainage system and to glacier-surface geometry changes (Magnússon and others, 2004) as other subglacial watershed divides that can be affected by changes in the subglacial water pressure (Flowers and others, 2003). The dependence of watershed divides on glacier surface and terminus geometries can cause migration of preferential subglacial watercourses and consequent changes in discharge ratios between adjacent rivers with an advancing or retreating glacier. The retreat of the Skeiðarárjökull outlet glacier from Vatnajökull ice cap has, for example, caused water formerly drained by the river Skeiðará to be rerouted to the river Gígjukvísl, with the result that the longest bridge in Iceland now crosses mostly dry riverbed.

2.2 Surface processes

Seasonal snow cover is substantial on Icelandic glaciers, and winter snow thickness can exceed 10 m in the upper part of the accumulation area (Figs 2.2 and 2.3) on glaciers in southern Iceland (Fig. 2.4). Large parts of the glaciers, where winter accumulation exceeds summer melt, remain snow-covered throughout the year; this is called the accumulation area of the glacier (Figs 2.2 and 2.3). The lower parts of the glaciers, where summer melt exceeds winter accumulation, are called the ablation area of the glacier (Figs 2.2 and 2.3). Thin seasonal snow cover is found in the lower parts of glaciers in southern Iceland, which extend nearly to sea level. At some locations there may be only a few days of snow cover each winter, and no winter snowpack accumulation.

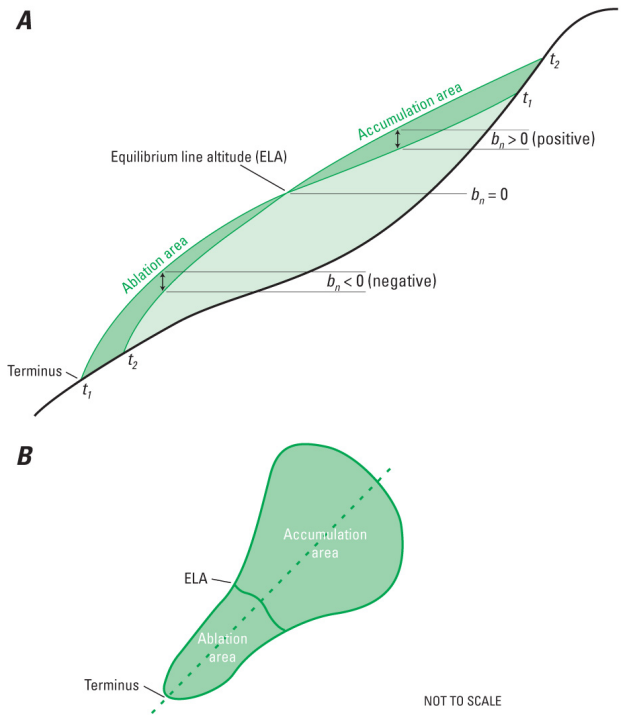

Figure 2.2. Glaciological division of glaciers: cross-sectional (A) and planar (B) view (from Williams and Ferrigno, 2012, fig. 72 A and B, p. A229).

Snow cover affects runoff from glaciers in a number of ways in addition to the seasonal snow storage. A portion of the surface meltwater and rain is retained in the snow by refreezing and through capillary processes. The amount of water retained in the snowpack depends on the temperature, porosity, crystal structure, and the thickness of the snowpack. These properties evolve during the course of the year and alter the hydrological processes acting within the snow (e.g. Fountain, 1996). The most apparent

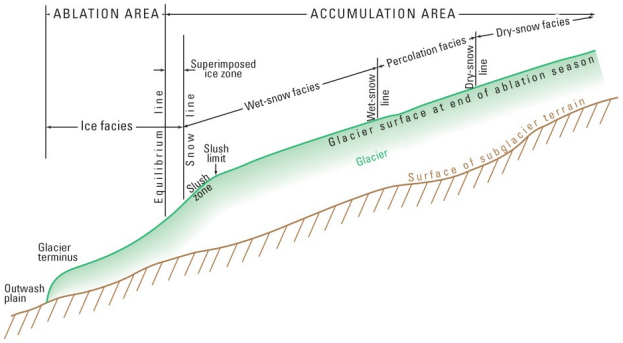

Figure 2.3. Glacier facies at the end of the balance year (from Williams and Ferrigno, 2012, fig. 4 A, p. 83).

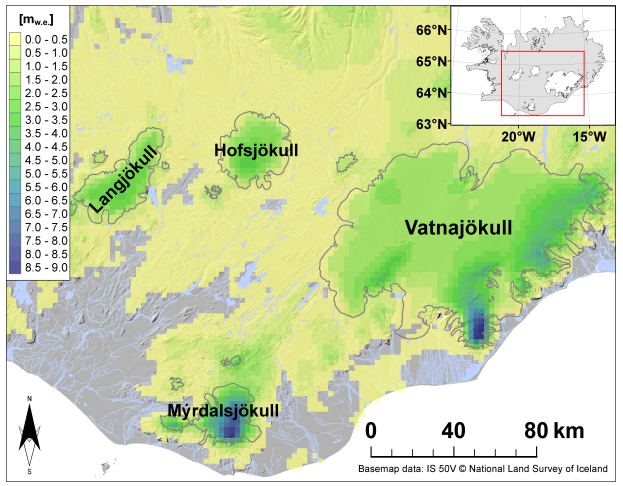

Figure 2.4. Calculated snow amounts ($m_{w.e.}$) for central and southeast Iceland; the accumulated values are from 1 September 2012 to 1 May 2013. Outlines of glaciers and ice caps are indicated with grey lines. The values are based on calculations by the weather model Harmonie at the Icelandic Meteorological Office.

and effective change is the thinning, and sometimes the complete melting, of the snowpack by summer ablation. The result is a gradual rise in elevation of the snowline in the ablation area on the glacier through the summer, exposing bare glacier ice and superimposed ice (not widely found in Iceland), and thus altering the hydrological characteristics of the surface. The residence time for water on the bare ice is much shorter than for a snow-covered surface; hence, diurnal variations in meltwater discharge entering the englacial hydrological system are much more pronounced as the summer progresses (e.g. Fountain, 1996). Water in the snowpack in the ablation area is only retained for a single melt season, until it drains out of the snowpack or the snowpack melts completely. In the accumulation area, water that refreezes within or below the winter snowpack may have the same fate as the surrounding snow. If it persists for several years it is transformed into glacier ice and is transported down-glacier into the ablation area, where it will be released decades or even centuries later by melting.

Water not retained in the snowpack percolates down until it meets the interface between ice and snow or firn and snow. Water flow at the base of the snowpack or firn is similar to groundwater flow in an unconfined aquifer until the water encounters crevasses, moulins or other vertical englacial conduits that allow the water to flow into the englacial hydrological system (Fountain and Walder, 1998). Substantial water flow has been observed at the firn/ice boundary in boreholes. This englacial flow causes the boreholes that do not reach the bed to fill up to the firn/ice boundary (Árnason and others, 1974; Thorsteinsson and others, 2002).

Figure 2.5. Water-saturated slushy snow and surface ponds in depressions on Tungnaárjökull in late spring on 11 June, 1999. Oblique aerial photograph no. 22130 by Oddur Sigurðsson, Icelandic Meteorological Office.

Saturated snow is sometimes observed in the lower part of snow pits in spring. The water table in the snowpack may reach the surface, forming large areas of water-saturated, slushy snow and ponds in depressions (Fig. 2.5). As melt progresses, the temporarily impounded water in such ponds has been observed on field expeditions to flow into moulins, crevasses or other surficial openings.

The entire accumulation area on Icelandic glaciers is located in the wet-snow facies (Fig. 2.3). The wintertime cold snowpack temperature is eliminated by refreezing

percolating meltwater during summer, leaving the entire snowpack and firn at the freezing point by autumn. This process is far more efficient than the cooling of the snowpack and firn by heat conduction during winter because the thermal conductivity of snow is low while latent heat release by freezing water is high (e.g. Cuffey and Paterson, 2010). The vertical temperature gradient in the snowpack, driving the heat conduction, is, furthermore, small in the maritime climate of Iceland with its relatively mild winters. The effect of refreezing is visible as ice lenses within the winter snowpack. The lenses become thinner and sparser at higher elevations but are still clearly visible. For example, numerous ice lenses with an aggregate thickness of $\sim$10 cm are found every year in snow cores drilled in spring at 1790 m a.s.l. at the summit of Hofsjökull, one of the highest ice caps, and the furthest inland in Iceland.

2.3 Englacial processes

Although solid glacier ice is virtually impermeable to the flow of water through intergranular veins (Fountain and Walder, 1998), very little water flows directly on the surface of glaciers, even within the lower parts of the ablation zone. Instead of flowing for long distances across the glacier surface, the water is diverted from surficial to englacial flow by crevasses, moulins or fractures in the ice (Fountain and Walder, 1998; Fountain and others, 2005).

Prominent surface channels of flowing meltwater abruptly terminate at moulins and, on low-lying, relatively flat outlet glaciers, the water plunges directly to the glacier bed in many cases. The surface channels and moulins are not as large on the ablation areas of outlet glaciers terminating at higher elevation but the system is similar in structure. Slower, more circuitous flow through other forms of englacial channels, such as crevasses and interconnected fractures in the ice, is believed to be dominant in the accumulation areas of Icelandic glaciers, but these systems are hard to observe directly.

2.4 Subglacial processes

Localized outlets of a channelized drainage system (Röthlisberger, 1972) are observed at the termini of most Icelandic glaciers in summer and early autumn. This indicates high-volume subglacial drainage channels with fast water flow under at least the lower part of the ablation area. Higher up on the glacier, under the accumulation area, in areas between the channels in the ablation zone and perhaps under the entire glacier in winter, water flow is expected to be in distributed cavities linked with poorly connected passages with slow water flow (Kamb, 1987).

In several cases on Icelandic glaciers, unusual situations have been observed to temporarily alter the basal hydraulic system in the accumulation and ablation areas. One example is a subglacial channel high up in the accumulation area maintained through the entire winter period by constant drainage from subglacial lake Grímsvötn after the 1996 Gjálp eruption. This is inferred to have led to lower basal water pressure and less basal sliding, causing observed reduction in ice flow velocities (Magnússon and

others, 2010). Increased transient drainage of water, caused by jökulhlaups from both Grímsvötn in 1996 and the eastern Skaftá cauldron in 1995, has, on the other hand, been observed to cause increased ice-flow velocities, due to a rise in water pressure at the glacier bed (Magnússon and others, 2007).

Another interesting example is provided by the effects of a surge of Skeiðarárjökull on the draining of a jökulhlaup from lake Grímsvötn in 1991 (Björnsson, 1998). Jökulhlaups from Grímsvötn normally drain with fast flow through tunnels when the glacier is not surging (Björnsson, 1974), but in this case the jökulhlaup did not manage to develop into a normal outburst flood. The surge caused it to flow through a distributed system and terminate when less than a quarter of the lake volume had drained. Water flow velocities were also much lower than normal: $0.15\,\mathrm{m\,s^{-1}}$compared to normal velocities above $1\,\mathrm{m\,s^{-1}}$ (Björnsson, 1998).

Figure 2.6. A surge wave on Síðujökull on 7 January, 1994. Water emerges at the glacier margin in a number of small outlets in front of the surge wave (left) while water is discharged in a few main outlets in parts of the margin where the wave has passed by (centre). This indicates distributed subglacial drainage in front of the surge wave, and channelized subglacial drainage behind the surge wave. Oblique aerial photograph no. 15576 by Oddur Sigurðsson, Icelandic Meteorological Office.

A surge wave propagating down Síðujökull in 1994 also had pronounced effects on the subglacial hydraulic system (Björnsson and others, 2003). At the front of the advancing surge wave, the subglacial channelized system was disrupted and a distributed-drainage pattern was inferred near the glacier margin but, as the surge wave passed, channelized drainage was re-established at the margin of Síðujökull (Fig. 2.6).

Icelandic glaciers generally respond to changes in subglacial water flow and subglacial accumulation of water in a similar way as observed elsewhere. That is, ice-flow velocity increase is observed, by continuous GPS measurements, in connection with rain events (Magnússon and others, 2011), jökulhlaups (Magnússon and others, 2011; Paper I), and beginning of spring melt (Paper III). Similar observations have been made on both large and small valley glaciers (e.g. Bartholomaus and others, 2008; Fudge and others, 2009), and on the Greenland ice sheet (for example, Rignot and Kanagaratnam,

2006; Doyle and others, 2015).

The response of the subglacial hydraulic system to increased meltwater input is nontrivial because the system adjusts to increased inflow by increasing the volumetric capacity of the basal channel network. Thus, changes in inflow rates may be more important than absolute inflow magnitudes that are sustained over longer time periods (Bartholomaus and others, 2008; Van de Wal and others, 2008). This is evidenced by the different effects of increased outflow from Grímsvötn in 1996 and 1997 and Skaftárkatlar in 1995, as mentioned above, that can either increase or decrease ice-flow velocities depending on circumstances.

2.5 Subglacial groundwater flow

Many glaciers in Iceland are underlain by unconsolidated glacial deposits, such as subglacial tills or heavily fractured bedrock. Part of the subglacial water flow takes place as groundwater flow in the till where such deposits are present. Recharge of subglacial water into deeper underlying glacial sediments and underlying bedrock is also widespread in Iceland, as discussed by Flowers and others (2003) and Sigurðsson (1990).

3 Methods

The results presented in this thesis are based on an interpretation of hydrologically induced glacier surface motions observed with continuous GPS measurements and discharge time-series from hydrometric stations in glacier rivers. Model simulations of the emptying of a cylindrically symmetric subglacial lake with the full-Stokes ice-dynamic model Elmer/Ice (Gagliardini and others, 2013) and degree–day modelling of melt on Skaftárjökull and Sátujökull glaciers are used for further interpretation of the measurements but are not the main topic of the research. Theoretical derivations and concepts such as Nye's (1976) equations for subglacial water flow in conduits, Jóhannesson's (2002) analysis of sheet-like water flow and propagation of a subglacial pressure wave and Kamb and Echelmeyer's (1986) estimates of longitudinal stress-gradient coupling are also used in the analysis. The propagation velocity of jökulhlaup flood fronts and the magnitude of basal overpressure are such that elastic deformation of the overlying ice may be important for separating the glacier from the bedrock. Elastic deformation of glacier ice is therefore considered, although that glacier flow is typically dominated by viscous deformation (Cuffey and Paterson, 2010). The methodology used in the processing of continuous GPS measurements and discharge measurements in glacier rivers and the analysis of subglacial water flow and ice dynamics is presented in more detail below, as they are a main theme in all three papers of the thesis.

3.1 GPS measurements of glacier surface motion

GPS measurements were used to monitor (i) the ice-shelf lowering during the 2006 jökulhlaup from the western Skaftá cauldron, (ii) how subglacial flood propagation affects glacier motion during jökulhlaups from Grímsvötn and the Skaftá cauldrons and (iii) hydrologically induced events in the motion of Sátujökull and Skaftárjökull. Dual-frequency Trimble GPS receivers were used in all cases. Recording intervals depended on available instrument storage space. For the Trimble NetRS and Trimble 5700 used on Hofsjökull and on Skaftárjökull, the recordings were made at continuous 15 s intervals. For the Trimble 4000SE GPS receiver used to monitor the ice-shelf lowering during the 2006 jökulhlaup from the western Skaftá cauldron the receiver was set to log for 5 minutes at 15 s intervals once per day.

The continuous 15 s data were processed with the GAMIT-Track utility (Herring and others, 2010) using a setup for long baselines. The daily data from the western Skaftá cauldron in 2006 were processed with the Trimble Geomatics Office software. All data were processed with respect to the next available base stations with high-quality data, resulting in baselines from $\sim$20 km and up to $\sim$85 km. The standard

deviation of unfiltered positions around a daily mean during periods of slow motion and low melt is approximately 4 cm in the vertical and 2 cm in the horizontal coordinates for the continuous data and may be used as an indication of the precision of the GPS measurements. Errors in the daily data from the western cauldron in 2006 are higher, but, based on fluctuations in the measurements between adjacent days during time periods of slow vertical movements before and after the jökulhlaup, the relative accuracy of the measured surface elevation is estimated to be better than 1 m.

Different post-processing filtering was applied depending on the purpose of the data acquisition. Ice movements are rapid and transient on timescales less than an hour during jökulhlaups, while the response to spring melt and rain-induced events is on the timescale of days so that more smoothing can be used without the filtering smoothing out the relevant signal.

For the jökulhlaups, horizontal velocities were calculated for 1 hour periods using filtered positions (2 hour wide triangular running average filter). During days prior to jökulhlaups, when we expect glacier motion to be approximately constant, the filtered velocity records reveal standard deviation of 8, 7 and 11 cm d^{-1} (3–5 mm h^{-1}) for the Skaftárjökull, 2004 Skeiðarárjökull and 2010 Skeiðarárjökull data, respectively.

For other events with timescales on the order of days, the locations were filtered with a 24 hour Gaussian filter and hourly values extracted. Hourly horizontal velocities were then extracted from location values 24 hours apart. Finally, daily median values were calculated from the hourly velocities. The standard deviation of the velocities for 7–10 day periods with approximately constant glacier motion was found to be 0.1–0.2 cm d^{-1}, which may be used as an indication of the uncertainty in the velocities.

3.2 Discharge measurements in glacier rivers

The discharge in Austari-Jökulsá at Austurbugur and Skaftá at Sveinstindur was measured by monitoring the water level in the river using a pressure transducer located upriver from a stable natural controlling cross section. The water level is then converted to discharge using a water-level–discharge rating curve that is constructed from discrete water-level and discharge measurements. The hydrometric data were quality-checked and corrected for biases, particularly disturbances due to ice forming at the river banks, as needed at the end of each hydrological year. Data missing because of instrument breakdown, ice formation or other causes were estimated using meteorological data from nearby weather stations or discharge from nearby rivers with similar discharge characteristics. The uncertainty of discharge measurements at Sveinstindur is estimated as $\pm 2\%$ (Jónsdóttir and others, 2001) and is expected to be similar for the measurements at Austurbugur, which are performed in the same way and with similar instruments. For further details on hydrological measurements in glacier rivers in Iceland see Einarsson (2012), and on instrumentation see Icelandic Meteorological Office (2017a,b).

Hydrological measurements in glacier rivers are often difficult. Glaciers erode the underlying strata by sliding and create large amounts of sediment that are carried by the rivers. These sediments give glacier rivers their characteristic milky colour and they create a number of problems in hydrometric measurements (Rist, 1990). Sensors get

buried in sand drifts travelling along the riverbed, silt jams up sensors and measuring pipes, and sediment accrual and removal from the controlling cross section disturbs the water-level–discharge relationship. The sediments also create large alluvial fans and sandur plains, causing the rivers to become braided and run in highly erodible, meandering channels (Rist, 1990). This makes it difficult to find good locations for hydrological measurements and stable cross sections. The magnitude of annual discharge variations also makes measurements harder, as the same instrument setup must be able to measure a range from a few $m^3\,s^{-1}$ to hundreds of $m^3\,s^{-1}$. Continuous discharge measurements are therefore not available from Skeiðará and Gígjukvísl, but discrete discharge measurements were made from bridges during jökulhlaups. Hydrographs for the 2004 and 2010 jökulhlaups from Grímsvötn are based on interpolation of such measurements.

3.3 Subglacial water flow

Subglacial water flow is generally assumed to be along an arborescent system of conduits melted into the overlying ice (Röthlisberger, 1972) or in a distributed system of interconnected cavities (Kamb, 1987). Water may also be present at the bed of glaciers as a thin water film (Walder, 1982; Creyts and Schoof, 2009), in canals incised into soft sediments or the bedrock below the glacier (Nye, 1973) or as flow in porous subglacial sediments and bedrock (Sigurðsson, 1990). Flow in subglacial conduits is analysed further below as it is important in the theory of slowly rising jökulhlaups (Nye, 1976) and in the response of the subglacial hydraulic system to increased inflow during the melt season. The situation of sheet-like water flow, encountered in a propagating subglacial pressure wave and in its wake, is also analysed as it is unusual and not as widely discussed in the literature as the other types of subglacial water flow.

Subglacial conduit flow

At least two sets of equations are required to describe subglacial water flow in addition to mass and energy conservation. One should describe the development of the size of the subglacial watercourse while the other describes the flow within the watercourse (Flowers, 2015). In traditional jökulhlaup modelling and the description of the development of subglacial conduits (Nye, 1976), the size of the conduit is described with its cross-sectional area, S. The cross-sectional area changes with melting at the conduit walls according to

$$\frac{\partial S}{\partial t} = \frac{m_\mathrm{i}}{\rho_\mathrm{i}}\,, \tag{1}$$

where t is time, m_i is the melt rate of the channel walls and ρ_i is density of ice. This equation neglects the effects of creep closure of the conduit, which is an acceptable assumption during the initial phase of jökulhlaups or for conduits formed in spring events as the water pressure is close to overburden in such conditions.

Assuming that the temperature of water flowing in the channel is not significantly different from the pressure melting point, which is valid for melt water in spring and

jökulhlaup floodwater several kilometres downstream from the source lake, the melt rate of the channel walls can be calculated as

$$m_i = \frac{Q}{L}\left(\frac{-\partial\phi}{\partial s} + c_t\rho_w c_w \frac{\partial p_w}{\partial s}\right) , \tag{2}$$

where g is the acceleration of gravity and L, ρ_w, c_w and c_t are the latent heat of fusion, the density, the heat capacity and the change in the melting point with pressure for water, respectively. An along-conduit horizontal coordinate is denoted by s, $\phi = \rho_w g z_b + p_w$ is the hydraulic potential, p_w is water pressure, z_b is elevation of the glacier bed and $\partial\phi/\partial s$ is the hydraulic gradient in the conduit. The term in parentheses is called the *melt-rate ability* of the conduit and denoted by μ by Magnússon and others (2011). It takes into account the thermodynamic effect, first analysed by Röthlisberger (1972), of the variation of the melting point of water with pressure on the rate of melting of the conduit walls, assuming that energy is released or spent as needed to lower or raise the temperature to maintain it at the local pressure melting point. This assumes instantaneous heat transfer from the water flow to the channel walls (see further discussion below).

The discharge, Q, along the subglacial conduit can be calculated using the Gauckler–Manning–Strickler formula for the mean flow speed $\bar{v}$ (Nye, 1976). Using $Q = S\bar{v}$ and assuming semi-circular channel geometry, the discharge may be expressed as

$$Q = \frac{S^{4/3}\left|\frac{\partial\phi}{\partial s}\right|^{1/2}}{n_m\sqrt{\rho_w g}(2/\pi)^{1/3}(2+\pi)^{2/3}} . \tag{3}$$

ρ_w is the density of floodwater and n_m is Manning's friction coefficient for the conduit walls and bottom.

The time-dependent development of S and Q can be calculated as a function of the hydraulic gradient and an estimate for an initial conduit cross-sectional area, S_0, derived for example from information about the subglacial discharge of water before a jökulhlaup or a spring event, using Nye's (1976) theory for jökulhlaups. Combining equations (1), (2) and (3), the time-dependent development of S can be expressed as

$$\frac{\partial S}{\partial t} = \frac{S^{4/3}\left|\frac{\partial\phi}{\partial s}\right|^{1/2}\left(\frac{-\partial\phi}{\partial s} + c_t\rho_w c_w\frac{\partial p_w}{\partial s}\right)}{\rho_i L n_m\sqrt{\rho_w g}(2/\pi)^{1/3}(2+\pi)^{2/3}} . \tag{4}$$

The local hydraulic potential gradient $\partial\phi/\partial s$ is estimated from the glacier bed and surface topographies, z_b and z_s. Assuming that the subglacial water pressure equals ice overburden as the subglacial hydraulic system is flooded with jökulhlaup water,

$$\frac{\partial\phi}{\partial s} = (\rho_w - \rho_i)g\frac{\partial z_b}{\partial s} + \rho_i g\frac{\partial z_s}{\partial s} . \tag{5}$$

The bed and surface gradients $\partial z_s/\partial s$ and $\partial z_b/\partial s$ should be estimated over a horizontal distance of about one ice thickness at each location.

For the above-mentioned assumption that conduit closure due to ice deformation is negligible due to water pressure close to overpressure, the equations predict unstable, approximately exponential growth of the discharge. The same holds true for a more

general set of equations where conduit closure is accounted for, as long as melt rate exceeds conduit closure (Nye, 1976). A positive feedback is created where more melting leads to more water flow which leads to more generation of frictional heat that then leads to more melting. This feedback and the growth in discharge will continue as long as water supply is available at the entrance of the conduit and melt rate exceeds conduit closure. Based on these equations, Nye (1976) presented an analytic solution for discharge, Q, as an asymptotic function that matched observation of a jökulhlaup from subglacial lake Grímsvötn in 1972, within 4%. This positive feedback of discharge growth is referred to in this thesis as the conduit-melt–discharge feedback. Nye (1976) assumed that the whole flood path was confined to a conduit and used the mean hydraulic gradient from the source lake to the glacier snout. Similar results could have been obtained by assuming that the flow is restricted by the conduit-melt–discharge feedback at a bottleneck somewhere along the flood path (Clarke, 1982). The hydraulic gradient at such a bottleneck could deviate substantially from the mean gradient, which would lead to different estimates of the Manning's friction factor, n_{m}, for the same hydrograph, than found by Nye (1976).

A related set of equations can be deduced by assuming steady-state conditions where conduit melt equals conduit closure due to ice deformation (Röthlisberger, 1972). The water pressure varies inversely with discharge for such conditions. A large conduit with high flow rate will therefore have a lower pressure than an adjacent smaller conduit with less flow. The large conduit thus tends to capture water from the smaller conduit, causing the system to form a connected arborescent structure. A similar tendency can be expected during transient conditions such as an input pulse of rain or melt. Larger conduits will transport the increased water with higher efficiency than the smaller ones and thereby create larger depressions in the englacial water table in the area around their upper end and along their path. However, recent modelling by Werder and others (2013), which incorporates channelized and distributed subglacial drainage in two horizontal dimensions, suggests that subglacial channel systems might in fact be only mildly arborescent for ice and bed surfaces without lateral variation, because a subglacial channel can only achieve a slight pressure reduction with respect to its surroundings where the pressure is approximately equal to the ice overburden pressure.

Sheet-like water flow

The observations and analysis presented in Paper I, concerning lifting induced by the propagation of a subglacial wave with water pressure higher than the ice overburden, indicate the formation of a wide subglacial watercourse with thickness on the order of 0.1–1 m, and with lateral width on the order of kilometres. Water flow in such volume is best described as sheet-like flow. Such sheet-like flow is unstable to irregularities in sheet thickness, so conduits are expected to eventually grow by melt–discharge feedback (Walder, 1982) in areas where the melt-rate ability of the conduit, μ, is positive (Magnússon and others, 2011). A crude estimate of the development of the thickness of such a sheet can be described with equations for lifting due to viscous (Equation (11), Paper I) and elastic deformation (Equation (12), Paper I) caused by water pressure higher than overburden. A detailed description of these processes is beyond the scope of this thesis.

Following Jóhannesson (2002), the discharge per unit width, q, in a subglacial sheet, which is much wider than the sheet thickness, h_w, may be calculated from Manning's formula as

$$q = \frac{h_w^{5/3}}{2^{2/3} n_m} \sqrt{\left(\frac{-\partial \phi_s}{\partial s} \right) / (\rho_w g)} \, . \tag{6}$$

The notation is the same as for channelized flow above except that the potential ϕ_s includes the sheet thickness h_w and is defined as $\phi_s = \rho_w g z_b + \rho_w g h_w + p_w$ where p_w is defined at the top of the sheet. The sheet thickness is considered as an average, $h_w = A_w / b_w$, over an effective width, b_w, of the flood path with a total cross-sectional area A_w, resulting in a Manning's hydraulic radius of $h_w/2$.

Macroporous water sheets can be stable for certain sheet thicknesses, in the presence of bed protrusions that partly support the overlying glacier (Creyts and Schoof, 2009). The sheet-like water flow considered in this thesis is not necessarily stable. It is a transient phenomenon in the subglacial propagating flood wave and in the initial flood path. However, a stable sheet flow might be maintained in jökulhlaups from the Skaftá cauldrons at a few locations along the flood path, where the melt-rate ability of conduits, μ, is negative due to adverse bed slopes.

Thermodynamics and heat transfer

The energy available for melting of ice in a subglacial hydraulic path may be used to calculate an upper bound for the volume of the part of the subglacial system created by melting,

$$V_{melt} = \frac{c_w \rho_w V_{in} T_{in} + g \rho_w V_{in} \Delta H - c_w \rho_w V_s T_s}{L \rho_i}, \tag{7}$$

in the same notation as above. T_{in} and T_s are the temperature of the floodwater at the input location and at the glacier snout. ΔH is the elevation difference between the input location and the glacier snout. Finally, V_{in} and V_s are the volumes of water input into the system and exiting the system at the glacier snout. The first term in the numerator on the right-hand side of the equation is the available thermal energy due to the initial heat of the water, the second term is the available potential energy and the third term is the thermal energy remaining in the water at the glacier snout. The kinetic energy in the water flow at the glacier snout is neglected as it is small compared with the other terms. This volume estimate is an upper bound as the potential energy component corresponds to flow all the way from the input location to the outlet and the thermal energy corresponding to the deviation of the subglacial floodwater temperature from the freezing point upstream from the snout is included in the estimate of the available energy.

The distribution of this melt along the path depends on the potential gradient and on the heat transport from the flow into the ice walls. The empirical equation for heat transport in a subglacial tunnel presented by Nye (1976) as a part of his jökulhlaup theory has been shown to be inconsistent with the rapid heat flow observed in subglacial water flow (Björnsson, 1992, 2010; Jóhannesson, 2002; Clarke, 2003) and this was indeed the reason for Nye's use of the simplifying assumption of instantaneous heat

transfer in his application of the theory to the 1972 Grímsvötn jökulhlaup. Nye's (1976) assumption of instantaneous heat transfer, therefore, seems to hold better than the empirical equation presented in his theory (Jóhannesson, 2002). Further research on the thermodynamics of subglacial water flow (e.g. Jarosch and Zwinger, 2015) indicates that more appropriate empirical relations may be obtained by combining laboratory data experiments with numerical modelling of subglacial water flow.

3.4 Ice dynamics

Ice is considered to be a shear thinning material under normal deformation rates and stresses encountered in glaciers (Cuffey and Paterson, 2010). Ice deformation is therefore described by connecting deformation rate, $\dot{e}_{ij}$, with the corresponding deviatoric stress, $\tau_{ij} = \sigma_{ij} + p$, with σ_{ij} denoting stress and p, ice pressure, through Glen's (1955) flow law for ice,

$$\dot{e}_{ij} = A\tau^{n-1}\tau_{ij} \ , \ 2\tau^2 = \sum \tau_{ij}^2 \ . \tag{8}$$

The exponent, n, has been found to be close to 3 for most conditions in glaciers, but lower values between 1 and 3 might be possible or even likely for special conditions such as stresses lower than 100 kPa and impure basal ice (Cuffey and Paterson, 2010). Ice flow calculations in this thesis are therefore based on $n = 3$. A is a temperature-dependent creep parameter, here taken as $2.4{\cdot}10^{-24}\ \mathrm{s}^{-1}\ \mathrm{Pa}^{-3}$, which is the value recommended by Cuffey and Paterson (2010) for ice at 0°C. This value is selected as the Icelandic glaciers are all temperate (Björnsson and Pálsson, 2008).

Glacier flow is typically dominated by viscous deformation (Cuffey and Paterson, 2010), but elastic deformation of ice may also be important for special circumstances with rapid changes in the stress field in the ice. The relative importance of viscous and elastic deformation in a given situation may be assessed by the the Maxwell time:

$$\tau_M = \frac{\eta}{G} \ , \tag{9}$$

where η is the effective viscosity of the material and G the shear modulus (Melosh, 2011). Both viscous and elastic deformation are important on timescales close to the the Maxwell time, but elastic deformation dominates on shorter timescales and viscous deformation on longer scales (Melosh, 2011). The Maxwell time for Skaftárjökull before the arrival of the flood front is found in Paper I to be of the order of several hours, which is longer than the observed 30–120 min duration of lifting associated with the passage of a subglacial flood front during the two jökulhlaups in 2008. The Maxwell time for the deforming ice above the pressure wave is, on the other hand, found to be several minutes, considerably shorter than the observed duration of lifting. The Maxwell time thus indicates that the subglacial flood front propagates below glacier ice where elastic effects are initially dominant, before the deformation pattern of the flood front is established, but strain softening induced by the separation of the glacier from the bed eventually leads to dynamics that are dominated by viscous deformation.

Elastic deformation of the overlying ice is therefore important for the separation of the glacier from the bedrock during jökulhlaups. It is accounted for in Paper I by

considering lifting of a an elastic plate according Pollard and Fletcher (2005). Elastic deformation of a material is connected to the stress deviator, unlike fluid dynamics where the deformation *rate* is connected to the stress deviator. Further discussion of elastic deformation and its possible effects on the passage of the flood front during jökulhlaups, based on Tsai and Rice's (2010, 2012) analysis on subglacial, turbulent, hydraulic fracture propagation in a medium with small fracture toughness, can be found in the methods section of Paper I.

4 Summary of papers

4.1 Paper I: A spectrum of jökulhlaup dynamics revealed by GPS measurements of glacier surface motion

Einarsson B, Magnússon E, Roberts MJ, Pálsson F, Thorsteinsson Th and Jóhannesson T (2016), *Annals of Glaciology*, **57**, 47–61

This paper builds on observations from continuous GPS measurements of glacier motion during jökulhlaups. The measurements are from (i) three locations along the flood path of a rapidly rising jökulhlaup from western Skaftá cauldron in August 2008, (ii) two locations along the same flood path which also conveyed a rapidly rising jökulhlaup from the eastern Skaftá cauldron in October 2008 and from (iii) a location on the flood path of two slowly rising jökulhlaups from the subglacial lake Grímsvötn in 2004 and 2010, a different location in the two events (Fig. 1.1). The observations from the two rapidly rising jökulhlaups show propagation of a subglacial pressure wave with negative effective pressure (overburden pressure of the glacier minus subglacial water pressure) that causes lifting of the glacier. These results are shown to be consistent with elastic and viscous deformation of ice caused by the negative effective pressure and subglacial, turbulent, hydraulic fracture propagation in a medium with small fracture toughness. The jökulhlaups are found to be associated with temporally increased basal slip in all cases. The observed lifting and subglacial water storage larger than the volume melted due to friction in the slowly rising jökulhlaups are inconsistent with assumptions typically made in theoretical and numerical modelling of jökulhlaups. The results on slowly rising jökulhlaups corroborate Björnsson's (2010) statement that "*current models may reconstruct discharge curves while not describing all the factual hydraulic and glaciodynamic processes of each jökulhlaup*". Observations of lifting in slowly rising jökulhlaups and inferred propagation of a rapidly rising jökulhlaup along conduits enlarged by the conduit-melt–discharge feedback, associated with slowly rising jökulhlaups (Nye, 1976), indicate that jökulhlaups should not be classified into the separate categories of slowly and rapidly rising floods. Rather, we argue that jökulhlaups show a spectrum of behaviour instead of being classifiable into two distinct categories, although, the traditional categories remain useful in discussions of flood characteristics.

Candidate's contribution

B.E. contributed to the design of the study along with the coauthors. B.E. participated in field expeditions for the setup and maintenance of the GPS instruments on Skaftárjökull. B.E. interpreted the data from Skaftárjökull, estimated possible conduit growth during the Skaftá jökulhlaups and calculated dimensions and propagating velocity of the subglacial pressure waves. B.E. did the initial processing of the GPS data from Skaftárjökull but they were later run by E.M. through the same work flow as the GPS data from Skeiðarárjökull for consistency. B.E. estimated the magnitude of negative effective pressure in the propagating pressure wave and compared the results with expected viscous and elastic lifting. B.E. also compared observed propagating velocity and lifting to the analysis of Tsai and Rice (2010, 2012) of subglacial, turbulent, hydraulic fracture propagation in a medium with small fracture toughness. B.E. wrote the introduction; the Skaftá jökulhlaups part of the study site description, the instrumentation and data-processing sections; the sections on analysis of conduit growth, and sheet-like water flow and propagation of a subglacial pressure wave; the results sections on observations of jökulhlaups from the Skaftá cauldrons and interpretation of observations of the Skaftá jökulhlaups; the discussion section and conclusions.

4.2 Paper II: Subglacial flood path development during a rapidly rising jökulhlaup from the western Skaftá cauldron, Vatnajökull, Iceland

Einarsson B, Jóhannesson T, Thorsteinsson Th, Gaidos E and Zwinger T (2017), *Journal of Glaciology*, **63**(240), 670–682

The main theme of this paper is, as for Paper I, the hydraulics of jökulhlaups and their interaction with the glacier. The study is based on data from a jökulhlaup from the western Skaftá cauldron in September/October 2006. Compared with Paper I, the focus is more on the ongoing processes in and around the subglacial lake in this study. The outflow from the lake is estimated from measurements of the lowering of the overlying ice shelf during the jökulhlaup and an estimation of the relationship between water volume in the subglacial lake and the ice shelf elevation. The volume–ice-shelf elevation relationship was deduced by modelling the emptying of a cylindrically symmetric subglacial lake with the full-Stokes ice-dynamic model Elmer/Ice. The modelling and comparison of DEMs of the cauldron at an empty and a full stage furthermore provide results on the geometry of the subglacial lake and the dynamics of the ice shelf during lowering. The results on the ice shelf dynamics are shown to be consistent with the results of the analytical cauldron subsidence model of Evatt and Fowler (2007).

The estimated outflow from the subglacial lake and measurements of proglacial discharge are used to determine the volume of water stored in the subglacial flow path, which is found to be $\sim$10 times larger than could be melted due to friction in the flow and initial heat of the floodwater. These results indicate that the initial flood path of this jökulhlaup is formed by mechanical processes such as lifting of the ice, hydraulic

fracturing as well as viscous and elastic deformation induced by water pressure higher than overburden pressure, as for the rapidly rising jökulhlaups presented in Paper I. The observations, therefore, imply that such floods can be explained by a coupled subglacial sheet–conduit mechanism where essentially all of the initial flood path is formed as a sheet by the propagation of a subglacial pressure wave. Analysis on the ice volume that can be melted by the initial heat of the floodwater, elongated surface depression formed over the uppermost part of the flood path and evidence of rapid heat transfer in jökulhlaups indicate that the subglacial pressure wave might be formed a few kilometres downstream of the lake but not at the beginning of the subglacial flood path. The first few kilometres of the flood path would then be formed mainly by melting due to rapid release of the initial heat of the floodwater. Rapidly and slowly rising jökulhlaups are, furthermore, discussed in the context of prehistoric jökulhlaups and proper assumptions for modelling of such past events, which are commonly assumed to be of the slowly rising type.

Candidate's contribution

This paper is partly built on the MS study of B.E. in 2009, under the supervision of T.J. B.E. reworked the design of the study together with T.J. Part of the material made by B.E. during the MS study is used in the paper such as: estimates for the travel speed of the subglacial flood front, temperature measurements in Skaftá during the jökulhlaup, and calculation of energy available for melt and resulting volumes of melted ice. As part of the MS study, B.E. participated in drilling expeditions to the western and eastern Skaftá cauldrons.

A new DEM of western Vatnajökull made with airborne lidar in July 2010 made it possible to improve the estimates of outflow from the western Skaftá cauldron during the jökulhlaup in September/October 2006, studied in the MS thesis. The study of this jökulhlaup was therefore repeated with refined methodology. Moreover, the focus was changed from modelling the jökulhlaup to modelling the geometry of the subglacial lake when the ice shelf is lowered as the lake is drained. Better estimates of outflow and new findings from Paper I also allowed further interpretation of the processes taking place during the formation of the subglacial flood path. The approach and the material of this paper is therefore substantially different from the MS thesis, and the paper contains a number of new findings.

The following tasks were performed as part of the PhD study. B.E. made the difference map used to estimate the shape of the subglacial lake. B.E. adopted an Elmer/Ice setup of cylindrically symmetric subglacial lake with variable lake volume, made by T.J. and T.Z., to the geometry of the western cauldron and magnitudes of jökulhlaups from there. B.E. furthermore ran the model, interpreted results and made comparisons to an analytic model of cauldron subsidence. B.E. recalculated floodwater outflow from the cauldron and estimated the transient volume of subglacial floodwater. B.E. participated in a field expedition in 2015 for further flood-water temperature measurements. B.E. wrote the first version of the manuscript.

4.3 Paper III: Hydrology and dynamics of two Icelandic outlet glaciers revealed by discharge and GPS measurements

Einarsson B and Jóhannesson T (2018), *To be submitted to the Journal of Glaciology.*

This paper focuses on the subglacial hydraulics of broad and gently sloping ice cap outlets and hydrologically induced forcing on basal slip. The study is based on (i) data from the three GPS stations on Skaftárjökull, which were set up for jökulhlaup research but provided months of observations under normal conditions, (ii) data from the continuous GPS measurements on Sátujökull and (iii) discharge time series from Austari-Jökulsá and Skaftá (Fig. 1.1). Melt on Skaftárjökull and Sátujökull is estimated with degree–day modelling, calibrated with 27 years of mass balance data from 14 stakes on Sátujökull. Estimates of longitudinal stress-gradient coupling lengths, based on the analysis of Kamb and Echelmeyer (1986), are used to estimate how far up- and down-glacier changes in basal drag will affect the glacier flow at each of the GPS instrument sites. Observed energy balance from an automatic weather station on Tungnaárjökull, provided by the Glaciology group at the Institute of Earth Sciences, University of Iceland, was also used for data interpretation.

These data show motion events of increased velocity (i) during the early melt season, (ii) contemporaneous with events of increased surface melt or rain and (iii) during the emptying of supraglacial slush ponds. They also show events of slower movement than late winter velocities prior to early-melt-season motion events and in the wake of motion events during the height of the melt season. The formation of an efficient, fast subglacial hydraulic system during the melt season is deduced from the observed energy balance on Tungnaárjökull, the diurnal variations in discharge in Skaftá and lack of response to certain runoff pulses. The effects of the passing of a jökulhlaup and high groundwater flow on the development of the subglacial hydraulic system are also discussed in the paper.

Candidate's contribution

B.E. designed the study together with T.J. B.E. participated in mass balance field expeditions on Hofsjökull, setup and maintenance of the GPS instruments on Skaftárjökull and discharge measurements and maintenance of the hydrometric stations at Austurbugur and Sveinstindur. As part of the PhD work, B.E. was responsible for the setup and operations of the GPS instruments on Sátujökull. B.E. set up runoff modelling and optimized model parameters. B.E. estimated longitudinal stress-gradient coupling lengths, runoff from the areas affecting each GPS site, snow line elevation, highest elevation of melt at each time and made order-of-magnitude estimates for groundwater flow. B.E. furthermore processed the GPS data and calculated daily mean velocities. B.E. extracted information on diurnal variations from the discharge data. B.E. identified motion and runoff events and interpreted them. B.E. inspected available satellite images for identification of slush pond drainage. B.E. wrote the first version of the manuscript.

5 Discussion

5.1 Glacial hydrology and glacier dynamics

Subglacial hydrology and its effect on glacier dynamics is a common theme of the three papers. The conclusion from Papers I and III is that water input exceeding the transport capacity of the subglacial hydraulic system reduces basal friction and causes increased basal slip. This holds independently of the water source as this is observed for (i) jökulhlaups, (ii) sharp increases in runoff due to melt or rain, (iii) the onset of melt in spring and (iv) the emptying of supraglacial slush ponds. The system is then observed to adjust to increased inflow, most likely by greater connectivity and volumetric capacity of cavities and the formation of an efficient fast-responding conduit network. These results are in agreement with previous studies on the connection between the hydrology of glaciers and their motion for situations different from those studied in this thesis (Iken and Bindschadler, 1986; Hooke and others, 1989; Jansson, 1995; Raymond and others, 1995; Iken and Truffer, 1997; Nienow and others, 1998, 2005; Mair and others, 2001, 2002a, 2002b; Zwally and others, 2002; Harper and others, 2005; Swift and others, 2005; Rignot and Kanagaratnam, 2006; Bartholomaus and others, 2008, 2011; Bell, 2008; Fudge and others, 2009; Bartholomew and others, 2010, 2011, 2012; Schoof, 2010; Doyle and others, 2015).

The extreme situations encountered during jökulhlaups, as presented in Papers I and II, create signals that are easily detectable with measurements due to the large signal-to-noise ratio. The observed lifting of the glacier during jökulhlaups in Skaftá, on the order of 0.1–1 m, described in Paper I, is, for example, well above the uncertainty range of the GPS measurements. This makes detection and identification of the ongoing processes easier than under the less extreme conditions studied in Paper III, where the magnitude of the lifting due to increased water input into the subglacial hydraulic system at the start of the melt season is less than the detection limit of the GPS measurements.

The transferability of processes and their importance, from extreme to normal conditions, must be kept in mind when drawing general conclusions about the hydraulic system of glaciers from observations of jökulhlaups. The importance of some processes can for example be controlled by a threshold value, such as for lifting, which does not play any role in subglacial hydraulics for water pressure lower than overburden but can suddenly become important when the effective pressure becomes negative. Based on a number of observations of lifting under less extreme conditions than in jökulhlaups (Iken and others, 1983; Mair and others, 2002a; Bartholomew and others, 2010; Magnússon and others, 2011) and the jökulhlaup results from Papers I and II, it seems to be necessary that lifting and the associated ice-dynamic processes are accounted for in models of the time-dependent evolution of the drainage system, as

done for example by Flowers and others (2004), Pimentel and Flowers (2011), Hewitt and others (2012) and Schoof and others (2012).

Based on these observations it seems that a special flow element that conceptually describes sheet-like flow formed by lifting and deformation caused by subglacial water pressure higher than overburden should be included in models of subglacial hydrology (see Flowers (2015) for further discussion on flow elements in subglacial hydrological modelling). Elements like this would differ, in at least the opening mechanism, from the sheet-like elements often used in modelling subglacial hydraulics, to represent average effects of interlinked cavities. Sheet-like flow might be important under conditions where the discharge capacity of the subglacial hydraulic system is exceeded and negative effective pressure arises. Such conditions appears to be common on broad and gently sloping temperate ice-cap outlets according to the results presented in Paper III. The dynamic response of the glacier caused by hydrologically induced changes in basal slip is also largest under such conditions, according to the results presented in Papers I and III.

5.2 Characteristics of jökulhlaups

In this thesis and the associated papers, we follow the convention in classifying jökulhlaups as rapidly or slowly rising based upon the rate of discharge increase during the rising phase of the flood. This is in accordance with Björnsson (2002) and Jóhannesson (2002). Other naming conventions such as linearly vs exponentially rising jökulhlaups have been used by other authors (Russell and others, 2005). In Paper I it is concluded that classification into two distinct categories of this type is too simple. Jökulhlaup behaviour appears to be more of a spectrum. Phenomena associated with rapidly rising jökulhlaups, such as lifting due to water pressure higher than overburden, are seen in slowly rising jökulhlaups, and phenomena associated with slowly rising jökulhlaups, such as flood paths formed by conduit-melt–discharge feedback, are seen in rapidly rising jökulhlaups.

The possibility of a rapid discharge increase during the later stages of large slowly rising jökulhlaups makes it hard to use the rate of discharge increase directly as a parameter to categorize jökulhlaups as done by Roberts (2005). That can lead to large slowly rising jökulhlaups being categorized as rapidly rising. The rate of discharge increase, scaled by the maximum discharge of the flood, might be a better parameter for categorization. Jökulhlaups can also be categorized according to whether their onset is abrupt or they start slowly with a gradually increasing discharge. The characteristic convex, approximately exponential, form of the discharge curve (caused by flood control by conduit-melt–discharge feedback (Nye, 1976)) is also a distinct feature of slowly rising jökulhlaups.

5.3 Rapidly rising jökulhlaups

As rapidly rising jökulhlaups have a fast discharge increase, they may be extremely dangerous since warning times for response are short. Results from Papers I and II on the subglacial propagation of the initial flood front in such floods are therefore discussed here in a special subsection. A few main results on slowly rising jökulhlaups are also discussed. Our observations from both slowly and rapidly rising jökulhlaups are in fact important for all jökulhlaup studies, as one of the conclusions from Paper I is that jökulhlaup behaviour appears to be more of a spectrum rather than two distinct categories of slowly and rapidly rising floods.

Jóhannesson (2002) described a propagating subglacial pressure wave, with water pressure higher than the overburden pressure of the glacier, as the mechanism for initial flood path creation in the rapidly rising jökulhlaup from Grímsvötn in October 1996. The observed surface lifting and subsequent lowering that propagates down Skaftárjökull during the initiation of two rapidly rising jökulhlaups from the Skaftá cauldrons in 2008, presented in Paper I, confirms the existence of such propagating subglacial pressure waves. The results presented in Paper II on the formation of the initial flood path by lifting and ice deformation in a small jökulhlaup from the western Skaftá cauldron in 2006 are also consistent with flood path formation by a propagating subglacial pressure wave. These results indicate that such pressure waves, forming a subglacial flood path by mechanical processes such as hydraulic fracturing, lifting of the ice and elastic and viscous deformation induced by water pressure higher than the ice overburden pressure, are intrinsic to rapidly rising jökulhlaups in general.

A jökulhlaup will become slowly rising if its drainage is constrained by the conduit-melt–discharge feedback (Nye, 1976) at a bottleneck somewhere along the flood path (Clarke, 1982). Whether all such bottlenecks are eliminated early in the flood might determine whether a jökulhlaup develops as a slowly or rapidly rising flood. A number of processes can eliminate such potential bottlenecks. The initial heat content available in the source lake can speed up conduit melting at a possible bottleneck close to the source lake as discussed in Paper II. Effective breaching of the ice dam at the edge of the source lake by flotation and dam lifting may facilitate flood path formation if outflow from the source lake would otherwise have been a limiting factor (Sugiyama and others, 2008; Björnsson, 2010). A propagating subglacial pressure wave as discussed in Papers I and II can also eliminate potential bottlenecks along the flood path because a sheet-like water flow formed in the wave and in its wake can act as a source for the growth of a nascent system of conduits (Flowers and others 2004), and can itself form an efficient flood path.

A delicate balance is required for a slowly rising jökulhlaup to develop by a positive feedback between water discharge and ice melting in a subglacial flood confined within a conduit along the whole distance from the source lake to the glacier terminus. The water pressure in the conduit, which is assumed to lie along the glacier bed, must remain below the ice overburden pressure at all locations as negative effective pressure would cause the glacier to be lifted from the bed and the floodwater would flow out of the conduit. However, longitudinal variations in the conduit dimensions arising from variations in floodwater temperature and in the frictional release of heat, will under many circumstances lead to water pressure that exceeds the local ice overburden

pressure, particularly in areas where the ice surface topography is concave in the direction of the flood path or if the source water temperature is above the pressure melting point. Measurements of subglacial water accumulation and glacier lifting in the 2004 and 2010 jökulhlaups from Grímsvötn, presented in Paper I, show that these conditions do arise in some slowly rising jökulhlaups. This situation often also arises in numerical simulations based on Nye's (1976) jökulhlaup theory, and then a rather arbitrary specification of the conduit development must be made as the theory is not valid for negative effective pressures. Both Clarke (2003) and Spring and Hutter (1981) assume that ice deformation leads to conduit enlargement without water escaping from the conduit when water pressure exceeds ice overburden pressure. There is, however, no physical justification for conduit enlargement through Nye's (1953) tunnel closure formula, which is used in the theory because the conduit is not sealed off from the surrounding of the base which is at a lower pressure. More appropriately, mechanical processes such as hydraulic fracturing and lifting due to subglacial water pressure higher than the ice overburden should be incorporated in modelling slowly rising jökulhlaups, as is also essential in modelling rapidly rising jökulhlaups, contrary to what is often done (Spring and Hutter, 1981; Fowler, 1999; Clarke, 2003; Kingslake, 2015).

The formation of part of the flood path by lifting in slowly rising jökulhlaups (Paper I) implies that the flood is constrained by conduit-melt–discharge feedback at some bottlenecks in between such areas. The hydraulic gradient over such limiting bottlenecks may deviate substantially from the mean gradient over the whole flood path. That complicates the calibration of friction coefficients from the mean hydraulic gradient as has often been done. Friction parameters (Manning's n and Darcy's f) are then fundamentally empirical parameters in a statistical relationship rather then physical parameters describing the roughness of the subglacial conduit. The high values of friction parameters obtained in calibrating jökulhlaup models (Nye, 1976; Spring and Hutter, 1982) might perhaps be caused by such deviations of the mean potential gradient from the actual potential gradient over bottlenecks restricting the flow. These high values therefore do not have a physical meaning and should not be used in jökulhlaup calculations where the hydrographs are unknown, such as for prehistoric floods. Modelling using more realistic, lower roughness values alone as done by Clarke (2003) is, however, not sufficient to produce a realistic description of those floods because glacier lifting is ignored in the modelling despite modelled water pressure higher than overburden and the heat transfer is too slow, resulting in unrealistic conduit growth and output temperature higher than indicated by observations. Theoretical studies of the palaeohydraulics of jökulhlaups from Lake Missoula, Montana, USA, (Clarke and others, 1984), and Lake Agassiz, North America (Clarke and others, 2004), are furthermore based on the assumption that these floods were of the slowly rising type and controlled by the melt–discharge feedback in a conduit. The discussion in Paper II shows that they could just as well have been on the rapidly rising side of the jökulhlaup spectrum, which would result in different quantitative conclusions, regarding e.g. flood duration and maximum discharge.

6 Conclusions

It is essential to work from a solid foundation when predicting the future fate of glaciers – never more so than now, when we know that we don't know the future, as it is not what it used to be, due to the anthropogenic effects on climate. We should seek to avoid unknown unknowns by working with the known knowns, which are physics and understanding of fundamental processes. The relative importance of each process and the combined effect of different processes ongoing in the hydrology of a glacier, and its interaction with their dynamics, can change. The present will, however, be the key to the future as it was the key to the past since physics and fundamental processes remain the same. Phenomenological and quantitative descriptions of processes, based on observations of the present hydrology and dynamics of glaciers under both normal and extreme conditions as presented in this thesis, are therefore especially important at this point in time.

The effect of runoff changes on the dynamics of glaciers and possible feedbacks of the dynamics on runoff are important for future projections of sea-level changes caused by glacier melting on Earth (Chu, 2014). Empirical relationships and ad hoc solutions should preferably be avoided in descriptions of the relationship between hydrology and sliding for such predictions, as we might be moving out of their valid range. This is currently unrealistically ambitious, but such empirical relationships and ad hoc solutions might be validated for the wide range of hydrological conditions encountered in extreme events such as jökulhlaups. It is also important to validate such solutions on different scales as for example on the broad and gently sloping Icelandic ice cap outlets. They fill an intermediate gap in the scale of glacier sizes as they are thicker and larger than most alpine valley glaciers but smaller and thinner than most outlets of the Greenland ice sheet. The results and interpretations presented in this thesis are of value for such comparison and calibration of models. Another valuable result is confirmation, by observations, of the existence of propagating subglacial pressure waves. Such waves might be much more common during jökulhlaup events of all magnitudes than previously thought and should be accounted for in all studies and modelling of rapidly rising jökulhlaups. Propagating pressure signals and lifting of the glacier might also be more important than hitherto believed in other circumstances than jökulhlaups when water input to the subglacial hydrological system varies rapidly.

References

Árnason B, Björnsson H and Theodórsson P (1974) Mechanical drill for deep coring in temperate ice. *Journal of Glaciology*, **13**(67), 133–139 (doi:10.3189/S0022143-000023443)

Bartholomaus TC, Anderson RS and Anderson SP (2008) Response of glacier basal motion to transient water storage. *Nature Geoscience*, **1**(1), 33–37 (doi: 10.1038/-ngeo.2007.52)

Bartholomaus TC, Anderson RS and Anderson SP (2011) Growth and collapse of the distributed subglacial hydrologic system of Kennicott Glacier, Alaska, USA, and its effects on basal motion. *Journal of Glaciology*, **57**(206), 985–1002 (doi: 10.3189/002214311798843269)

Bartholomew ID, Nienow P, Mair D, Hubbard A, King MA and Sole A (2010) Seasonal evolution of subglacial drainage and acceleration in a Greenland outlet glacier. *Nature Geoscience*, **3**, 408–411

Bartholomew ID, Nienow P, Sole A, Mair D, Cowton T, King MA and Palmer S (2011) Seasonal variations in Greenland ice sheet motion: inland extent and behaviour at higher elevations. *Earth and Planetary Science Letters*, **307**, 271–278

Bartholomew ID, Nienow P, Sole A, Mair D, Cowton T and King MA (2012) Short-term variability in Greenland ice sheet motion forced by time-varying meltwater drainage: implications for the relationship between subglacial drainage system behavior and ice velocity. *Journal of Geophysical Research*, **117**, F03002 (doi:10.1029/2011JF002220)

Bell RE (2008) The role of subglacial water in ice-sheet mass balance. *Nature Geoscience*, **1**(5), 297–304 (doi:10.1038/ngeo186)

Björnsson H (1974) Explanation of jökulhlaups from Grímsvötn, Vatnajökull, Iceland. *Jökull*, **24**, 1–26

Björnsson H (1975) Subglacial water reservoirs, jökulhlaups and volcanic eruption. *Jökull*, **25**, 1–11

Björnsson H (1988) *Hydrology of ice caps in volcanic regions.* Societas Scientarium Islandica, University of Iceland, Reykjavík, Iceland

Björnsson H (1992) Jökulhlaups in Iceland: prediction, characteristics and simulation. *Annals of Glaciology*, **16**, 95–106

Björnsson H (1998) Hydrological characteristics of the drainage system beneath a surging glacier. *Nature*, **395**, 771–774 (doi:10.1038/27384)

Björnsson H (2002) Subglacial lakes and jökulhlaups in Iceland. *Global and Planetary Change*, **35**, 255–271 (doi:10.1016/S0921-8181(02)00130-3)

Björnsson H (2010) Understanding jökulhlaups: from tale to theory. *Journal of Glaciology*, **56**(200), 1002–1010 (doi: 10.3189/002214311796406086)

Björnsson H (2017) *The glaciers of Iceland. A historical, cultural and scientific overview*. Atlantis Press. (doi:10.2991/978-94-6239-207-6)
Björnsson H, Pálsson F, Sigurðsson O and Flowers GE (2003) Surges of glaciers in Iceland. *Annals of Glaciology*, **36**, 82–90 (doi:10.3189/172756403781816365)
Björnsson H and Pálsson F (2008) Icelandic glaciers. *Jökull*, **58**, 365–386
Björnsson H, Pálsson F, Guðmundsson S, Magnússon E, Aðalgeirsdóttir G, Jóhannesson T, Sigurðsson O, Thorsteinsson Th and Berthier E (2013) Contribution of Icelandic ice caps to sea level rise: trends and variability since the Little Ice Age. *Geophysical Research Letters*, **40**, 1,546–1,550 (http://doi.wiley.com/10.1002/grl.50278)
Chu VW (2014) Greenland ice sheet hydrology: a review. *Progress in Physical Geography* **38**(1) 19–54 (doi:10.1177/0309133313507075)
Clarke GKC (1982) Glacier outburst floods from "Hazard Lake", Yukon Territory, and the problem of flood magnitude prediction. *Journal of Glaciology*, **28**(98), 3–21
Clarke GKC (2003) Hydraulics of subglacial outburst floods: new insights from the Spring–Hutter formulation. *Journal of Glaciology*, **49**(165), 299–313 (doi: 10.3189/-172756503781830728)
Clarke GKC, Mathews WH and Pack RT (1984) Outburst floods from glacial Lake Missoula. *Quaternary Research*, **22**(3), 289–299
Clarke GKC, Leverington DW, Teller JT and Dyke AS (2004) Paleohydraulics of the last outburst flood from glacial Lake Agassiz and the 8200 BP cold event. *Quaternary Science Reviews*, **23**, 389–407 (doi:10.1016/j.quascirev.2003.06.004)
Creyts TT and Schoof CG (2009) Drainage through subglacial water sheets. *Journal of Geophysical Research*, **114**, F04008 (doi:10.1029/2008JF001215)
Crochet P (2013) Sensitivity of Icelandic river basins to recent climate variations. *Jökull*, **63**, 71–90
Crochet P, Jóhannesson T, Jónsson T, Sigurðsson O, Björnsson H, Pálsson F and Barstad I (2007) Estimating the spatial distribution of precipitation in Iceland using a linear model of orographic precipitation. *Journal of Hydrometeorology*, **8**, 1,285–1,306
Cuffey KM and Paterson WSB (2010) *The physics of glaciers. Fourth edition.* Oxford, Elsevier
Doyle SH, Hubbard A, Van de Wal RSW, Box JE, Van As D, Scharrer K, Meierbachtol TW, Smeets PCJP, Harper JT, Johansson E, Mottram RH, Mikkelsen AB, Wilhelms F, Patton H, Christoffersen P and Hubbard B (2015) Amplified melt and flow of the Greenland ice sheet driven by late-summer cyclonic rainfall. *Nature Geoscience*, **8**, 647–653 (doi:10.1038/ngeo2482)
Einarsson B (2009) *Jökulhlaups in Skaftá: a study of a jökulhlaup from the Western Skaftá cauldron in the Vatnajökull ice cap, Iceland*. MS thesis, University of Iceland, also available as technical report VI 2009-006 from the Icelandic Meteorological Office
Einarsson B (2012) *Available discharge time-series from glacier-covered catchments in Iceland.* Reykjavík, Icelandic Meteorological Office, Technical Report BE/2012-01
Einarsson B and Jónsson S (2010) *The effect of climate change on runoff from two watersheds in Iceland.* Reykjavík, Icelandic Meteorological Office, Report 2010-16
Evatt GW and Fowler AC (2007) Cauldron subsidence and subglacial floods. *Annals of Glaciology*, **45**, 163–168 (doi:10.3189/172756407782282561)
Flowers GE (2015) Modelling water flow under glaciers and ice sheets. *Proceedings*

of the Royal Society London A: Mathematical, Physical Engineering Sciences, **471**(2176) (doi:10.1098/rspa.2014.0907)

Flowers GE, Björnsson H and Pálsson F (2003) New insights into the subglacial and periglacial hydrology of Vatnajökull, Iceland, from a distributed physical model. *Journal of Glaciology*, **49**(165), 257–270 (doi:10.3189/172756503781830827)

Flowers GE, Björnsson H, Pálsson F and Clarke GKC (2004) A coupled sheet–conduit mechanism for jökulhlaup propagation. *Geophysical Research Letters*, **31**(5), L05401 (doi:10.1029/2003GL019088)

Flowers GE, Marshall SJ, Björnsson H and Clarke GKC (2005) Sensitivity of Vatnajökull ice cap hydrology and dynamics to climate warming over the next 2 centuries. *Journal of Geophysical Research*, **110**, F02011 (doi:10.1029/2004JF000200)

Fountain AG (1996) Effect of snow and firn hydrology on the physical and chemical characteristics of glacial runoff. *Hydrological Processes*, **10**, 509–521

Fountain AG and Walder JS (1998) Water flow through temperate glaciers. *Reviews of Geophysics*, **36**(3), 299–328

Fountain AG, Schlichting RB, Jansson P and Jacobel RW (2005) Observations of englacial water passages: a fracture-dominated system. *Annal of Glaciology*, **40**, 25–30

Fowler AC (1999) Breaking the seal at Grímsvötn, Iceland. *Journal of Glaciology*, **45**(151), 506–516

Fudge TJ, Harper JT, Humphrey NF and Pfeffer WT (2009) Rapid glacier sliding, reverse ice motion and subglacial water pressure during an autumn rainstorm. *Annals of Glaciology*, **50**(52), 101–108

Gagliardini O, Zwinger T, Gillet-Chaulet F, Durand G, Favier L, De Fleurian B, Greve R, Malinen M, Martín C, Råback P, Ruokolainen J, Sacchettini M, Schäfer M, Seddik H and Thies J (2013) Capabilities and performance of Elmer/Ice, a new-generation ice sheet model. *Geoscientific Model Development*, **6**(4), 1299–1318

Gaidos E, Glazer B, Harris D, Heshiki Z, Jeppsson N, Miller M, Thorsteinsson Th, Bergur E, Kjartansson V, Stefansson A, Quinn de Camargo LG, Johannesson T, Roberts MJ, Skidmore M and Lanoil B (2007) A simple sampler for subglacial water bodies. *Journal of Glaciology*, **53**(180), 157–158 (doi:10.3189/1727565077-81833820)

Gaidos E, Marteinsson V, Thorsteinsson Th, Jóhannesson T, Rafnsson AR, Stefánsson A, Glazer B, Lanoil B, Skidmore M, Han S, Miller M, Rusch A and Foo W (2009) An oligarchic microbial assemblage in the anoxic bottom waters of a volcanic subglacial lake. *The International Society for Microbial Ecology Journal*, **3**, 486–497 (doi:10.1038/ismej.2008.124)

Glen JW (1955) The creep of polycrystalline ice. *Proceedings of the Royal Society London A: Mathematical, Physical Engineering Sciences*, **228**(1175), 519–538 (doi:10.1098/rspa.1955.0066)

Harper JT, Humphrey NF, Pfeffer WT, Fudge T and O'Neel S (2005) Evolution of subglacial water pressure along a glacier's length. *Annals of Glaciology*, **40**, 31–36

Herring TA, King RW and McClusky SC (2010) *Introduction to GAMIT/GLOBK. Release 10.4.* Massachusetts Institute of Technology, Cambridge, MA. `www-gpsg.mit.edu/~simon/gtgk`

Hewitt IJ, Schoof C and Werder MA (2012) Flotation and open water flow in a model

for subglacial drainage. Part II: Channel flow. *Journal of Fluid Mechanics*, **702**, 157–187 (doi:10.1017/jfm.2012.166)

Hooke RLeB, Calla P, Holmlund P, Nilsson M and Stroeven A (1989) A 3 year record of seasonal variations in surface velocity, Storglaciären, Sweden. *Journal of Glaciology*, **35**(120), 235–247

Icelandic Meteorological Office (2017a) *Rennslisskýrsla vatnsárið 2015/2016, V228, Austari-Jökulsá, Austurbugur [Discharge report for the water year 2015/2016, V299, Austari-Jökulsá; Austurbugur].* Reykjavík, Icelandic Meteorological Office [In Icelandic]

Icelandic Meteorological Office (2017b) *Rennslisskýrsla vatnsárið 2015/2016, V299, Skaftá; Sveinstindur [Discharge report for the water year 2015/2016, V299, Skaftá; Sveinstindur].* Reykjavík, Icelandic Meteorological Office [In Icelandic]

Iken A, Röthlisberger H, Flotron A and Haeberli W (1983) The uplift of Unteraargletscher at the beginning of the melt season – a consequence of water storage at the bed? *Journal of Glaciology*, **29**(101), 28–47

Iken A and Bindschadler RA (1986) Combined measurements of subglacial water pressure and surface velocity of Findelengletscher, Switzerland: conclusions about drainage system and sliding mechanism. *Journal of Glaciology*, **32**(110), 101–119

Iken A and Truffer M (1997) The relationship between subglacial water pressure and velocity of Findelengletscher, Switzerland, during its advance and retreat. *Journal of Glaciology*, **43**(144), 328–338

Jansson P (1995) Water pressure and basal sliding on Storglaciären, northern Sweden. *Journal of Glaciology*, **41**(138), 232–240

Jarosch AH and Zwinger T (2015) *Explicit numerical modeling of heat transfer in glacial channels.* American Geophysical Union, Fall Meeting 2015, abstract #C54B-05

Jóhannesson T (2002) Propagation of a subglacial flood wave during the initiation of a jökulhlaup. *Hydrological Sciences Journal*, **47**(3), 417–434

Jóhannesson T, Aðalgeirsdóttir G, Björnsson H, Crochet P, Elíasson, EB, Guðmundsson S, Jónsdóttir JF, Ólafsson H, Pálsson F, Rögnvaldsson Ó, Sigurðsson O, Snorrason Á, Blöndal Sveinsson ÓG and Thorsteinsson Th (2007). *Effect of climate change on hydrology and hydro-resources in Iceland.* Reykjavík, National Energy Authority – Hydrological Service, Report OS-2007/011

Jónsdóttir JF (2008) A runoff map based on numerically simulated precipitation and a projection of future runoff in Iceland. *Hydrological Sciences Journal*, **53**(1), 100–111

Jónsdóttir JF, Kristjánsdóttir GB and Zóphóníasson S (2001) *Skaftá við Sveinstind, vhm 166 Rennslislykill nr. 5 [Skaftá by Sveinstindur, vhm 166 Discharge water elevation relationship number 5].* National Energy Authority, Reykjavík, Report OS-2001/001

Jónsson T (1991) Ný meðaltöl veðurþátta, 1961–1990 [New averages of temperature, precipitation, wind speed, and sunshine in Iceland, 1961–1990]. *Jökull*, **41**, 81–87 [In Icelandic]

Kamb B (1987) Glacier surge mechanism based on linked cavity configuration of the basal water conduit system. *Journal of Geophysical Research*, **B92**, 9083–9100

Kamb B and Echelmeyer K (1986) Stress coupling in glacier flow: I. Longitudinal averaging of the influence of ice thickness and surface slope. *Journal of Glaciology*,

31(111), 267–284

Kingslake J (2015) Chaotic dynamics of a glaciohydraulic model. *Journal of Glaciology*, **61**(227), 493–502 (doi: 10.3189/2015JoG14J208)

Magnússon E, Björnsson H, Pálsson F and Dall J (2004) Glaciological application of InSAR topography data of western Vatnajökull acquired in 1998. *Jökull*, **54**, 17–36

Magnússon E, Rott H, Björnsson H and Pálsson F (2007) The impact of jökulhlaups on basal sliding observed by SAR interferometry on Vatnajökull, Iceland. *Journal of Glaciology*, **53**(181), 232–240 (doi:10.3189/172756507782202810)

Magnússon E, Björnsson H, Rott H and Pálsson F (2010) Reduced glacier sliding caused by persistent drainage from a subglacial lake. *The Cryosphere*, **4**, 13–20

Magnússon E, Björnsson H, Rott H, Roberts MJ, Pálsson F, Guðmundsson S, Bennett RA, Geirsson H and Sturkell E (2011) Localized uplift of Vatnajökull, Iceland: subglacial water accumulation deduced from InSAR and GPS observations. *Journal of Glaciology*, **57**(203), 475–484 (doi:10.3189/002214311796905703)

Mair D, Nienow P, Willis I and Sharp M (2001) Spatial patterns of glacier motion during a high-velocity event: Haut Glacier d'Arolla, Switzerland. *Journal of Glaciology*, **47**(156), 9–20

Mair DWF, Sharp MJ and Willis IC (2002a) Evidence for basal cavity opening from analysis of surface uplift during a high-velocity event: Haut Glacier d'Arolla, Switzerland. *Journal of Glaciology*, **48**(161), 208–216

Mair D, Nienow P, Sharp M, Wohlleben T and Willis I (2002b) Influence of subglacial drainage system evolution on glacier surface motion: Haut Glacier d'Arolla, Switzerland. *Journal of Geophysical Research*, **107**(B8) (doi:10.1029/2001JB000514)

Melosh HJ (2011) *Planetary surface processes*, Cambridge, Cambridge University Press

Nienow PW, Sharp MJ and Willis IC (1998) Seasonal changes in the morphology of the subglacial drainage system, Haut Glacier d'Arolla, Switzerland. *Earth Surface Processes and Landforms*, **23**, 825–843

Nienow PW, Hubbard AL, Hubbard BP, Chandler DM, Mair DWF, Sharp MJ and Willis IC (2005) Hydrological controls on diurnal ice flow variability in valley glaciers. *Journal of Geophysical Research*, **110**, F04002 (doi:10.1029/2003JF000112)

Nye JF (1953) The flow law of ice from measurements in glacier tunnels, laboratory experiments and the Jungfraufirn borehole experiment. *Proceedings of the Royal Society London A: Mathematical, Physical Engineering Sciences*, **219**(1139), 477–489

Nye JF (1973) Water at the bed of a glacier, in Glen J and Adie RJD eds., *Symposium on the Hydrology of Glaciers*, International Association of Scientific Hydrology, 189–194

Nye JF (1976) Water flow in glaciers: jökulhlaups, tunnels and veins. *Journal of Glaciology*, **17**(76), 181–207

Pimentel S and Flowers GE (2011) A numerical study of hydrologically driven glacier dynamics and subglacial flooding. *Proceedings of the Royal Society London A: Mathematical, Physical Engineering Sciences*, **467**, 537–558 (doi:10.1098/rspa.-2010.0211)

Pollard DD and Fletcher RC (2005) *Fundamentals of structural geology.* Cambridge, Cambridge University Press

Radić V and Hock R (2014) Glaciers in the Earth's hydrological cycle: assessments of glacier mass and runoff changes on global and regional scales. *Surveys in Geophysics*, **35**(3), 813–837 (doi:10.1007/s10712-013-9262-y)

Raymond CF, Benedict RJ, Harrison WD, Echelmeyer KA and Strum M (1995) Hydrological discharges and motion of Fels and Black Rapids Glaciers, Alaska, U.S.A.: implications for the structure of their drainage systems. *Journal of Glaciology*, **41**(138), 290–304

Rignot E and Kanagaratnam P (2006) Changes in the velocity structure of the Greenland Ice Sheet. *Science*, **311**(5763), 986–990 (doi:1126/science.1121381)

Rist S (1990) *Vatns er þörf [Water is a necessity].* Reykjavík, Bókaútgáfa Menningarsjóðs, 248 pp [In Icelandic]

Roberts MJ (2005) Jökulhlaups: a reassessment of floodwater flow through glaciers *Reviews of Geophysics*, **43**, RG1002 (doi:10.1029/ 2003RG000147)

Röthlisberger H (1972) Water pressure in intra- and subglacial channels. *Journal of Glaciology*, **11**(62), 177–203

Russell AJ, Fay H, Marren PM, Tweed FS and Knudsen Ó (2005) Icelandic jökulhlaup impacts, in Caseldine C ed., *Iceland: modern processes and past environments.* London, Elsevier, 153–203

Schoof C (2010) Ice-sheet acceleration driven by melt supply variability. *Nature*, **468** (doi:10.1038/nature09618)

Schoof C, Hewitt IJ and Werder MA (2012) Flotation and open water flow in a model for subglacial drainage. Part I: Linked cavities. *Journal of Fluid Mechanics*, **702**, 126–156 (doi:10.1017/jfm.2012.165)

Sigurðsson F (1990) Groundwater from glacial areas in Iceland. *Jökull*, **40**, 119–146

Sigurðsson O and Einarsson B (2005) *Jökulhlaupaannáll 1989–2004 [Catalogue of jökulhlaups in Iceland 1989–2004].* Reykjavík, National Energy Authority, Report OS-2005-031

Snorrason Á, Einarsson B, Pagneux E, Harðardóttir J, Roberts MJ, Sigurðsson O, Thórarinsson Ó, Crochet P, Jóhannesson T and Thorsteinsson Th (2012) Floods in Iceland, in Kundzewicz ZW, ed., *Changes in flood risk in Europe: International Association of Hydrological Sciences (IAHS) Special Publication*, **10**, 257–276.

Shreve RL (1972) Movement of water in glaciers. *Journal of Glaciology*, **11**(62), 205–214

Spring U and Hutter K (1981) Numerical studies of jökulhlaups. *Cold Regions Science and Technology*, **4**(3), 227–244

Spring U and Hutter K (1982) Conduit flow of a fluid through its solid phase and its application to intraglacial channel flow. *The International Journal of Engineering Science*, **20**(2), 327–363

Sugiyama S, Bauder A, Huss M, Riesen P and Funk M (2008) Triggering and drainage mechanisms of the 2004 glacier-dammed lake outburst in Gornergletscher, Switzerland. *Journal of Geophysical Research*, **113**, F04019 (doi:10.1029/2007JF000920)

Swift DA, Nienow PW, Hoey TB and Mair DWF (2005) Seasonal evolution of runoff from Haut Glacier d'Arolla, Switzerland and implications for glacial geomorphic processes. *Journal of Hydrology*, **309**, 133–148 (doi:10.1016/j.jhydrol.2004.11.016)

Thorsteinsson T, Sigurðsson O, Jóhannesson T, Larsen G and Wilhelms F (2002) Ice core drilling on the Hofsjökull ice cap. *Jökull*, **51**, 25–41

Thorsteinsson T, Elefsen SO, Gaidos E, Lanoil B, Johannesson T, Kjartansson V, Marteinsson VT, Stefansson A and Thorsteinsson T (2007) A hot water drill with built-in sterilization: design, testing and performance. *Jökull*, **57**, 71–82

Tsai VC and Rice JR (2010) A model for turbulent hydraulic fracture and application to crack propagation at glacier beds. *Journal of Geophysical Research*, **115**, F03007 (doi: 10.1029/2009JF001474)

Tsai VC and Rice JR (2012) Modeling turbulent hydraulic fracture near a free surface. *Journal of Applied Mechanics*, **79**, 031003 (doi: 10.1115/1.4005879)

Van de Wal RSW, Boot W, Van den Brocke MR, Smeets CJ, Reijmer CH, Donker JJA and Oerlemans J (2008) Large and rapid melt-induced velocity changes in the ablation zone of the Greenland Ice Sheet. *Science*, **321**(5885), 111–113 (doi:10.-1126./science.1158540)

Walder JS (1982) Stability of sheet flow of water beneath temperate glaciers and implications for glacier surging. *Journal of Glaciology*, **28**(99), 273–293

Werder MA, Hewitt IJ, Schoof C and Flowers GE (2013) Modeling chanelized and distributed subglacial drainage in two dimensions. *Journal of Geophysical Research*, **118**, 1–19 (doi:10.1002/jgrf.20146)

Williams RS Jr and Ferrigno JG (2012) Glaciers (A-2), in Williams, RS Jr and Ferrigno JG, eds., *Satellite image atlas of glaciers of the world.* U.S. Geological Survey Professional Paper 1386-A (State of the Earth's Cryosphere at the Beginning of the 21st Century: Glaciers, Global Snow Cover, Floating Ice, and Permafrost and Periglacial Environments). `http://pubs.usgs.gov/pp/p1386a/`

Zwally HJ, Abdalati W, Herring T, Larson K, Saba J and Steffen K (2002) Surface melt-induced acceleration of Greenland ice-sheet flow. *Science*, **297**, 218–222

Þórarinsson S (1974) *Vötnin stríð. Saga Skeiðarárhlaupa og Grímsvatnagosa. [The swift flowing rivers. The history of Grímsvötn jökulhlaups and eruptions].* Reykjavík, Bókaútgáfa Menningarsjóðs. 254 pp [In Icelandic]

Paper I

A spectrum of jökulhlaup dynamics revealed by GPS measurements of glacier surface motion.

Einarrson B, Magnússon E, Roberts MJ, Pálsson F, Thorsteinsson Th and Jóhannesson T (2016)

Annals of Glaciology, **57**, 47–61 (doi:10.1017/aog.2016.8)

Annals of Glaciology 57(72) 2016 doi: 10.1017/aog.2016.8

A spectrum of jökulhlaup dynamics revealed by GPS measurements of glacier surface motion

Bergur EINARSSON,[1] Eyjólfur MAGNÚSSON,[2] Matthew J. ROBERTS,[1] Finnur PÁLSSON,[2] Thorsteinn THORSTEINSSON,[1] Tómas JÓHANNESSON[1]

[1]*Icelandic Meteorological Office, Bústaðavegur 9, IS-108 Reykjavík, Iceland*
E-mail: bergur@vedur.is
[2]*Institute of Earth Sciences, University of Iceland, Sturlugata 7 Askja, IS-101 Reykjavík, Iceland*

ABSTRACT. GPS campaigns on glaciers during jökulhlaups show how subglacial floods affect glacier motion and shed light on the dynamics of such floods. Three such campaigns have been carried out on southern and western Vatnajökull, southeast Iceland, over known jökulhlaup paths. Two slowly rising jökulhlaups from Grímsvötn and two rapidly rising jökulhlaups from the western and eastern Skaftá cauldrons were captured in these campaigns, with maximum discharge ranging from 240 to 3300 $m^3 s^{-1}$. Glacier surface movements measured in these campaigns are presented along with the corresponding discharge curves. The measurements are interpreted as indicating: (1) initiation of rapidly rising jökulhlaups with a propagating subglacial pressure wave, (2) decreased glacier basal friction during jökulhlaups, (3) subglacial accumulation of water in slowly rising jökulhlaups and (4) lifting of the glacier caused by subglacial water pressure exceeding overburden in both rapidly and slowly rising jökulhlaups. The latter two observations are inconsistent with assumptions that are typically made in theoretical and numerical modelling of jökulhlaups. Both viscous and elastic deformation of the glacier as well as turbulent hydraulic fracture at the ice/bedrock interface are important in the dynamics of the subglacial pressure wave at the front of rapidly rising jökulhlaups.

KEYWORDS: glacier flow, glacier hydrology, jökulhlaups (GLOFs), subglacial lakes

INTRODUCTION

Jökulhlaups (glacier outburst floods) from subglacial geothermal areas, marginal lakes and subglacial volcanic eruptions are common in Iceland (e.g. Björnsson, 1975, 1976, 2002). These floods overfill the subglacial hydrological system and have a substantial effect on the dynamics of the glaciers, where they occur (Anderson and others, 2005; Magnússon and others, 2007; Sugiyama and others, 2007; Bartholomaus and others, 2008, 2011; Stearns and others, 2008; Riesen and others, 2010). Jökulhlaups can be categorized into two main groups, rapidly and slowly rising (Björnsson, 2002), which are characterized by marked differences in the hydrographs.

The hydrographs of slowly rising jökulhlaups have been explained with a model of melt enlargement of an ice tunnel (Nye, 1976) or melt enlargement of a constriction (bottleneck) at the location of a seal near the source lake (Clarke, 1982; Björnsson, 1992). Clarke (2003) developed the theory of Nye (1976) further based on Spring and Hutter (1981, 1982) and showed that the effective pressure (ice overburden minus water pressure) in a flood through a subglacial tunnel may become negative in parts of the flood path. Negative effective pressure is expected to lead to water escaping the tunnel due to hydraulic fracturing at the ice/bedrock interface and lifting of the glacier, creating a wider and more complex flood path at the corresponding location. Glacier uplift and widespread velocity increase have been observed for slowly rising jökulhlaups from the subglacial lake Grímsvötn in 1996 (Magnússon and others, 2007) and the marginal lake Gornersee, Switzerland, in 2005 (Huss and others, 2007), indicating that the flood path of slowly rising jökulhlaups is not always restricted to one or more tunnels. Björnsson (2010) therefore states that '*current models may reconstruct discharge curves while not describing all the factual hydraulic and glaciodynamic processes of each jökulhlaup*'.

In contrast, it has been proposed that the flood path of rapidly rising jökulhlaups is created by the propagation of a subglacial pressure wave (Jóhannesson, 2002) at the front of sheet flow underneath the glacier (Björnsson, 2002; Flowers and others, 2004). During rapidly rising jökulhlaups from Grímsvötn and from the lake beneath the western Skaftá ice cauldron, the estimated water volume stored in the flood paths was an order of magnitude larger than could be stored in conduits formed by melting. Lifting and deformation of the overlying glacier was, therefore, important in their dynamics (Björnsson, 2002). Indications of subglacial water pressure higher than ice overburden, and associated glacier lifting have been observed for rapidly rising jökulhlaups from Grímsvötn in 1996 (Björnsson, 1997; Roberts and others, 2000) and for Gornersee in 2004 (Huss and others, 2007; Sugiyama and others, 2008). Indications of subglacial sheet flow in the early stages of a rapidly rising jökulhlaup from the eastern Skaftá cauldron have also been observed (Magnússon and others, 2007), but direct observations of the propagation of a subglacial pressure wave have not been reported.

The propagation mechanism of jökulhlaups at the glacier bed is poorly understood. Continuous GPS measurements on the glacier surface can provide valuable information on the effect of jökulhlaups on the motion of the glacier and shed light on jökulhlaup dynamics. Three GPS campaigns have been carried out on southern and western Vatnajökull, Iceland, over jökulhlaup paths from subglacial lakes at Grímsvötn and the Skaftá cauldrons. Glacier surface movements during jökulhlaups from these campaigns are

presented and interpreted in this paper. Similarities and differences in the initiation of rapidly and slowly rising jökulhlaups are addressed based on observations of both types of jökulhlaups. Based on these observations, we argue that jökulhlaups show a spectrum of behaviour instead of being classifiable into two distinct categories, although, the traditional categories remain useful in discussions of flood characteristics. We identify physical processes that we infer to be acting at the glacier bed and within the glacier during the floods and compare our observations with the conceptual background of existing models.

Subglacial water flow and variations in subglacial water pressure have attracted increasing attention in recent years as a likely cause of large variations in ice-flow velocities that have been observed on the main outlets of the Greenland ice sheet and some of the ice streams of Antarctica (e.g. Rignot and Kanagaratnam, 2006; Fricker and others, 2007; Stearns and others, 2008; Doyle and others, 2015). The focus of this paper is on subglacial water flow in the context of jökulhlaup dynamics, but the subject has a wider relevance, as improved understanding of subglacial hydrology is important for understanding the response of glaciers and ice sheets to hydrological variations such as changes in meltwater input due to climate change.

THE STUDY SITES AND THE INVESTIGATED JÖKULHLAUPS

This study was conducted over two jökulhlaup paths in the Vatnajökull ice cap, at the Skeiðarárjökull and Skaftárjökull outlet glaciers in the southern and western parts of the ice cap, respectively (Fig. 1).

Jökulhlaups from Skeiðarárjökull originate in the Grímsvötn subglacial lake (Fig. 1) (Björnsson, 1974; Thórarinsson, 1974). The lake is formed by geothermal melting in a ~10 km wide and ~300 m deep subglacial volcanic caldera (Björnsson, 1974). The lake accumulates basal meltwater produced by geothermal and volcanic activity in addition to surface meltwater and rain (Björnsson and Kristmannsdóttir, 1984). Most jökulhlaups from Grímsvötn are classified as slowly rising (Björnsson, 2002) and the exponential rise of the discharge during these jökulhlaups has been physically explained by invoking the conduit-melt–discharge feedback (Nye, 1976; Björnsson, 1992). A jökulhlaup in November 1996 that rose to a maximum discharge of ~50 000 $m^3 s^{-1}$ at the terminus in a little over a day after outflow from Grímsvötn started (Björnsson, 1997, 2002; Snorrason and others, 1997) is, however, an example of a rapidly rising jökulhlaup (Björnsson, 2002; Jóhannesson, 2002). This jökulhlaup released ~3 km^3 of meltwater from an eruption in Gjálp north of Grímsvötn (Guðmundsson and others, 1997) and damaged the seal of the Grímsvötn subglacial lake, altering the characteristics of jökulhlaups after 1996. Less water can now accumulate in Grímsvötn, hence the volume of jökulhlaups is smaller. At the same time, their duration became shorter. The peak flow of the two largest post-1996 jökulhlaups, in the autumn of 2004 and 2010, ~3000 $m^3 s^{-1}$, is therefore, comparable with typical jökulhlaups prior to 1996. A GPS station was operated on Skeiðarárjökull during the 2004 and 2010 jökulhlaups. The station was located ~1 km up-glacier of the outlet of the ~50 km long flood path in 2004 (denoted by SKE2) and ~9 km up-glacier of the outlet in 2010 (denoted by SKE1) (Figs 1 and 2). Previous studies have shown water

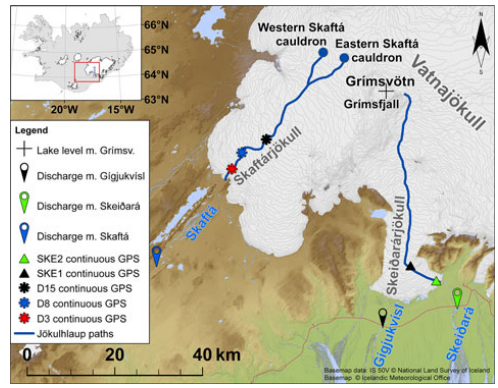

Fig. 1. Location of the subglacial lakes at Grímsvötn and the Skaftá cauldrons. Estimated flood paths, based on the gradient of the hydraulic potential, and location of GPS stations, discharge measurement sites and hydrometric stations.

accumulation at SKE1 during a jökulhlaup and also during an intense rain event (Magnússon and others, 2011).

Jökulhlaups in the Skaftá river from western Vatnajökull have been known since 1955 (Björnsson, 1977). These jökulhlaups originate from two subglacial lakes under 1–3 km wide and 50–150 m deep depressions in the glacier surface, commonly referred to as ice cauldrons, formed by geothermal melting. The average time interval between jökulhlaups from each cauldron is ~2 a. The jökulhlaups travel ~40 km under a glacier that reaches maximum thickness of ~750 m and emerge in the Skaftá river at the terminus of Skaftárjökull outlet glacier (Figs 1 and 2). A hydrometric station is located in the river by Sveinstindur, 25 km downstream of the glacier margin (Fig. 1). The hydrographs of all measured jökulhlaups from the Skaftá cauldrons have been rapidly rising (Zóphóníasson, 2002). Three continuous GPS stations were installed over the flood path of jökulhlaups from the Skaftá cauldrons in 2008, located 3, 8 and 15 km from the glacier margin and denoted D3, D8 and D15, respectively. Two jökulhlaups occurred during the GPS campaign, one with a maximum discharge of 240 $m^3 s^{-1}$ from the western cauldron in August 2008 and the other with a maximum discharge of 1290 $m^3 s^{-1}$ from the eastern cauldron in October 2008.

The jökulhlaup paths from Grímsvötn and the Skaftá cauldrons have similar length and ice thickness, whereas the vertical relief is larger for Grímsvötn (Fig. 2). The Grímsvötn ice-flow basin (~300 km^2) is an order of magnitude larger than the ice-flow basins of each of the Skaftá cauldrons (~20 and ~30 km^2 for the western and eastern cauldron, respectively) and accumulates an order of magnitude more meltwater annually in the subglacial lake (Björnsson, 1974, 1977, 2002; Pálsson and others, 2006). The jökulhlaups from Grímsvötn have been more varied in size and characteristics than jökulhlaups from the Skaftá cauldrons, some released in connection with subglacial volcanic eruptions and others caused by the continuous accumulation of water in the lake. The jökulhlaups from the Skaftá cauldrons, on the other hand, vary in size over an order of magnitude and are all caused by slow accumulation of water from geothermal melting, surface melting and rain.

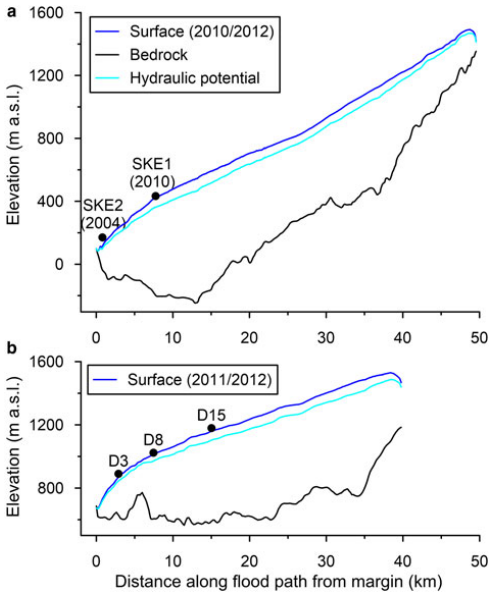

Fig. 2. Longitudinal profiles of bedrock and ice surface along jökulhlaup paths from Grímsvötn (a) and the western Skaftá cauldron (b) (see Fig. 1). The lower 32 km of the flood paths from the western and eastern Skaftá cauldrons are identical and the elevation profiles for the upper parts are so similar that they are nearly indistinguishable at the scale of this figure. Therefore, only the path from the western cauldron is shown in (b). The locations of the GPS stations are indicated. The elevation of the GPS stations corresponds to the glacier surface at the time of each measurement campaign. Bedrock elevation is based on radio-echo soundings (Björnsson, 1988; Björnsson and others, 1999; Magnússon, 2008; Magnússon and others, 2009).

METHODS

Instrumentation

The GPS instruments used to monitor the two events from the Skaftá cauldrons and the 2010 event from Grímsvötn were installed on top of the glacier surface on quadropods, while the GPS instrument used in the 2004 event from Grímsvötn was installed on a pole drilled into the ice. The height of the instruments deployed on the quadropods is affected by surface melting as they are lowered with the surface. Observed elevation changes at all instruments are affected by the local surface slope and the down-glacier movement of the ice. These processes are not corrected for and need to be accounted for, when the elevation data are studied over periods of days or periods with large horizontal movements.

The GPS instruments used during recording of all events were Trimble NetRS (Trimble 5700 in 2004) dual-frequency receivers recording at 15 s intervals. At the time of October 2008 jökulhlaup, the D15 instrument at the highest elevation was snowed in and out of power. The D8 instrument at the second highest elevation lost power on 14 October. The maximum discharge during the October event had been reached at that time and recession had started but was not fully completed. SKE2, the station running in 2004 on Skeiðarárjökull, was taken down on 6 November, while the glacier was still subsiding after the 2004 jökulhlaup from Grímsvötn.

Data processing

The GPS data were processed with the GAMIT-Track utility (Herring and others, 2010) using a set up for long baselines. The August and October events on Skaftárjökull in 2008 were processed with respect to a base station at Skrokkalda (SKRO) in August and Ísakot (ISAK) in October, giving baselines of ~35 and ~85 km, respectively. The stations operated on Skeiðarárjökull were processed using Höfn (HOFN) as base station at ~100 km distance. The standard deviation of unfiltered positions around a daily mean during periods of slow motion and low melt is ~4 cm in the vertical and 2 cm in the horizontal coordinates and may be used as an indication of the precision of the GPS measurements. Horizontal velocities were calculated for 1 h periods using filtered positions (2 h wide triangular filter). During days prior to the jökulhlaups, when we expect the glacier motion to be approximately constant, the velocity records reveal standard deviation of 8, 7 and 11 cm d^{-1} (3–5 mm h^{-1}) for the Skaftárjökull, 2004 Skeiðarárjökull and 2010 Skeiðarárjökull data, respectively.

The volume of water stored in lake Grímsvötn can be calculated from the mapped hypsometry of the caldera, where the lake is located and the thickness and surface elevation of the lake ice cover (Guðmundsson and others, 1995). The elevation is from a fixed station on the ice cover above the deepest part of the lake. In 2004, the elevation was measured with a navigation GPS (code-based GPS). In 2010, the elevation was calculated from barometric measurements at the station on the ice cover and at a nunatak at ~3 km distance using temperature measurements at the two locations. In both cases, the uncertainty of the daily average elevation is 2–4 m but the derived total elevation drop was 42 m in 2004 and 54 m in 2010. The hypsometry of the caldera is from Guðmundsson and others (1995), updated with post-1996 radio-echo sounding measurements (unpublished data of the Institute of Earth Sciences) to compensate for changes caused by the 1996 Gjálp eruption. The ice-cover thickness is based on radio-echo sounding measurements in 2000.

The amount of additional meltwater produced by friction during the Grímsvötn jökulhlaups can be calculated from the loss of potential energy in the 1280 m descent from the water level in the subglacial lake to the ice margin. We assume that the temperature of the water stored at Grímsvötn is at the pressure-melting point (Ágústsdóttir and Brantley, 1994).

To enable integration of the cumulative jökulhlaup discharge in Gígjukvísl in 2010, we assume that the river discharge increases linearly from a background value at 10:00 on 31 October, when river level starts rising significantly at the bridge, to the first discharge measurement 4 h later. We assume linear change in discharge between discharge measurements, except for the peak discharge. The peak discharge was estimated at ~3000 m^3 s^{-1} at 11:30 on 3 November based on the intersection of exponential approximations to the observed discharge before and after the maximum (unpublished data of the Icelandic Meteorological Office) (Fig. 3). The last discharge measurement was carried out in the afternoon on 4 November, but three additional values

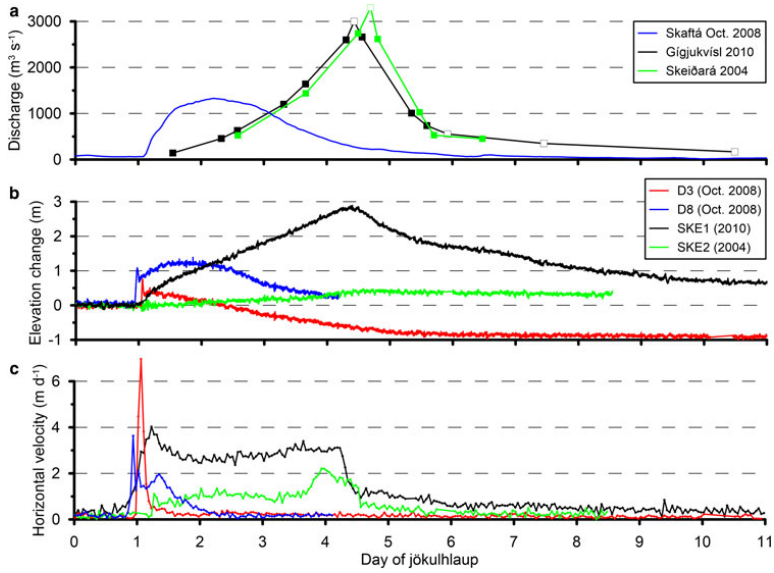

Fig. 3. (a) Discharge during the 2004 jökulhlaup from Grímsvötn (green), the 2010 jökulhlaup from Grímsvötn (black) and the October 2008 jökulhlaup from the eastern Skaftá cauldron (blue), (unpublished data from the discharge database of the Icelandic Meteorological Office). Discrete discharge measurements are indicated with filled squares and estimated discharge values are indicated with hollow squares. (b, c) Observed elevation changes (b) and horizontal velocities (c) of the glacier surface during the jökulhlaups. The 2004 results (green) are from SKE2, a location 1 km from the glacier margin of Skeiðarárjökull, while the 2010 results (black) are from SKE1, a location 9 km from the margin. Results at two different locations over the flood path of the October 2008 jökulhlaup from the eastern Skaftá cauldron at 3 km, D3 (red), and 8 km, D8 (blue), from the glacier margin are presented.

of the discharge were derived using the measured river level at the bridge and a linear approximation relating river level and discharge based on simultaneous measurements of the discharge and river level. The river is assumed to have reached background discharge at midnight on 11 November when the river level fully settled.

To estimate water storage in the subglacial flood path of the jökulhlaups, we calculate the difference between the integrated water added into the flood path (flow from Grímsvötn plus meltwater produced by friction) and the outflow of jökulhlaup water from the glacier margin estimated by shifting the Gígjukvísl discharge back 1 h (corresponding to estimated travel time from the glacier margin to the bridge) minus an estimated fixed background discharge of 29 $m^3\,s^{-1}$, which leads to equal volume released out of Grímsvötn and discharged into Gígjukvísl. This magnitude of the background discharge can be considered realistic for Gígjukvísl at this time of year.

Analysis of local conduit growth

Estimation of local conduit growth, assuming a steady supply of water from above through a sheet-like flood path formed by a subglacial pressure wave, can be used to investigate possible conduit development during the creation of the flood path at selected locations.

Here, the discharge, Q, along a subglacial conduit is calculated using the Gauckler–Manning–Strickler formula for the mean flow speed $\bar{v}$, as is traditional in jökulhlaup modelling (e.g. Nye, 1976; Clarke, 2003). Using $Q = S\bar{v}$, where S is the cross-sectional area of the conduit, and assuming semicircular channel geometry, the discharge may be expressed as

$$Q = \frac{S^{4/3}|\partial\phi/\partial s|^{1/2}}{n_m\sqrt{\rho_w g}(2/\pi)^{1/3}(2+\pi)^{2/3}}. \quad (1)$$

ρ_w is the density of flood water, n_m is Manning's friction coefficient for the conduit walls and bottom and g is the acceleration of gravity. An along-conduit horizontal coordinate is denoted by s, $\phi = \rho_w g z_b + p_w$ is the hydraulic potential, p_w is the water pressure, z_b is the elevation of the glacier bed and $\partial\phi/\partial s$ is the hydraulic gradient in the conduit.

The time-dependent development of S and Q can be calculated as a function of the hydraulic gradient and an estimate for an initial conduit cross-sectional area, S_0, derived for example from information about the subglacial discharge of water before the jökulhlaup, using Nye's (1976) theory for jökulhlaups. Creep closure of the conduit during the initial phase of the flood is neglected as the water pressure is assumed to be close to overburden, where this equation is applied. The time-dependent development of S will therefore only be controlled by melting of the conduit walls and is given by

$$\frac{\partial S}{\partial t} = \frac{m_i}{\rho_i}, \quad (2)$$

where t is time, m_i is the melt rate of the channel walls and ρ_i is the density of ice. All initial heat of the flood water in the source lake is assumed to have been dissipated before the

flood reaches the location of the GPS instruments, as they are tens of kilometres downstream from the source lake, and heat transfer in subglacial water flow towards the surrounding ice is very rapid (Björnsson, 1992; Jóhannesson, 2002). Due to the rapid heat flow, flood water temperature is assumed to be maintained at the pressure-melting point, so that all released frictional heat is spent locally for melting of ice. Under these assumptions the melt rate of the channel walls will be

$$m_\mathrm{i} = \frac{Q}{L}\left(\frac{-\partial\phi}{\partial s} + c_\mathrm{t}\rho_\mathrm{w}c_\mathrm{w}\frac{\partial p_\mathrm{w}}{\partial s}\right), \quad (3)$$

where L, c_w and c_t are the latent heat of fusion, the heat capacity and the change of the melting point with pressure for water, respectively. The term in parentheses is the *melt-rate ability* of the conduit, denoted μ by Magnússon and others (2011). It takes into account the thermodynamic effect, first analysed by Röthlisberger (1972), of the variation of the melting point of water with pressure on the rate of melting of the conduit walls, assuming that energy is released or spent as needed to lower or raise the temperature to maintain it at the local pressure-melting point. Combining Eqns (1–3), the time-dependent development of S can be expressed as

$$\frac{\partial S}{\partial t} = \frac{S^{4/3}|\partial\phi/\partial s|^{1/2}((-\partial\phi/\partial s) + c_\mathrm{t}\rho_\mathrm{w}c_\mathrm{w}(\partial p_\mathrm{w}/\partial s))}{\rho_\mathrm{i}Ln_\mathrm{m}\sqrt{\rho_\mathrm{w}g}(2/\pi)^{1/3}(2+\pi)^{2/3}}. \quad (4)$$

The local hydraulic potential gradient $\partial\phi/\partial s$ is estimated from the glacier bed and surface topographies, z_b and z_s. Assuming that the subglacial water pressure equals ice overburden as the subglacial hydraulic system is flooded with jökulhlaup water,

$$\frac{\partial\phi}{\partial s} = (\rho_\mathrm{w} - \rho_\mathrm{i})g\frac{\partial z_\mathrm{b}}{\partial s} + \rho_\mathrm{i}g\frac{\partial z_\mathrm{s}}{\partial s}. \quad (5)$$

The bed and surface gradients $\partial z_\mathrm{s}/\partial s$ and $\partial z_\mathrm{b}/\partial s$ are estimated over a horizontal distance of one ice thickness at each location.

Analysis of sheet-like water flow and propagation of a subglacial pressure wave

Following Jóhannesson (2002), discharge per unit width, q, in a subglacial sheet, which is much wider than the sheet thickness, h_w, may be calculated from Manning's formula as

$$q = \frac{h_\mathrm{w}^{5/3}}{2^{2/3}n_\mathrm{m}}\sqrt{\frac{-\partial\phi_\mathrm{s}/\partial s}{\rho_\mathrm{w}g}}. \quad (6)$$

The notation is the same as above for channelized flow, except that the potential ϕ_s includes the sheet thickness h_w and is defined as $\phi_\mathrm{s} = \rho_\mathrm{w}gz_\mathrm{b} + \rho_\mathrm{w}gh_\mathrm{w} + p_\mathrm{w}$, where p_w is defined at the top of the sheet. The sheet thickness is considered as an average, $h_\mathrm{w} = A_\mathrm{w}/b_\mathrm{w}$, over an effective width, b_w, of the flood path with a total cross-sectional area, A_w, resulting in a Manning's hydraulic radius of $h_\mathrm{w}/2$.

The difference, $\Delta p = p_\mathrm{w} - p_\mathrm{i}$, between the water pressure and ice overburden near the front of the subglacial pressure wave drives the uplift of the glacier at the flood front and thereby the propagation of the front. It may be expressed as

$$\Delta p = p_\mathrm{w} - p_\mathrm{i} = \phi_\mathrm{s} - (\rho_\mathrm{w} - \rho_\mathrm{i})gz_\mathrm{b} - \rho_\mathrm{i}gz_\mathrm{s} - \rho_\mathrm{w}gh_\mathrm{w}. \quad (7)$$

If the propagating flood front is thicker than the sheet that follows, as hypothesized by Jóhannesson (2002), then the potential gradient, $\partial\phi_\mathrm{s}/\partial s$, within this thicker flow will be smaller than higher upstream. The longitudinal profile of ϕ_s will thus be flatter within the thicker flood front and the water pressure within it will approach a hydrostatic pressure distribution. A propagating front of this type implies a lifting of the glacier surface and a subsequent lowering as the pressure wave passes by, when viewed from a fixed position on the flood path. The water pressure at the base of the glacier can be assumed to be approximately equal to overburden, when lifting stops and the vertical displacement reaches maximum.

If the distance between the front of the flood and the position of maximum vertical displacement can be estimated, as well as the potential gradient within the pressure wave with greater sheet thickness, then Eqn (7) can be used to derive an estimate for the pressure difference, Δp, at the flood front. We assume that the geometry of the propagating pressure wave is approximately constant, so that the depth-averaged velocity of the flow of water is approximately the same within and behind the wave over the time span needed for the wave to pass, and that the discharge behind the pressure wave is driven by the local gradients of the bed and surface topographies. Then the potential gradients within and behind the pressure wave, $\partial\phi_\mathrm{wave}/\partial s$ and $\partial\phi_\mathrm{sb}/\partial s$, according to Eqn (6), modified for flow speed, will satisfy

$$\frac{\partial\phi_\mathrm{wave}}{\partial s} = \left(\frac{h_\mathrm{sb}}{h_\mathrm{wave}}\right)^{4/3}\frac{\partial\phi_\mathrm{sb}}{\partial s}, \quad (8)$$

and the gradient within the pressure wave may be calculated from estimates of the sheet thickness within and behind the wave, h_wave and h_sb.

Glacier flow is typically dominated by viscous deformation (Cuffey and Paterson, 2010), but the propagation velocity of the flood front and the magnitude of the basal overpressure are such that elastic deformation of the overlying ice may also be important for the separation of the glacier from the bedrock during jökulhlaups. The relative importance of viscous and elastic deformation in a given situation may be assessed by the Maxwell time

$$\tau_\mathrm{M} = \frac{\eta}{G}, \quad (9)$$

where η is the effective viscosity of the material and G the shear modulus (Melosh, 2011). The effective viscosity of ice (and thereby the Maxwell time) depends on the deviatoric stress, τ_E, as ice is a shear thinning fluid with

$$\eta = \frac{B^n}{2\tau_E^{n-1}}, \quad (10)$$

where B and n are parameters in Glen's flow law (Cuffey and Paterson, 2010). Both viscous and elastic deformation are important on timescales close to the the Maxwell time, but elastic deformation dominates on shorter timescales and viscous deformation on longer scales (Melosh, 2011). For typical values of shear and longitudinal stresses and strain rates on temperate glaciers, the Maxwell time is of the

order of several hours. As the ice viscosity is reduced by the deformation induced by the propagating pressure wave, Eqn (10) predicts that the Maxwell time will be shorter in the vicinity of the wave than elsewhere.

Jóhannesson (2002) derived an approximate expression for the rate of viscous lifting, w_v, at a flood front of transverse width b_w with water pressure locally higher than the ice overburden

$$w_v = \frac{2h_i}{n+2}\left(\frac{b_w}{2h_i}\right)^{n+1}\left(\frac{\Delta p}{B}\right)^n, \quad (11)$$

where $h_i = z_s - z_b$ is the ice thickness. In case the transverse width is not shorter than the length of the pressure wave as assumed by Jóhannesson, the equation may be assumed to provide an order-of-magnitude estimate for the rate of lifting, if b_w is replaced by the shortest horizontal dimension of the pressure wave over which vertical shear motion associated with the lifting takes place. This equation ignores the effect of strain softening due to the horizontal shearing in the downslope flow of the glacier, which may be estimated to be an order of magnitude smaller than the shear rate induced by the propagation of the flood fronts that are analysed here.

Equation (11) only considers lifting of the glacier by viscous deformation, but elastic deformation may also be expected to play a role in the dynamics of the pressure wave. The magnitude of elastic lifting, ϵ_e, of the overlying ice after the passage of the initial flood front may be crudely estimated with the theory of elastic plates (Pollard and Fletcher, 2005) as

$$\epsilon_e = \frac{\Delta p}{cR}a^4. \quad (12)$$

a is the horizontal dimension of the area affected by overpressure Δp acting at the bottom of the plate, $R = Eh_i^3/(12(1-\nu^2))$ is the flexure rigidity of the plate and E and ν are the Young's modulus and the Poisson ratio of the plate material, respectively. If the shortest horizontal dimension of the area, a, is much smaller than the longest horizontal dimension, the constant $c = 384$, but if the area is circular with diameter a, $c = 1024$. This equation provides an order-of-magnitude estimate for the elastic response of the glacier if a is the shortest dimension of the subglacial pressure wave.

Elastic lifting according to Eqn (12) approximately captures the effect of elasticity after the passage of the flood front, but not the possible influence of elastic deformation on the propagation of the subglacial front. Subglacial, turbulent, hydraulic fracture propagation in a medium with small fracture toughness has been analysed by Tsai and Rice (2010, 2012) based on linear elastic fracture mechanics (LEFM) for a horizontal fracture that grows parallel to a free surface, both for a short fracture and for a fracture that eventually becomes long compared with the ice thickness. They take into account the time needed for the water flow to fill the fracture as it propagates down-glacier and grows in thickness utilizing the Gauckler–Manning–Strickler approximation to represent turbulent friction in the fracture. The analysis is intended to shed light on the emptying of supraglacial lakes, and does not fully correspond to the situation analysed here, as Tsai and Rice assume maximum effective pressure at a fixed inflow location. This leads to a steadily growing separation between ice and bedrock all the way between the inflow location and tip of the propagating fracture at the ice/bedrock interface. The analysis of Tsai and Rice (2012) may be expected to approximately represent the tip of a propagating jökulhlaup, if the inflow location is assumed to correspond to a moving position at a distance $L_{\Delta p}$ behind the tip although their solution regarding the variation of pressure and discharge along the flood front will not be fully consistent in this case. This leads to the following expression (in our notation) for propagation velocity of the crack tip:

$$U_{tip} = \theta\sqrt{\frac{\Delta p}{\rho_w}}\left(\frac{\Delta p}{E'}\right)^{2/3}\left(\frac{L_{\Delta p}}{k}\right)^{1/6}, \quad (13)$$

where θ is a non-dimensional multiplicative factor (denoted ϕ by Tsai and Rice), $E' = E/(1-\nu^2)$ and k is the Nikuradse roughness height. Tsai and Rice (2012) give an approximation for the factor $\theta \approx 5.13 + 0.64(L_{\Delta p}/h_i) + 0.94(L_{\Delta p}/h_i)^2$, valid for $L_{\Delta p}/h_i \le 5$, and the Nikuradse roughness height is related to the Manning's friction coefficient by $n_m = (0.0380\ \mathrm{s\,m^{-1/2}})\,k^{1/6}$.

The analysis of Tsai and Rice also yields approximate solutions for the crack opening (again in our notation)

$$h_w = \frac{\hat{w}\Delta p L_{\Delta p}}{E'}. \quad (14)$$

The time-varying spatial average of the non-dimensional crack opening, $\hat{w}$, is approximately given as a function of the ratio of the crack length to the ice thickness $\hat{w}_{avg} \approx 1.72 + 0.89(L_{\Delta p}/h_i)^2$, and the ratio of the maximum opening to the average opening may be read off figure 5 in Tsai and Rice (2012) for $0.02 \le L_{\Delta p}/h_i \le 5$.

The vertical uplift rates predicted by viscous deformation (Eqn (11)), the lifting predicted by plate elasticity (Eqn (12)) and the crack opening given by the LEFM analysis of Tsai and Rice (Eqn (14)) are not directly comparable with our jökulhlaup observations, as the lifting shown by the GPS instruments will be the result of both elastic and viscous deformation. We will calculate the contributions of the different processes described above and compare them to our observations to investigate, which processes are likely to be important for the propagation of the subglacial pressure wave.

RESULTS

Observations of jökulhlaups from the Skaftá cauldrons

The October 2008 jökulhlaup in Skaftá

The October 2008 jökulhlaup from the eastern Skaftá cauldron was among the larger jökulhlaups in Skaftá, reaching maximum discharge of flood water at Sveinstindur of 1290 $m^3\,s^{-1}$ (Fig. 3). The total volume of flood water was 0.27 km^3. A delay of 3 h is estimated for the propagation of the flood from the glacier margin to Sveinstindur, based on a simple calculation for wave propagation in open channels. The discharge at the glacier margin started rising at 02:45 on 11 October, reached a maximum ~26 h later at 05:00 on 12 October, and was back to expected base flow ~19 October.

On-site observations showed flow from large continuous segments of the ~5 km wide glacier margin of the Skaftárjökull outlet glacier during the beginning of the jökulhlaup. Around midday on 11 October, substantial flow was still observed from an overflight from large continuous parts of the glacier margin, but a few main outlets

discharged most of the water. During a field trip late in the evening of 11 October, the jökulhlaup was observed to discharge from a few main outlets.

Indications of high water pressure near the terminus during the initiation of the jökulhlaup, such as water flowing out of moulins and a ~2 km long, transverse thrust fault formed through the glacier ~1 km from the ice margin, were observed from an overflight and during a field trip. The formation of the fault, which was ~2 m high, was associated with an M2 glacier originated earthquake at 02:05 on 11 October located near the glacier terminus by Iceland's seismic network (unpublished data of the Icelandic Meteorological Office). Breaking-up of the glacier snout was observed as well.

The arrival of the jökulhlaup at GPS station D8 at 22:30 on 10 October was associated with lifting of 1.06 m in 50 min followed by lowering of 0.41 m in 50 min (Fig. 4). A second phase of slower lifting then started, with total vertical displacement of 0.58 m in 11 h. The vertical position of the station then remained constant for ~14 h at a total displacement of 1.23 m, compared with the initial elevation before the jökulhlaup. The glacier surface started to fall at 01:30 on 12 October and had been lowered by 0.77 m when the station lost power on 14 October.

The ice movement at station D3 at the beginning of the flood was similar to the movement at D8 with a delay of ~2.1–2.5 h, with lifting of 0.84 m in 40 min followed by lowering of 0.47 m in 60 min (Fig. 4). A second phase of slower lifting then started with total lifting of 0.12 m in 2 h followed by slow lowering over the next 5 d by 1.25 m in total, after which no further changes in elevation were observed. The station was thus 0.76 m lower after the jökulhlaup than before.

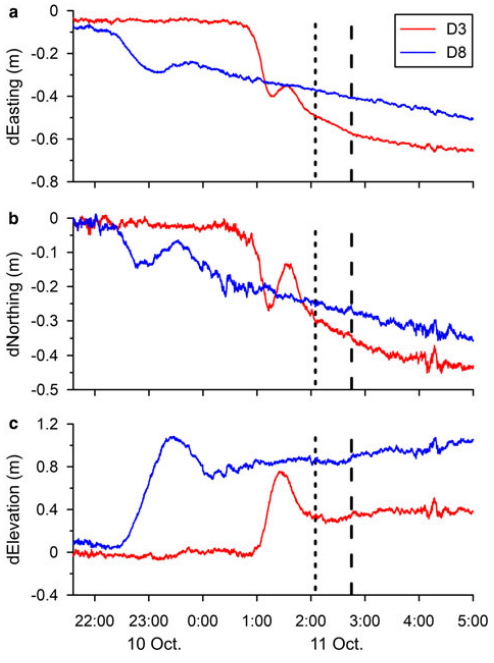

Fig. 4. Observed horizontal displacements (a, b) and elevation changes (c) during the October 2008 jökulhlaup from the eastern Skaftá cauldron at 3 km, D3 (red), and 8 km, D8 (blue), from the glacier margin. The onset of discharge increase at the glacier margin is indicated with a dashed vertical line and the timing of an M2 earthquake near the terminus with a dotted line.

Substantial changes in horizontal velocity were observed at both D8 and D3 during the jökulhlaup (Fig. 3). The onset of horizontal motion was more gradual and started some tens of minutes before the vertical motion (Fig. 4). Rapid horizontal movements coincided with rapid vertical movements, and the horizontal velocity generally increased during lifting and started to decrease as soon as lifting stopped. Reversed loop motion (in a vertical section) was superimposed on the above-described general displacement pattern at both stations. The reverse motion occurs around the time of maximum uplift during the passage of the subglacial wave at the onset of the jökulhlaup at each location. The timing and relative magnitude of changes in the south–north and west–east velocity components often did not coincide during the jökulhlaup, causing temporary changes in the ice-flow direction by several tens of degrees.

Lowering due to surface melting is estimated at 2–3 mm d^{-1} by simple degree-day calculations, both at D8 and D3, and can be ignored compared with the observed vertical motions. Lowering due to the movement of the instruments down the surface gradient of the glacier, with the horizontal flow, is 2–4 mm d^{-1} at both stations for days before and after the jökulhlaup. During the jökulhlaup, bed slip is substantial, leading to a combination of normal ice flow following the surface gradient and block flow controlled by the bed gradient. Using the higher of the two gradients leads to estimated lowering of 25 mm d^{-1} at D8 and 45 mm d^{-1} at D3 at the time of maximum horizontal velocities during the jökulhlaup. This is one to three orders of magnitude smaller than the observed vertical velocities and is also ignored here.

The propagation velocity of the subglacial flood front is estimated as 0.5–0.6 m s^{-1} between D8 and D3 and 0.4–0.5 m s^{-1} between D3 and the glacier margin, based on the timing of the onset of lifting and the time of the beginning of discharge increase at the glacier margin. The propagation velocities allow an estimation of the length of the subglacial pressure wave (Jóhannesson, 2002), which is assumed here to cause the first phase of lifting and subsequent lowering, to be 3.0–3.5 km at D8 and 2.3–3.5 km at D3.

The overpressure, Δp, at the flood front may be calculated from Eqns (7) and (8). The water pressure at the base of the glacier is assumed to be equal to overburden when lifting stops and the vertical displacement reaches maximum at the distance $L_{\Delta p}$ from the flood front. $L_{\Delta p}$ is found to be 1.8–1.5 km at D8 and 0.9–1.3 km at D3. This leads to $\Delta p = 0.16$–0.18 MPa at D8 and $\Delta p = 0.17$–0.25 MPa at D3. The correction for the effect of friction in the water flow within the flood front expressed by Eqn (8) amounts to ~50% of the estimated overpressure.

The August 2008 jökulhlaup in Skaftá

The August 2008 jökulhlaup from the western Skaftá cauldron was a relatively small event, with a maximum discharge of flood water at Sveinstindur of 240 $m^3 s^{-1}$ (Fig. 5) and total volume of flood water of 0.10 km^3. A delay of 3.5 h is in this case estimated for the flood propagation from the glacier margin to Sveinstindur. The start of the flood at the glacier margin was obscured by the diurnal discharge variation in the base flow from the glacier. Conductivity started to rise

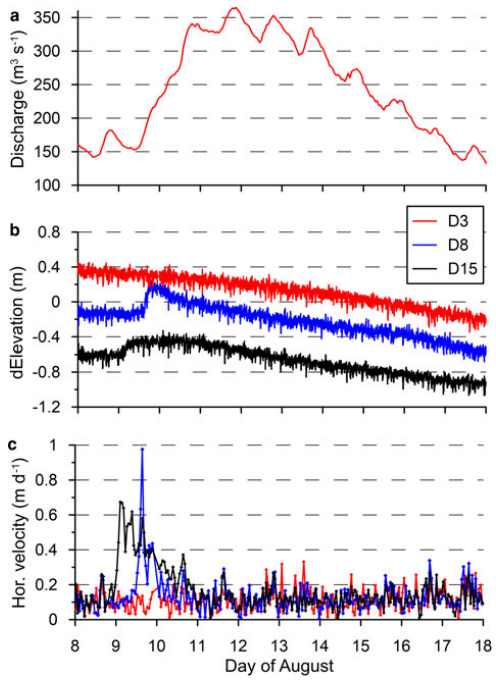

Fig. 5. (a) Discharge during the August 2008 jökulhlaup from the western Skaftá cauldron (unpublished data from the database of the Icelandic Meteorological Office). (b, c) Observed elevation changes (b) and horizontal velocities (c) of the glacier surface at 3 km, D3 (red), 8 km, D8 (blue), and 15 km, D15 (black), from the glacier margin during the jökulhlaup.

at ~19:00 on 8 August, indicating some flood water from the geothermal source lake at the margin. Notable discharge increase was first observed around noon on 9 August and the discharge increased sharply until the evening of 10 August. The maximum in discharge, on 11 August, might have been caused by diurnal variation in base flow rather than a maximum in flood water discharge. The discharge receded back to expected base flow ~17–18 August. During a field trip on 10 August, the jökulhlaup was observed to flow out of a few main outlets and no evidence of a widespread outflow from the glacier margin or flow out of fractures through the glacier surface was observed.

Slow lifting started at D15 ~00:30 on 9 August (Fig. 5). About 3 h later, the rate of lifting suddenly increased by a factor of 4 and rapid lifting sustained for 2 h. The rate of lifting then decreased substantially and slow lifting took place for the next 11 h, reaching total vertical displacement of 0.15 m. A flat maximum in the displacement was then maintained for ~20 h. Slow lifting started at D8 ~07:30 on 9 August. About 7 h later, the rate of lifting was accelerated by a factor of 15–20 and rapid lifting took place for 1 h. This was followed by slower lifting for 3 h and maximum vertical displacement of 0.35 m was reached at 19:00. After the maximum was reached, slow lowering took place at both locations until ~15 August when the stations reached the rate of lowering expected from melting and down-glacier ice movement. The total vertical displacement of the instruments over the course of the jökulhlaup was equal to the expected lowering due to melting and downslope movement of the GPS instruments with the ice, within +/−5 cm and ±10 cm for D15 and D8, respectively.

Substantial changes in horizontal velocities were observed at both D15 and D8 during the jökulhlaup. The horizontal velocity generally increased during lifting and started to decrease as soon as lifting stopped. A short event of reversed motion in the south–north direction took place at D8 around the time of maximum vertical displacement. The timing and relative magnitude of changes in south–north and west–east velocity components did not coincide during the jökulhlaup, as for the October event, causing temporary changes in the ice-flow direction by tens of degrees.

No changes were observed at D3 during the jökulhlaup (Fig. 5). The vertical movement was as expected, due to surface melting and down-glacier ice movement. The horizontal velocities were approximately constant.

As for the October 2008 jökulhlaup, the effect of surface melting and down-glacier movement with the ice of the GPS instruments at D15 and D8 on the measured vertical velocities is small in comparison with the velocity changes induced by the jökulhlaups and can be ignored.

The propagation velocity of the subglacial flood front is estimated at ~0.2 m s^{-1} between D15 and D8. The propagation velocity cannot be calculated between D8 and D3 as no signal of the flood front was observed at D3. The propagation velocity between D8 and the glacier snout is uncertain, as the start of flood at the ice margin is unclear, but it can be inferred to have been in the range 0.1–0.3 m s^{-1}.

The length of the subglacial pressure wave is harder to estimate than for the October event because the lowering in the wake of the pressure wave is hard to distinguish. The distance from the flood front to the point of maximum vertical displacement can be estimated at $L_{\Delta p}$ = 1–2 km for D15 and $L_{\Delta p}$ = 2–4 km at D8. The potential gradient that drives the sheet flow inside the pressure wave cannot be calculated from Eqn (8) because the sheet thickness behind the wave, h_{sb}, cannot be estimated. Assuming that the correction for head loss within the pressure wave is 50% of the estimated overpressure, similar to that for the October event, leads to Δp = 0.05–0.10 MPa at D15 and Δp = 0.15–0.31 MPa at D8.

Interpretation of observations of the Skaftá jökulhlaups

Observations of outflow from large continuous segments of the glacier margin during the beginning of the October 2008 jökulhlaup in Skaftá suggest drainage from a subglacial sheet-like flow in the wake of a pressure wave and lifting due to basal water pressure higher than ice overburden (Sugiyama and others, 2008). Such sheet-like flow is unstable to irregularities in sheet thickness, so conduits are expected to eventually grow by melt–discharge feedback (Walder, 1982) in areas where the melt-rate ability of the conduit, μ, is positive (Magnússon and others, 2011). The development of the subglacial flood path in the wake of the pressure wave is consequently dependent on the local value of μ. Contraction of the flood path into a few main conduits near the glacier margin is expected as μ is positive there and up to the location of D3.

The second phase of lifting at D3 and subsequent lowering, while the discharge of the October jökulhlaup was still increasing (Fig. 3), can be interpreted as an evolution of an

initial sheet-like flood path into efficient conduits. Increasing discharge for a sheet-like subglacial flood path implies a thicker sheet and lifting of the glacier surface, whereas conduit growth can increase the efficiency of the flood path without increased bed separation. Draining of the water stored in the sheet into the growing conduits then leads to the observed lowering. Lower surface elevation at D3 at the end of the jökulhlaup may be due to the closure of such a conduit or erosion of bed sediments by the flood (Ng, 1998) but this cannot be ascertained on the basis of the available observations.

Sustained lifting while local inflow was increasing at D8 during the October jökulhlaup and at D15 during the August jökulhlaup implies increased flood path efficiency by thickening of the sheet during the whole event with little or no conduit growth. This is consistent with the adverse bed slope at D15, i.e. more than four times the magnitude of the surface slope (Fig. 2), which may be expected to cause glaciohydraulic supercooling at this location (Alley and others, 1998; Clarke, 2005). This leads to negative melt-rate ability μ that prevents melt enlargement of conduits. Adverse bed slope a short distance downstream of D8 may be expected to inhibit conduit growth there too as further discussed below.

A second phase of uplift was not detected at D8 during the August 2008 Skaftárjökull jökulhlaup, which had an order-of-magnitude smaller discharge and much smaller induced surface motions compared with the October flood. The reason for this difference in induced ice motion at D8 between the August and October events is not obvious but could be related to transverse variability across the subglacial path in the much smaller August flood that is not resolved by our point observations.

The difference between the ice motion at D3 and D8 induced by the October jökulhlaup and the difference between ice motion at D8 in the October and the August jökulhlaups demonstrates the importance of local surface and bed topographies for the path development and shows that detailed temporal and spatial modelling of the flood path development and ice dynamics is needed to understand rapidly rising jökulhlaups.

The subglacial propagation velocities for the two jökulhlaups in Skaftá are in the range 0.1–0.6 m s^{-1}, similar to ~0.5 m s^{-1} estimated by Magnússon and others (2007) for a small jökulhlaup in Skaftá in 1995 and 0.2–0.4 m s^{-1} for a jökulhlaup from the western cauldron in 2006 (unpublished data from the Icelandic Meteorological Office). These speeds are substantially lower than the mean propagation velocity of ~1.3 m s^{-1} for the large jökulhlaup from Grímsvötn in November 1996 (Björnsson, 2002), indicating that large subglacial floods propagate faster along the glacier bed as would be expected from the larger spatial dimensions of the subglacial flood tongue and higher overpressure of the larger floods.

Dynamics of the flood front at Skaftárjökull

The uplift associated with the passage of a subglacial pressure wave can be caused by horizontal compression of the glacier due to longitudinal velocity gradients across the front as well as by viscous and elastic lifting of the glacier from the bed. The contribution due to horizontal compression for the two jökulhlaups can be estimated to be <5–15% based on the thickness of the glacier, $L_{\Delta p}$ and horizontal motion accumulated between the arrival of the wave and maximum horizontal velocity and is therefore ignored here.

The Maxwell time for the glacier before the arrival of the flood front is of the order of several hours, which is longer than the observed 30–120 min duration of lifting associated with the passage of the flood front. The Maxwell time for the deforming ice above the pressure wave is considerably shorter. Using Eqns (9) and (10) and physical parameters from Table 1, it is found to be several minutes for overpressures of 0.15–0.35 MPa at D3 and D8 in both jökulhlaups and <2 h for an overpressure of 0.05–0.10 MPa, which was estimated at D15 during the August jökulhlaup. The Maxwell time thus indicates that the flood front propagates in glacier ice where elastic effects are initially dominant, before the deformation pattern of the flood front is established, but strain softening induced by the separation of the glacier from the bed eventually leads to dynamics that are dominated by viscous deformation.

The vertical ice velocity due to viscous deformation and the elastic lifting in connection with the passage of the flood front may be calculated with Eqns (11) and (12) from estimates of the overpressure and the shortest horizontal dimension of the pressure wave. In a similar manner, the propagation velocity of the flood front and the maximum crack opening predicted by the LEFM theory of Tsai and Rice (2010, 2012) can be found with Eqns (13) and (14). Because of the approximate nature of these analyses, the results is expected to be interpreted as order-of-magnitude estimates, intended to give an indication of the plausibility of the pressure wave as a conceptual model for the propagating subglacial flood front. The calculated vertical velocities and elastic lifting fall within wide ranges, $w_v = 0.03$–55 m d^{-1} and $\epsilon_e = 0.05-0.3$ m, for overpressures of 0.15–0.35 MPa acting over horizontal dimensions in the range 1–2 km, and using parameters from Table 1. The viscous vertical velocities correspond to total viscous lifting of 0.01–2 m during the passage of the wave. The lowest estimated value of 0.05 MPa for the overpressure at D15 in August leads to much lower velocities that cannot be considered realistic. More reasonable velocities can be obtained if a longer length scale is chosen as Eqn (11) is very sensitive to the choice of the length scale. The observed rates of vertical lifting, $w_v = 1-30$ m d^{-1}, and maximum lifting of 0.15–0.98 m, are on the same orders of magnitude but the wide ranges preclude detailed comparison for each location in the two jökulhlaups. The analysis indicates that the pressure wave has a lateral width

Table 1. Physical parameters used in conduit growth calculations

Parameter	Symbol	Value
Acceleration of gravity	g	9.82 m s^{-2}
Density of ice	ρ_i	910 kg m^{-3}
Density of water	ρ_w	1000 kg m^{-3}
Latent heat of fusion	L	3.34×10^5 J kg^{-1}
Glen ice rheology flow-law exponent	n	3
Glen ice rheology flow-law rate factor	B	7.5×10^7 Pa s$^{1/3}$
Pressure-melting coefficient	c_t	7.4×10^{-8} K Pa^{-1}
Heat capacity of water	c_w	4.22×10^3 J kg^{-1} K^{-1}
Young's modulus for ice	E	8.7×10^9 Pa
Poisson's ratio of ice	ν	0.31
Shear modulus for ice	G	3.7×10^9 Pa

greater than or equal to the along-flood-path length because a narrower wave, of the order of several hundred metres wide for example, would lead to much lower vertical velocities (of the order of mm d^{-1}) and maximum elastic lifting (of the order of mm) that cannot be reconciled with the observation of the propagating flood front.

The LEFM theory of Tsai and Rice (2012) leads to crack-tip propagating velocities $U_{tip} = 0.02-9$ m s^{-1} for overpressures $\Delta p = 0.05-0.35$ MPa, $L_{\Delta p} = 1-2$ km, $(L_{\Delta p}/h_i) = 2-5$, Nikuradse roughness heights calculated from Manning's friction factor, $n_m = 0.01-0.1$ m$^{-1/3}$ s as reported for subglacial conditions by Cuffey and Paterson (2010), and physical parameters from Table 1. This range overlaps the observed flood front velocities of 0.1–0.6 m s^{-1} for the jökulhlaups. The predicted elastic lifting at the point of maximum overpressure is found to be 0.02–3.6 m, again overlapping the observed lifting of 0.15–0.98 m. A narrower range of overpressures, 0.15–0.35 MPa and a middle-of-the-range value, $n_m =$ 0.033 m$^{-1/3}$ s, for the Manning roughness, corresponding to natural river beds, leads to crack-tip velocities in the range 0.4–3 m s^{-1} and maximum lifting of 0.08–3.6 m. These calculations indicate that turbulent, hydraulic fracture at the tip of the pressure wave is an important physical process in the propagation of the flood front and that both elastic and viscous deformations contribute to the lifting of the glacier.

Local conduit growth at Skaftárjökull

The field observations of the October 2008 jökulhlaup show development from sheet flow to conduits at the glacier margin over the course of the jökulhlaup, and the GPS measurements at D3 during the August jökulhlaup indicate that the subglacial water flow at D3 was confined to conduits for the whole jökulhlaup. Farther up-glacier, this jökulhlaup appears to have started with the propagation of a pressure wave implying sheet flow. Conditions for conduit development can be analysed in terms of the melt rate ability, $\mu = -(\partial\phi/\partial s) + c_t\rho_w c_w(\partial p_w/\partial s)$, using Eqn (4) to estimate conduit enlargement based on the local flood path geometry, an estimate for an initial conduit size and physical parameters from Table 1. The modelled conduit development and estimated initial cross-sectional area is highly dependent on the selected Manning's coefficient for friction, n_m. We will consider the same range of n_m as above but use $n_m = 0.033$ m$^{-1/3}$ s, corresponding to natural river beds, when we need a single explicit value.

The melt-rate ability is negative at D15 and a short distance downstream from D8 so conduit growth is not expected at those locations as further discussed below. The melt-rate ability is positive at D3, so conduits are predicted to grow there. An initial cross section of 6–30 m^2 for a conduit at D3 in August 2008 is estimated for the range of n_m given above, if a single conduit that carries the measured pre-jökulhlaup river discharge is assumed (after subtraction of runoff from the watershed below this location (Kristinsson, 2005)). The increased carrying capacity of such a conduit in 2 d is 100–1000 m^3 s^{-1}, and 720 m^3 s^{-1} for $n_m = 0.033$ m$^{-1/3}$ s. The observed discharge increase during the first 2 d of the jökulhlaup is 170 m^3 s^{-1}. So this analysis shows that conduit growth starting from the late-summer subglacial hydrological conditions at D3 can accommodate the observed rise in the discharge of the August 2008 jökulhlaup, which is consistent with the GPS measurements at D3 that show no lifting of the glacier for this jökulhlaup.

Estimating a plausible initial cross-sectional area in August is harder at D8 than D3. Assuming an initial cross-sectional area of 10 m^2 as an upper bound results in conduit growth that is an order of magnitude too slow to accommodate the observed discharge increase. The initial rise in the discharge at this location is, thus, hard to explain without invoking sheet flow, which is consistent with the GPS measurements that show lifting of the glacier indicating sheet flow at the beginning of the jökulhlaup.

Similar calculations using the measured base discharge before the October 2008 jökulhlaup to estimate initial cross-sectional areas for a conduit at D3 and D8 indicate that conduit growth is two orders of magnitude too slow to accommodate the rapid initial discharge increase of the October flood.

Observations of jökulhlaups from Grímsvötn

The two jökulhlaups from Grímsvötn are similar in terms of duration, discharge and total volume (Fig. 3). The lowering of the Grímsvötn ice cover corresponds to the release of ~0.5 and 0.6 km^3 during the 2004 and 2010 jökulhlaups, respectively. An additional ~0.1 km^3 of meltwater was produced during the 2004 eruption in Grímsvötn (Guðmundsson and others, 2009), starting around the peak of the jökulhlaup. Up to ~0.2 km^3 or ~1/3 of the flood water was stored in the flood path beneath the glacier (Fig. 6) during the 2010 jökulhlaup. Despite significant uncertainty in the ice-cover elevation at any given time, the peak subglacial water storage is fairly well established (uncertainty <25%) due to the time lag between the outflow from Grímsvötn and the observed river discharge. Analysis of the 2004 jökulhlaup (not shown) similar to that used to derive Figure 6 for the 2010 jökulhlaup shows that when the eruption started in 2004, ~0.2 km^3 of water was already stored in the subglacial flood path. This flood water storage is an order of magnitude larger than the volume of a conduit formed by melting during these floods.

Seismic tremor measured at Grímsfjall, ~1 km from the lake, and elevation measurements on the Grímsvötn ice cover suggest that water started to flow out of the lake no

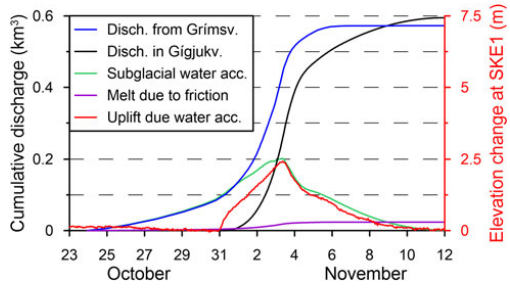

Fig. 6. Observed accumulated drainage out of Grímsvötn (blue) and accumulated discharge at the glacier margin in Gígjukvísl (black) during the 2010 jökulhlaup from Grímsvötn. Subglacial storage (green) is estimated as the difference of the two curves plus the calculated amount of melt due to friction in the flow (magenta). Estimated uplift due to water accumulation (red) at SKE1 is presented by the right *y*-axis.

later than 26 and 27 October in 2004 and 2010, respectively. The influence of the flood water on glacier motion at the GPS station was in both cases observed ~3.5 d later, but increased conductivity was measured in Gígjukvísl on 29 October during the 2010 jökulhlaup, a day before acceleration of surface motion was detected. Timing of the onset of increased discharge at the glacier margin is uncertain in the two jökulhlaups as only water stage is measured in Gígjukvísl (in 2010) and Skeiðará (in 2004) and the calculation of discharge from water stage for braided glacial rivers on a sediment bed is uncertain. Clear signs of increased discharge are seen shortly after 01:30 on 30 October in 2004 and 10:00 on 31 October in 2010 but the discharge may have started to increase up to a day earlier in both cases. The delay due to the flow from the glacier margin to the water stage and discharge measurement sites may be estimated to be ~1 h.

The horizontal and vertical displacement records at the GPS stations do not indicate the propagation of a pressure wave at the beginning of the jökulhlaups as is observed on Skaftárjökull in August and October 2008. The effect on the glacier motion is quite different between the stations (Fig. 3). In 2010, gradual acceleration in horizontal motion probably starts ~18:00 on 30 October at SKE1 located 9 km from the glacier margin, where the glacier is ~600 m thick (Fig. 2). The velocity increases from 0.4 m d^{-1} between 17:00 and 18:00 to 2.1 m d^{-1} around midnight and continues to accelerate to a peak velocity of 4.0 m d^{-1} between 05:00 and 06:00 the following morning. Uplift of the station starts shortly before midnight, ~6 h later than the horizontal acceleration. The station rises by 0.4 m until 06:00 the following morning, when the rate of rise slows down by half. The vertical rise remains constant at ~0.8 m d^{-1} and the horizontal velocity ~3 m d^{-1} for 3 d until 06:00 on 3 November. The rise then stopped and the station remained at approximately constant elevation for 6 h, while the peak discharge of the jökulhlaup passed the station. While the GPS station remained at this elevation, the horizontal velocity decreased from 3.1 to 1.1 m d^{-1}. The station subsided for ~1 week after the discharge peaked, by 0.9 m during the first 24 h, but then at a gradually slower rate and the horizontal velocity decreased gradually from 1.1 m d^{-1} to a typical winter velocity value of 0.3 m d^{-1}.

In the morning of 30 October 2004, strong acceleration from ~0.15 m d^{-1} between 06:00 and 07:00 to ~1.0 m d^{-1} between 07:00 and 08:00 was observed at the GPS station SKE2, 800 m from the glacier margin where the ice thickness is ~200 m (Fig. 2). The start of the rise at the station is slow. The timing of the start is therefore inaccurate but seems to be ~3 h later. The station rises ~0.20 m during the next 2 d and the horizontal velocity fluctuates ~1 m d^{-1}. Around 17:00 on 1 November, the station starts accelerating steadily from 1.1 m d^{-1} between 17:00 and 18:00 to 2.2 m d^{-1} between 22:00 and 23:00. The rise also becomes faster ~22:00; the station rose by 0.15 m during the following 12 h. An eruption started in Grímsvötn in the evening of 1 November. A seismic tremor measured at Grímsfjall indicates the onset of the eruption at 21:50, a few hours after the horizontal velocity at SKE2 started increasing and at approximately the same time as the uplift rate increased. The horizontal velocity decreases gradually from 2.2 m d^{-1} at midnight to 1.4 m d^{-1} between 12:00 and 13:00 the following day, around the time when the maximum vertical displacement has been reached. Then the horizontal velocity was reduced by half to 0.7 m d^{-1} in 1 h after which the glacier gradually decelerated. The station stayed at the peak elevation for ~8 h, while the peak discharge of the jökulhlaup passed this location, and then started subsiding slowly. When the station was taken down 4 d later, it had subsided by 0.11 m and the subsidence was still ongoing. The daily horizontal displacement of the station at that time was 0.15 m, whereas the daily displacement prior to the jökulhlaup was ~0.08 m.

The total vertical displacement at both stations on Skeiðarárjökull is positive, most likely due to adverse bed slope below the stations (Fig. 2). During rapid basal sliding, the glacier may be assumed to move effectively as a solid block along the bed, causing the bed slope to control the direction of ice motion at the surface. It is difficult to estimate the bed slope underneath the station accurately based on the existing bedrock data (Björnsson and others, 1999; Magnússon, 2008; Magnússon and others, 2009). The slope of the 3-D total displacement vector during the jökulhlaups, 2.6° at SKE1 in 2010 and 3.6° at SKE2 in 2004, is within the likely range of adverse bed slope at both locations. If we compensate for vertical motion due to block movement along the bed using the above slope values, the residual vertical displacement may be assumed to be caused by water accumulation and depletion. It reaches a maximum of 2.5 m at SKE1 in 2010 (Fig. 6) and 0.17 cm at SKE2 in 2004. Uplift due to water accumulation may be somewhat underestimated at SKE2 because the station was still subsiding when it was taken down.

As mentioned above, the damage done to the seal at Grímsvötn by the catastrophic jökulhlaup in November 1996 altered the characteristics of slowly rising jökulhlaups from the subglacial lake. Figure 7 compares the rise of the 2004 and 2010 jökulhlaups studied here with seven earlier slowly rising jökulhlaups for which discharge measurements are available (Rist, 1955, 1973; unpublished data from the Icelandic Meteorological Office). The timescale needed for the flood discharge to rise by a factor of $e = 2.7$ was shortened from 3–6 d to slightly over a day in 1996. This distinct change indicates that the timescale of the rise in discharge is controlled by conditions at a particular location of the flood path rather than the large-scale path geometry, such as the vertical relief, the total path length or the overall scale for the ice thickness or potential gradient, as these quantities did not change fundamentally in 1996.

Interpretation of observations of the Grímsvötn jökulhlaups

The lifting at SKE1 on Skeiðarárjökull during the 2010 jökulhlaup shares a number of characteristics with the second phase of lifting at D8 on Skaftárjökull during the October 2008 jökulhlaup, such as close resemblance to the variation in discharge (see Figs 3 and 6). The geometry of the flood path at the two locations is similar, with an adverse bed slope, steep enough to prevent the development of conduits, less than one ice thickness farther down-glacier (Fig. 2). We interpret the rise in the ice surface as an indication of widespread subglacial accumulation of water that we expect to occur upstream of locations with adverse bed slope and conditions for supercooling that prevent the formation of efficient conduits. This accumulation is driven by two processes. Firstly, the rising discharge carried by sheet flow over the adverse bed slope requires a correspondingly greater sheet thickness, h_w, that may be expected to reach

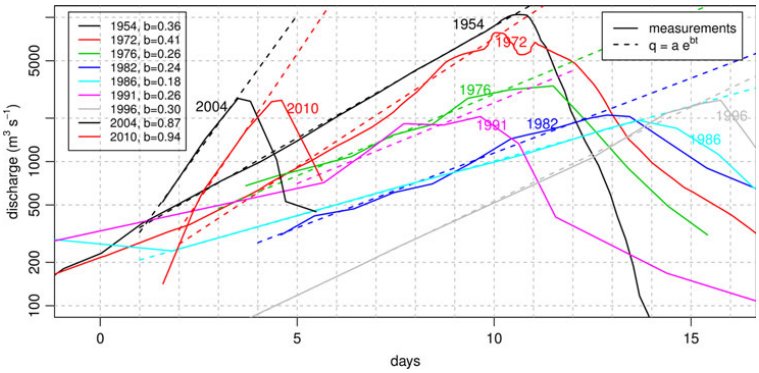

Fig. 7. Discharge variation with time for nine slowly rising jökulhlaups from Grímsvötn. The dashed lines show a log–linear fit, $Q = ae^{bt}$, to the rising limb of each curve, where t is time in days since the start of the rise in discharge and a and b are statistical parameters. The slope of the least-squares line, b (d^{-1}), for each jökulhlaup is given in the legend. The timescale needed for the exponential approximation to the discharge to rise by a factor of $e = 2.7$ is given by $1/b$. It was shortened by a factor of ~3–4 after the catastrophic jökulhlaup in 1996.

some distance up-glacier from the start of the back slope, due to rigidity of the ice on timescales of hours, further enhanced by block flow of the glacier up the adverse bed slope. Secondly, the smaller efficiency of the path without conduits on the adverse bed slope will lead to greater hydraulic gradient there, which leads to comparatively high subglacial water pressures, lifting and accumulation of water upstream (Magnússon and others, 2011).

Uplift and subsequent subsidence over the duration of the jökulhlaup is also observed at SKE2 in 2004, probably due to water accumulation upstream of adverse bed slope, but an order of magnitude smaller than at SKE1 in 2010 (Fig. 3). The reason for this difference in magnitude is not clear but might be related to the short distance (800 m) to the glacier margin where the water pressure becomes equal to atmospheric pressure and remnants of conduits from the previous summer may still be present due to slow creep closure under thin ice.

Subglacial accumulation of water of the magnitude encountered at both Skaftárjökull and Skeiðarárjökull during the jökulhlaups considered here, can be expected to greatly reduce basal drag over large areas by drowning bed roughness elements and decreasing effective pressure at the bed (Iken and Bindschadler, 1986). This change in the force balance of the glacier, from local control to global control (Cuffey and Paterson, 2010), is a probable explanation for the observed changes in horizontal velocities and ice-flow direction during the jökulhlaups. Similar increase in horizontal velocity and changes in flow direction in connection with enhanced basal slip during jökulhlaups or intense rainfall events have been observed before for Skeiðarárjökull (Magnússon and others, 2007, 2011) and observed and modelled for Gornergletscher, Switzerland (Sugiyama and others, 2007; Riesen and others, 2010).

DISCUSSION

The GPS measurements of ice motion during the four jökulhlaups described above, show many features that shed light on the dynamics of the subglacial hydrological system during rapid changes in water input. The dynamics are apparently complex and depend among other things on the state of the subglacial hydrological system before the flood and the local geometry of the glacier surface and the bed.

Grímsvötn is well known in the glaciological literature, and the jökulhlaup in 1972 (Rist, 1973) was used by Nye (1976) in his development of a dynamical theory for slowly rising jökulhlaups where the conduit-melt–discharge feedback was first used as an explanation for the rise in jökulhlaup discharge with time. In its original form, this theory assumes that the rise of the flood is driven by the average potential gradient from the source lake to the outlet. The change in the character of slowly rising jökulhlaups from Grímsvötn in 1996, when the timescale of the rise in discharge was shortened by a factor of ~3–4 (Fig. 7), indicates that the dynamics of slowly rising jökulhlaups is more complex than can be reconciled with Nye's theory and points to local control or bottlenecks in the path (Clarke, 1982, 2003) that determine the rise in discharge. It appears that the damage done to the seal in 1996 moved the control of the flood to a different location where conditions allowed a much more rapid rise in discharge. This implies that Manning's friction coefficient, determined from Nye's theory by statistical fitting to the variation of the discharge with time using a single along-path average of the potential gradient, must be considered as a phenomenological parameter that does not have a clear meaning in terms of conduit roughness or other physical properties of the path. The same applies to similar theories based on along-path averages of the potential gradient and conduit cross section (e.g. Clarke, 1982).

The lifting of the glacier surface shown by the GPS measurements and the subglacial accumulation of water in the 2004 and 2010 jökulhlaups reveal another interesting aspect of slowly rising jökulhlaups that cannot be accounted for by Nye's theory or its later developments (e.g. Spring and Hutter, 1981, 1982; Clarke, 2003). Subglacial water accumulation at Skeiðarárjökull has also been observed before the change of the timescale of discharge rise in 1996, for a jökulhlaup under normal conditions (Magnússon and others, 2007) and for a jökulhlaup during a surge (Björnsson, 1998). The subglacial accumulation of 0.2 km^3 of flood water in the 2010 jökulhlaup corresponds to a 2 m

thick and 2 km wide tongue of water extending along the entire 50 km long flood path. Of course, the water stored subglacially does not have this simple geometry. Most likely, it was accumulated in a few areas along the flood path of greater width and water depth where subglacial ponding is favoured by the local glacier surface and bed topographies. The discharge from glacier margin during the jökulhlaup is a combination of outflow from the source lake, with a delay because of the time needed for the water to flow down-glacier, and the release of ponded flood water stored subglacially. In spite of the fact that Nye's theory does not account for this subglacial ponding, the rise in discharge can be reproduced surprisingly well by the theory with parameters statistically determined to fit the observed discharge curve as mentioned above. This points to local control or bottlenecks in the path that determine the rise in discharge by conduit-melt–discharge feedback. These bottlenecks would not necessarily be located at a seal below the thickest ice as envisioned by Clarke (1982). They could be located in regions of channel growth between areas of subglacial storage and glacier lifting. Melting at such bottlenecks could be driven by a potential gradient that differs substantially from both the average potential gradient for the whole flood path and the gradient predicted by modelling assuming conduit flow along the path (Spring and Hutter, 1981, 1982; Clarke, 2003). This again indicates that such theories should be considered phenomenological rather than physical so that the parameters, such as the Manning's coefficient, n_m, and the variables, such as the channel cross section, S, may not have a clear physical meaning.

Jökulhlaups in Skaftá appear to be fundamentally different from jökulhlaups from Grímsvötn in having a much more rapid rise in discharge that does not have the near-exponential form so characteristic of most floods from Grímsvötn (Fig. 7). The GPS measurements show that the initiation of these rapidly rising floods is associated with a wave of surface lifting and subsequent subsidence moving down-glacier, in agreement with the concept of a localized, subglacial pressure wave suggested by Jóhannesson (2002). A several-km wide pressure wave followed by sheet flow is, furthermore, consistent with observations that indicate reduced basal friction over a several-km wide flood path for a jökulhlaup at Skaftárjökull in 1995 (Magnússon and others, 2007). Order-of-magnitude agreement between theoretical predictions and the observed ice velocities, lifting of the glacier and the down-glacier propagating velocities of the jökulhlaup wave indicates that viscous and elastic deformation as well as turbulent hydraulic fracture at the tip of the flood front are all important processes in the propagation of the pressure wave.

We have not identified quantitative conditions that determine whether a jökulhlaup develops as a rapidly rising flood, with an initial subglacial pressure wave, or slowly, with a near-exponential rise in the discharge. This must be considered as the main unresolved question in the study of jökulhlaups. Both these types of jökulhlaups appear from our observations to be associated with widespread subglacial ponding of flood water at preferred locations along the flood path where a substantial part of the flood volume is temporarily accumulated and released. This implies considerable challenges for quantitative understanding and modelling of jökulhlaups as detailed modelling of widespread lifting, and related dynamic effects on the movement of the overlying ice, requires an integrated modelling of subglacial water flow and ice movement that has not been attempted so far in jökulhlaup studies.

CONCLUSIONS

We have presented several different types of movement of the overlying ice in response to jökulhlaups. They include rapid vertical uplift, often followed by (partial) subsidence, during the initiation of the flood, uplift and subsequent subsidence that takes place during the entire flood, horizontal acceleration, temporary change in horizontal ice-flow direction by up to tens of degrees and temporary reverse ice motion during uplift and subsidence creating backward loop motion. These observations can be interpreted in terms of the development of the jökulhlaup at the bed of the glacier. The observations of jökulhlaups at Skeiðarárjökull in 2004 and 2010 indicate subglacial water pressure higher than overburden, lifting and lateral water storage in typical slowly rising jökulhlaups. The rapid uplift at the beginning of jökulhlaups in Skaftá indicates the passage of a subglacial pressure wave that forms the initial flood path of rapidly rising jökulhlaups. We, furthermore, interpret observations from a rapidly rising jökulhlaup in Skaftá in August 2008 such that parts of the initial flood path were formed by conduit-melt–discharge feedback as is considered typical for slowly rising jökulhlaups. The classification of jökulhlaups into two distinct categories, rapidly and slowly rising, therefore, seems to be too simple. Jökulhlaup behaviour appears to be more of a spectrum. Extremely rapidly rising jökulhlaups, such as the large November 1996 jökulhlaup from Grímsvötn and large jökulhlaups from the eastern Skaftá cauldron, where most of the initial flood path is formed by propagation of a subglacial pressure wave (Jóhannesson, 2002), will then form one end of the spectrum. Slowly rising jökulhlaups, confined in a conduit enlarged by melt–discharge feedback for the whole flood path, are then at the other end of the spectrum. The slowly rising jökulhlaups from Grímsvötn after the November 1996 event, which rise much faster than jökulhlaups before November 1996 as discussed above, and rapidly rising jökulhlaups from the western Skaftá cauldron that rise much more slowly than large jökulhlaups from the eastern cauldron, are examples of events that seem to be of an intermediate type between the two extremes in the spectrum of rapidly and slowly rising jökulhlaups.

ACKNOWLEDGEMENTS

The Icelandic Research Fund, the Landsvirkjun (National Power Company of Iceland) Research Fund, the Icelandic Road Administration, the Kvískerja fund and the Iceland Glaciological Society provided financial and field support, which made this study possible. We thank Helgi Björnsson and Alexander H. Jarosch for stimulating discussion about jökulhlaups, Oddur Sigurðsson for photographs and descriptions from the overflight over the October 2008 jökulhlaup in Skaftá, and the many people who worked with us in the field, in particular our technicians Vilhjálmur S. Kjartansson and Gunnar Sigurðsson. We are grateful to the Scientific Editor Gwenn Flowers and the reviewers Victor C. Tsai and Jason Amundson for constructive comments that significantly improved the manuscript. This publication is contribution No. 68 of the Nordic Centre of Excellence SVALI, 'Stability

and Variations of Arctic Land Ice', funded by the Nordic Top-level Research Initiative (TRI).

REFERENCES

Ágústsdóttir AM and Brantley SL (1994) Volatile fluxes integrated over four decades at Grímsvötn volcano, Iceland. *J. Geophys. Res.*, **99**, 9505–9522

Alley RB, Lawson DE, Evanson EB, Strasser JC and Larson GJ (1998) Glaciohydraulic supercooling: a freeze-on mechanism to create stratified, debris-rich basal ice: II. Theory. *J. Glaciol.*, **44**(148), 563–569

Anderson RS, Walder JS, Anderson SP, Trabant DC and Fountain AG (2005) The dynamic response of Kennicott Glacier, Alaska, USA, to the Hidden Creek Lake outburst flood. *Ann. Glaciol.*, **40**, 237–242 (doi: 10.3189/172756405781813438)

Bartholomaus TC, Anderson RS and Anderson SP (2008) Response of glacier basal motion to transient water storage. *Nat. Geosci.*, **1**(1), 33–37 (doi: 10.1038/ngeo.2007.52)

Bartholomaus TC, Anderson RS and Anderson SP (2011) Growth and collapse of the distributed subglacial hydrologic system of Kennicott Glacier, Alaska, USA, and its effects on basal motion. *J. Glaciol.*, **57**(206), 985–1002 (doi: 10.3189/002214311798843269)

Björnsson H (1974) Explanation of jökulhlaups from Grímsvötn, Vatnajökull, Iceland. *Jökull*, **24**, 1–26

Björnsson H (1975) Subglacial water reservoirs, jökulhlaups and volcanic eruption. *Jökull*, **25**, 1–11

Björnsson H (1976) Marginal and supraglacial lakes in Iceland. *Jökull*, **26**, 40–51

Björnsson H (1977) The cause of jökulhlaups in the Skaftá river, Vatnajökull. *Jökull*, **27**, 71–78

Björnsson H (1988) *Vatnajökull, western part subglacial bedrock surface, Map 1:200 000*. Science Institute, University of Iceland, Reykjavík

Björnsson H (1992) Jökulhlaups in Iceland: prediction, characteristics and simulation. *Ann. Glaciol.*, **16**, 95–106

Björnsson H (1997) Grímsvatnahlaup fyrr og nú. In Haraldsson H ed. *Vatnajökull. gos og hlaup 1996*. Icelandic Public Roads Administration, Reykjavík, 61–77

Björnsson H (1998) Hydrological characteristics of the drainage system beneath a surging glacier. *Nature*, **395**, 771–774 (doi: 10.1038/27384)

Björnsson H (2002) Subglacial lakes and jökulhlaups in Iceland. *Glob. Planet. Change*, **35**, 255–271 (doi: 10.1016/S0921-8181(02)00130-3)

Björnsson H (2010) Understanding jökulhlaups: from tale to theory. *J. Glaciol.*, **56**(200), 1002–1010 (doi: 10.3189/002214311796406086)

Björnsson H and Kristmannsdóttir H (1984) The Grímsvötn geothermal area, Vatnajökull, Iceland. *Jökull*, **34**, 25–50

Björnsson H, Pálsson F and Magnússon E (1999) *Skeiðarárjökull: Landslag og rennslisleiður vatns undir sporði*. Science Institute, University of Iceland, Reykjavík, Report RH-11-1999

Clarke GKC (1982) Glacier outburst floods from 'Hazard Lake', Yukon Territory, and the problem of flood magnitude prediction. *J. Glaciol.*, **28**(98), 3–21

Clarke GKC (2003) Hydraulics of subglacial outburst floods: new insights from the Spring–Hutter formulation. *J. Glaciol.*, **49**(165), 299–313 (doi: 10.3189/172756503781830728)

Clarke GKC (2005) Subglacial processes. *Ann. Rev. Earth Planet. Sci.*, **33**, 247–276 (doi: 10.1146/annurev.earth.33.092203.122621)

Cuffey KM and Paterson WSB (2010) *The physics of glaciers*, 4th edn. Elsevier, Oxford

Doyle SH and *et al*. (2015) Amplified melt and flow of the Greenland ice sheet driven by late-summer cyclonic rainfall. *Nat. Geosci.*, **8**, 647–653 (doi: 10.1038/ngeo2482)

Flowers GE, Björnsson H, Pálsson F and Clarke GKC (2004) A coupled sheet–conduit mechanism for jökulhlaup propagation. *Geophys. Res. Lett.*, **31**(5), L05401 (doi: 10.1029/2003GL019088)

Fricker HA, Scambos T, Bindschadler R and Padman L (2007) An active subglacial water system in West Antarctica mapped from space. *Science*, **315**(5818), 1544–1548 (doi: 10.1126/science.1136897)

Guðmundsson MT, Björnsson H and Pálsson F (1995) Changes in jökulhlaup sizes in Grímsvötn, Vatnajökull, Iceland, 1934–1991, deduced from in situ measurements of subglacial lake volume. *J. Glaciol.*, **41**(138), 263–272

Guðmundsson MT, Sigmundsson F and Björnsson H (1997) Ice–volcano interaction of the 1996 Gjálp subglacial eruption, Vatanjökull, Iceland. *Nature*, **389**, 954–957 (doi: 10.1038/40122)

Guðmundsson MT and 7 others (2009) Energy partitioning in the phreatomagmatic basaltic eruption of Grímsvötn in 2004. In *American Geophysical Union, Fall Meeting 2009*, abstract #V11B-1952

Herring TA, King RW and McClusky SC (2010) *Introduction to GAMIT/GLOBK. Release 10.4*. Massachusetts Institute of Technology, Cambridge, MA. http://www-gpsg.mit.edu/~simon/gtgk

Huss M, Bauder A, Werder M, Funk M and Hock R (2007) Glacier-dammed lake outburst events of Gornersee, Switzerland. *J. Glaciol.*, **53**(181), 189–200 (doi: 10.3189/172756507782202784)

Iken A and Bindschadler RA (1986) Combined measurements of subglacial water pressure and surface velocity of Findelengletscher, Switzerland: conclusions about drainage system and sliding mechanism. *J. Glaciol.*, **32**(110), 101–119

Jóhannesson T (2002) Propagation of a subglacial flood wave during the initiation of a jökulhlaup. *Hydrol. Sci. J.*, **47**(3), 417–434 (doi: 10.1080/02626660209492944)

Kristinsson B (2005) *Rennslismælingar í vestari kvísl Skaftár við vhm 470 og samanburður við rennsli Skaftár hjá Sveinstindi, vhm 161, árin 1997–2004*. National Energy Authority, Reykjavík, Report BK-2005/01

Magnússon E (2008) Glacier hydraulics explored by means of SAR-interferometry. (PhD dissertation, University of Innsbruck)

Magnússon E, Rott H, Björnsson H and Pálsson F (2007) The impact of jökulhlaups on basal sliding observed by SAR interferometry on Vatnajökull, Iceland. *J. Glaciol.*, **53**(181), 232–240 (doi: 10.3189/172756507782202810)

Magnússon E, Pálsson F and Björnsson H (2009) *Breytingar á austanverðum Skeiðarárjökli og farvegi Skeiðarár 1997–2009 og framtíðarhorfur [Changes at the eastern part of Skeiðarárjökull outlet glacier and the river Skeiðará, 1997–2009, and future prospects]*. Institute of Earth Sciences, University of Iceland, Reykjavík, Report RH-08-2009

Magnússon E and 8 others (2011) Localized uplift of Vatnajökull, Iceland: subglacial water accumulation deduced from InSAR and GPS observations. *J. Glaciol.*, **57**(203), 475–484 (doi: 10.3189/002214311796905703)

Melosh HJ (2011) *Planetary surface processes*. Cambridge University Press, Cambridge

Ng FSL (1998) Mathematical modelling of subglacial drainage and erosion. (DPhil thesis, University of Oxford)

Nye JF (1976) Water flow in glaciers: jökulhlaups, tunnels and veins. *J. Glaciol.*, **17**(76), 181–207

Pálsson F, Björnsson H, Haraldsson HH and Magnússon E (2006) *Vatnajökull: mass balance, meltwater drainage and surface velocity of the glacial year 2004–2005*. Institute of Earth Sciences, University of Iceland, Reykjavík, Report RH-06-2006

Pollard DD and Fletcher RC (2005) *Fundamentals of structural geology*. Cambridge University Press, Cambridge

Riesen P, Sugiyama S and Funk M (2010) The influence of the presence and drainage of an ice-marginal lake on the flow of Gornergletscher, Switzerland. *J. Glaciol.*, **56**(196), 278–286 (doi: 10.3189/002214310791968575)

Rignot E and Kanagaratnam P (2006) Changes in the velocity structure of the Greenland Ice Sheet. *Science*, **311**(5763), 986–990 (doi: 10.1126/science.1121381)

Rist S (1955) Skeiðarárhlaup 1954. *Jökull*, **5**, 30–36
Rist S (1973) Jökulhlaupaannáll 1971, 1972 og 1973. *Jökull*, **23**, 55–60
Roberts MJ, Russell AJ, Tweed FS and Knudsen O (2000) Ice fracturing during jökulhlaups: implications for englacial flood water routing and outlet development. *Earth Surf. Process. Landf.*, **25** (13), 1429–1446 (doi: 10.1002/1096-9837(200012)25:13<1429)
Röthlisberger H (1972) Water pressure in intra- and subglacial channels. *J. Glaciol.*, **11**(62), 177–203
Snorrason Á and *et al*. (1997) Hlaupið á Skeiðarársandi haustið 1996. Útbreiðsla, rennsli og aurburður. In Haraldsson H ed. *Vatnajökull. Gos og hlaup 1996*. Icelandic Public Roads Administration, Reykjavík, 79–137
Spring U and Hutter K (1981) Numerical studies of jökulhlaups. *Cold Reg. Sci. Technol.*, **4**(3), 227–244
Spring U and Hutter K (1982) Conduit flow of a fluid through its solid phase and its application to intraglacial channel flow. *Int. J. Eng. Sci.*, **20**(2), 327–363
Stearns LA, Smith BL and Hamilton GS (2008) Subglacial floods cause rapid increase in flow speed of a major East Antarctic outlet glacier. *Nat. Geosci.*, **1**, 827–831 (doi: 10.1038/ngeo0356)
Sugiyama S, Bauder A, Weiss P and Funk M (2007) Reversal of ice motion during the outburst of a glacier-dammed lake on Gornergletscher, Switzerland. *J. Glaciol.*, **53**(181), 889–898 (doi: 10.3189/172756507782202847)
Sugiyama S, Bauder A, Huss M, Riesen P and Funk M (2008) Triggering and drainage mechanisms of the 2004 glacier-dammed lake outburst in Gornergletscher, Switzerland. *J. Geophys. Res.*, **113**, F04019 (doi: 10.1029/2007JF000920)
Thórarinsson S (1974) *Vötnin stríð. Saga Skeiðarárhlaupa og Grímsvatnagosa [The swift flowing rivers. The history of Grímsvötn jökulhlaups and eruptions]*. Bókaútgáfa Menningarsjóðs, Reykjavík
Tsai VC and Rice JR (2010) A model for turbulent hydraulic fracture and application to crack propagation at glacier beds. *J. Geophys. Res.*, **115**, F03007 (doi: 10.1029/2009JF001474)
Tsai VC and Rice JR (2012) Modeling turbulent hydraulic fracture near a free surface. *J. Appl. Mech.*, **79**, 031003 (doi: 10.1115/1.4005879)
Walder JS (1982) Stability of sheet flow of water beneath temperate glaciers and implications for glacier surging. *J. Glaciol.*, **28**(99), 273–293
Zóphóníasson S (2002) *Rennsli í Skaftárhlaupum 1955–2002 [Discharge in jökulhlaups in Skaftá 1955–2002]*. National Energy Authority, Reykjavík, Report SZ-2002/01

Paper II

Subglacial flood path development during a rapidly rising jökulhlaup from the western Skaftá cauldron, Vatnajökull, Iceland.

Einarsson B, Jóhannesson T, Thorsteinsson Th, Gaidos E and Zwinger T (2017)
Journal of Glaciology, **63**(240), 670–682 (doi:10.1017/jog.2017.33)

Journal of Glaciology (2017), **63**(240) 670–682 doi: 10.1017/jog.2017.33

Subglacial flood path development during a rapidly rising jökulhlaup from the western Skaftá cauldron, Vatnajökull, Iceland

BERGUR EINARSSON,[1] TÓMAS JÓHANNESSON,[1] THORSTEINN THORSTEINSSON,[1] ERIC GAIDOS,[2] THOMAS ZWINGER[3]

[1]*Icelandic Meteorological Office, Reykjavík, Iceland*
[2]*Department of Geology & Geophysics, University of Hawai'i, Honolulu, Hawai'i, USA*
[3]*CSC – IT Center for Science Ltd., Espoo, Finland*
Correspondence: Bergur Einarsson <bergur@vedur.is>>

ABSTRACT. Discharge and water temperature measurements in the Skaftá river and measurements of the lowering of the ice over the subglacial lake at the western Skaftá cauldron, Vatnajökull, Iceland, were made during a rapidly rising glacial outburst flood (jökulhlaup) in September 2006. Outflow from the lake, flood discharge at the glacier terminus and the transient subglacial volume of floodwater during the jökulhlaup are derived from these data. The 40 km long initial subglacial path of the jökulhlaup was mainly formed by lifting and deformation of the overlying ice, induced by water pressure in excess of the ice overburden pressure. Melting of ice due to the heat of the floodwater from the subglacial lake and frictional heat generated by the dissipation of potential energy in the flow played a smaller role. Therefore this event, like other rapidly rising jökulhlaups, cannot be explained by the jökulhlaup theory of Nye (1976). Instead, our observations indicate that they can be explained by a coupled subglacial-sheet–conduit mechanism where essentially all of the initial flood path is formed as a sheet by the propagation of a subglacial pressure wave.

KEYWORDS: glacier hydrology, jökulhlaups (GLOFs), subglacial lakes

1. INTRODUCTION

Jökulhlaups in the river Skaftá from western Vatnajökull occur at 1–2 year intervals with volumes of 0.05–0.4 km^3 and maximum discharge of 50–3000 m^3 s^{-1} (Björnsson, 1977; Zóphóníasson, 2002; unpublished data from the Icelandic Meteorological Office). The floods originate from two subglacial lakes below 50–150 m deep and 1–3 km wide depressions (cauldrons) in the ~450 m thick surrounding ice cap. Together, the depressions drain ~50 km^2 of the ice cap (Pálsson and others, 2006) (Fig. 1). The jökulhlaups travel ~40 km subglacially before they emerge at the terminus of the outlet glacier Skaftárjökull.

Jökulhlaups in Skaftá reach maximum discharge in 1–3 days and typically recede in 1–2 weeks (Björnsson, 2002) (Fig. 2). They are on the 'rapidly rising' side of the spectrum of 'rapidly rising' to 'slowly rising' jökulhlaups (Einarsson and others, 2016). The hydrograph of slowly rising jökulhlaups, such as most floods from Grímsvötn subglacial lake in Vatnajökull, gradually rises to maximum discharge in 1–3 weeks and recedes in <1 week, often in only 1–3 days (Björnsson, 2002) (Fig. 2). Jökulhlaups from subglacial and marginal lakes at other locations in Iceland may rise even more rapidly than jökulhlaups in Skaftá and can reach maximum discharge in less than half a day (Thórarinsson, 1974; Sigurðsson and Einarsson, 2005; Jónsson and Þórarinsdóttir, 2011). The hydrographs of slowly rising jökulhlaups are reasonably well explained by the theory of conduit-melt–discharge feedback, developed by Nye (1976). The rapid initial increase of the hydrograph during jökulhlaups in Skaftá is difficult to explain with Nye's theory without invoking implausibly high temperature for the lake water (Björnsson, 1992), and many aspects of the dynamics of rapidly rising jökulhlaups are still unresolved. As rapidly rising jökulhlaups have a fast discharge increase, they may be extremely dangerous since warning times for response are short.

The fundamental reasons that govern whether a jökulhlaup develops as a rapidly rising or slowly rising flood are not fully understood. The predominant discharge development mechanism appears to be different for these two types of floods. Hydraulic uplift of the glacier, caused by water pressure exceeding glacier overburden pressure in a propagating subglacial pressure wave, is likely to be an important component in the flood path formation for rapidly rising jökulhlaups (Björnsson, 2002; Jóhannesson, 2002; Flowers and others, 2004; Roberts, 2005; Einarsson and others, 2016). Flood path formation by coupled subglacial sheet of water and conduit flow has been used for modelling of rapidly rising jökulhlaups (Flowers and others, 2004). The formation of the initial sheet has been proposed to be caused by ice dam flotation near the subglacial lake (Björnsson, 2002, 2010; Flowers and others, 2004; Sugiyama and others, 2008) and hydraulic jacking along the flood path (Flowers and others, 2004). Positive feedback between discharge and melting in the sheet leads to the creation of conduits that carry an increasing proportion of the water as the flood develops. The subglacial flood path of slowly rising jökulhlaups is, on the other hand, thought to be mainly formed by melting by frictional heat released in the flow by dissipation of potential energy and the initial heat of the source water (Nye, 1976; Spring and Hutter, 1981, 1982). Recent research on jökulhlaups from Grímsvötn indicates that lifting of the glacier may also play a role in flood path formation of some slowly rising jökulhlaups (Björnsson, 2010; Magnússon and others, 2011; Einarsson and others, 2016).

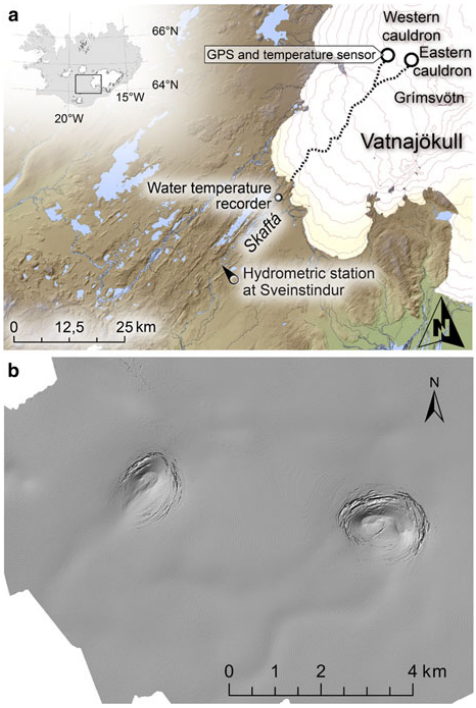

Fig. 1. (a) The Skaftá cauldrons and subglacial lakes in the western Vatnajökull ice cap and the upper part of the watershed of the Skaftá river. The inferred subglacial paths of jökulhlaups (dotted lines) and locations of instruments described in the text are shown. (b) A hillshade of a DEM of the cauldron area measured by lidar (acronym for 'light detection and ranging') in 2010.

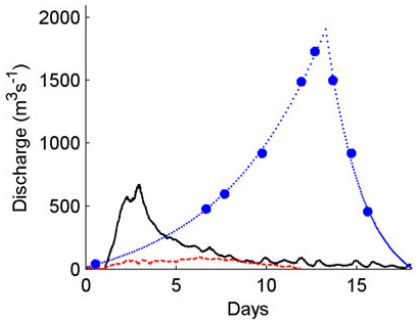

Fig. 2. Comparison of the hydrographs of a large rapidly rising jökulhlaup in 2002 (solid curve) and the small jökulhlaup in 2006 with a rapid initial rise, which is the subject of this paper (dashed curve), both from the western Skaftá cauldron. The hydrograph of a typical slowly rising jökulhlaup from Grímsvötn in 1986 (dotted curve) is also shown. The hydrograph of the Grímsvötn jökulhlaup is based on discrete discharge measurements which are shown as dots. The rapid rise of the hydrograph of the 2006 jökulhlaup is more clearly visible in Figure 6 which shows the same discharge curve with the vertical scale expanded.

The discharge development of a jökulhlaup seems to depend on both local conditions at each site and the initial conditions for each particular flood. Both rapidly rising and slowly rising jökulhlaups can originate from the same source location. As an example, the 1861, 1892, 1938 and the November 1996 jökulhlaups from Grímsvötn in Vatnajökull were all of the rapidly rising type (Thórarinsson, 1974; Björnsson, 2002), whereas over 20 jökulhlaups from Grímsvötn in the decades from 1940 to 2010 were slowly rising (Thórarinsson, 1974; Björnsson, 2002; Sigurðsson and Einarsson, 2005; unpublished data from the Icelandic Meteorological Office). Different drainage mechanisms for different outbursts from the same source location have likewise been identified for Gornersee in Switzerland (Huss and others, 2007).

Subglacial water flow and variations in subglacial water pressure have attracted increasing attention in recent years as a likely cause of the large variations in ice flow velocities that have been observed on the main outlets of the Greenland ice sheet and some of the ice streams of Antarctica (e.g. Rignot and Kanagaratnam, 2006; Fricker and others, 2007; Stearns and others, 2008; Doyle and others, 2015). Subglacial accumulation of water has been observed or inferred at many locations on large and small glaciers and found to be associated with substantial increases in ice flow velocities (e.g. Iken and Bindschadler, 1986; Fudge and others, 2009; Magnússon and others, 2011). Jökulhlaups provide one of the best opportunities to study the response of the subglacial hydraulic system to large and sudden variations in water flow, and lessons learned from studies of jökulhlaups may be useful for understanding variations in basal sliding and ice flow in glaciers and ice sheets in general (Bell, 2008).

To gain understanding of the energy balance, heat dissipation and flood path formation and development in rapidly rising jökulhlaups, a campaign to monitor the Skaftá cauldrons and the Skaftá river was initiated in 2006. This paper reports our results on the subglacial hydrology of the September 2006 jökulhlaup from the western Skaftá cauldron. Outflow from the subglacial lake and transient storage of water in the subglacial flood path are derived and used, together with water temperature measurements in the subglacial lake and near the terminus, to shed light on the dynamics of the flood path development for this type of flood. The emptying of a cylindrically symmetric subglacial lake is simulated with the full-Stokes ice-dynamic model Elmer/Ice (Gagliardini and others, 2013) to deduce a relationship between water volume in the lake and ice-shelf elevation for calculations of outflow from the lake and for analysing the size of the subglacial lake in relation to the observed dimensions of the ice-surface depression.

2. DATA AND METHODS

The ice shelf covering the western Skaftá cauldron was penetrated by a hot water drill in June 2006 (Thorsteinsson and others, 2007). (The term 'ice shelf' is used in this paper to describe the ice cover overlying the subglacial lakes as the weight of the ice is to a large extent supported by flotation. The ice shelves are, however, fundamentally different from the large ice shelves at the margins of ice sheets and glaciers in, for example, Antarctica, Greenland and Canada.) A temperature sensor was deployed at the bottom of the lake and connected with a cable to a data logger on the surface

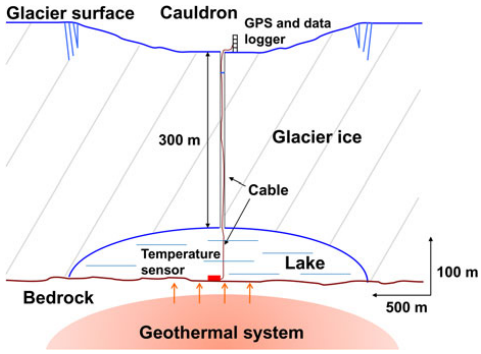

Fig. 3. Schematic drawing of the western Skaftá cauldron showing the ~300 m thick floating ice shelf penetrated by a drillhole into the ~100 m deep subglacial lake and the scientific instruments deployed in the lake and on the glacier surface in the campaign in 2006. Note that the vertical scale is exaggerated five-fold.

(Fig. 3). A differential GPS instrument was placed at the centre of the cauldron, and a water temperature logger was placed in the Skaftá river, 3 km downstream of the port where the river emerges from beneath the ice (Fig. 1).

2.1. Proglacial discharge

The proglacial discharge in Skaftá was measured at the hydrometric station at Sveinstindur, 25 km downstream of the glacier margin. The discharge at the river outlet at the glacier terminus was back-calculated with flood routing using the 1-D HEC-RAS hydraulic model for unsteady flow in open channels (Jónsson, 2007). In addition to the jökulhlaup component, the discharge measured at Sveinstindur includes the normal discharge from the glacier and from several relatively small tributaries. These additional discharge components were estimated, based on a comparison with river discharge records for similar weather conditions, and subtracted from the measured discharge to yield a discharge estimate for the flood originating from the cauldron (Einarsson, 2009). The uncertainty in this discharge estimate arises from the uncertainty of the discharge measurement at Sveinstindur and the uncertainties of the estimates for base flow and for rain and melt-induced runoff from the watershed during the period 26 September to 2 October. The uncertainties of the base flow (±5 m^3 s^{-1}) and rain and melt runoff (±10 m^3 s^{-1}) are relatively large for this small jökulhlaup in 2006, compared with the uncertainty of discharge measurement at Sveinstindur (±2%; see Jónsdóttir and others, 2001). This leads to ±12 m^3 s^{-1} uncertainty in the jökulhlaup discharge and ±20% uncertainty in the estimated flood volume and rate of outflow from the subglacial lake because subtraction of base flow and melt-induced runoff increases the relative uncertainty in the final results.

2.2. Glacier surface elevation over the subglacial lake

The elevation of the ice shelf varies in response to changes in the volume of water in the subglacial lake. The elevation of the surface of the ice shelf was measured near the centre of the cauldron with a Trimble 4000SE GPS receiver equipped with a Trimble 4000ST L1 Geodetic antenna. The receiver logged data at 15 seconds intervals for 5 minutes at 08:00 every morning. The average of the measurements from each 5 minutes logging interval provided one GPS location per day during the period 14 September to 25 October. The data were processed with the Trimble Geomatics Office software using base station data from the stations GFUM (Grímsfjall, length of baseline ~20 km) and SKRO (Skrokkalda, length of baseline ~37 km). Based on fluctuations in the measurements between adjacent days during time periods of slow vertical movements before and after the jökulhlaup, the relative accuracy of the measured surface elevation is estimated to be <1 m.

2.3. The geometry of the cauldron and the subglacial lake

The difference of two 5 m × 5 m DEMs of the cauldron between filled and empty stages was used to deduce the geometry of the part of the subglacial volume that is emptied out in jökulhlaups. A DEM based on aerial synthetic aperture radar (SAR) measurements from August 1998 was made of western Vatnajökull by Magnússon (2003). A jökulhlaup with a peak discharge of 149 m^3 s^{-1} and total volume of 0.116 km^3 drained from the western cauldron in September 1998, <1 month after the aerial survey, so the western cauldron was nearly filled at the time of the survey. A second DEM of the Skaftá cauldron area was made with airborne lidar in July 2010 (Jóhannesson and others, 2013). The western cauldron was at a low water level at the time of the lidar survey, as a jökulhlaup with a peak discharge of ~410 m^3 s^{-1} and total volume of 0.190 km^3 drained the western cauldron in June 2010, ~1 month before the survey.

Our inferred geometry of the subglacial volume is not based on direct measurements immediately before and after the 2006 flood and may be affected by changes in ice thickness in the 12 years between the SAR and lidar ice-surface measurements in 1998 and 2010 when seven other jökulhlaups are recorded (Zóphóníasson, 2002; unpublished data from the Icelandic Meteorological Office). The shape of the ice surface of the western cauldron shortly before a jökulhlaup is flat and smooth and is expected to be very similar for different floods. The general size and shape of the cauldron at the end of a jökulhlaup has been monitored from many reconnaissance flights during and after the floods and is also found to be rather similar for the events that have been observed (O. Sigurðsson, personal communication, 2016). The geometry of ice thickness changes over the subglacial lake in a jökulhlaup cycle are therefore expected to be rather similar between cycles. The general lowering of the glacier surface due to a negative mass balance since 1998 is accounted for by subtracting the elevation difference in the adjacent area unaffected by the cauldron subsidence. The subglacial lake is not fully emptied out in jökulhlaups so that large parts of the ice shelf do not touch the underlying bedrock at the end of the floods. Small-scale transient changes due to melting at the underside of the ice shelf, caused by possible spatial variations in the subglacial geothermal activity, are, therefore, not expected to affect the inferred geometry of the volume that is emptied out in jökulhlaups. The inferred geometry of the subglacial volume is affected by a hump near the centre of the cauldron. The hump is most likely an ice-dynamic thrust phenomenon connected to ice flow into the cauldron and therefore does

not represent the shape of the subglacial lake. This effect is small compared with other uncertainties in the estimation of the geometry of the lake.

2.4. The hypsometry of the subglacial lake

The water volume in the subglacial lake is not a simple function of the lake geometry and water level as for lakes in bedrock basins because the geometry of the lake may change with the ice-shelf elevation. A hypsometric curve, i.e. lake water volume as a function of ice-shelf elevation, for the lowering of the ice shelf was calculated with the full-Stokes ice-dynamic model Elmer/Ice (Gagliardini and others, 2013) by simulating the emptying of a cylindrically symmetric subglacial lake below an ice cover with the approximate dimensions of the western Skaftá cauldron. The question to be addressed by the simulation is whether the subglacial water body maintains a similar shape as the ice shelf is lowered and the lake is emptied or whether the lake geometry changes substantially due to internal shear within the ice shelf near the lake edge such that the grounding line at the lateral boundary moves inward as the shelf lowers. These two possibilities correspond to different relationships between the rate of lowering of the ice shelf and the rate of outflow from the subglacial lake, leading to different trajectories between the two known points on the volume–ice-shelf-elevation curve that are determined by the observed total outflow and surface lowering. Our modelling is simplistic and meant to capture the main physical processes that determine the shape of the hypsometric curve but not the 2006 event in detail. The model setup is, thus, based on a simplified geometry of the western cauldron and general characteristics of jökulhlaups released from there and the final results are scaled to the observed volume and ice shelf lowering in the 2006 event. The physical basis of our model formulation is in principle similar to the analytical model of cauldron subsidence during jökulhlaups developed by Evatt and Fowler (2007) but there are differences in the geometrical and physical assumptions as will be further described in Section 4.

The Skaftá cauldrons and ice flow in their vicinity are close to being cylindrically symmetric in geometry (Figs 1 and 3). A cylindrically symmetric model configuration was chosen because the detailed geometry of the ice-flow basin away from the subglacial lake, which deviates from cylindrical symmetry, is not expected to influence the form of the calculated hypsometric curve to a significant degree.

We take the overall shape and size of the subglacial lake as given, based on the inferred geometry of the volume emptied out in the 2010 jökulhlaup. This shape is dynamically determined over many jökulhlaup cycles and it is outside the scope of this paper to derive and analyse this time-dependent geometry by modelling. The modelled lake is assumed to have a convex shape and maximum depth of ~100 m at the centre at the start of a jökulhlaup and to be covered with an ice shelf with surface geometry based on the 1998 SAR DEM (see Fig. 4, which explains the notation used to describe the model geometry). The glacier and the lake are underlain by flat bedrock in the model set-up.

The dynamic and kinematic boundary conditions at the ice surface and the ice/bed interface are formulated with a stress-free upper surface, as is customary in ice flow models of this kind (e.g. Gagliardini and others, 2013), and a constant uniform positive surface mass balance b_s. The stress-free upper surface is assumed to have a smooth geometry, ignoring the dynamic effect of surface crevasses that are observed to be formed in a concentric pattern during the subsidence of the ice shelf. The lidar measurements in 2010, shortly after a jökulhlaup, showed crevasse depths up to 40 m, which should be considered a minimum as the lidar is not likely to have reached to the bottom of the deepest crevasses. Crevasses formed over a timescale of several days during a jökulhlaup may be estimated to be on the order of 100 m deep (Cuffey and Paterson, 2010, Eqn (10.6), p. 449). As the surrounding glacier is ~450 m thick, the crevasses may have some effect on the ice dynamics but neglecting them is not likely to have a dominating effect on our results considering other simplifications in our modelling specification.

The kinematic boundary condition at the bottom of the ice takes geothermal melting of ice, m_g, into account within the radius of the geothermal area r_g. The dynamic boundary condition at the ice/bed interface assumes Weertman sliding, $u_b = C\,\tau_b^{m-1}\,\tau_b$, where u_b is the bed-parallel velocity component, τ_b is the basal shear stress and C and m are parameters.

Water pressure in the lake, p_w, is assumed to be hydrostatic:

$$p_w = \rho_w g\,(z_w - z), \tag{1}$$

where z_w is the piezometric height of the lake, and the dynamic boundary condition at the ice/water interface is formulated in terms of the water pressure that is set equal to the (negative of the) surface normal stress in the ice at the shear-stress-free bottom of the ice shelf. The position of the grounding line, where the ice/water interface meets the ice/bed interface, is part of the solution and evolves with time. Its

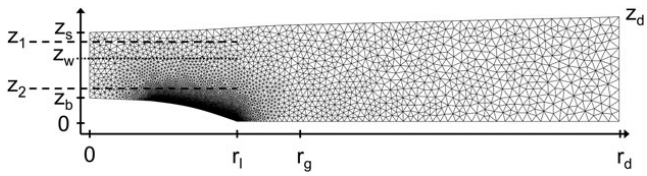

Fig. 4. The Elmer/Ice computational finite-element mesh for the cylindrically symmetric model of a glacier on a flat bed overlying a subglacial lake with dimensions corresponding to the western Skaftá cauldron. The figure explains the notation used to define the geometry of the model: the elevation of the ice surface, z_s, and the bottom of the ice, z_b, the time-dependent piezometric water level of the subglacial water lake, z_w, the radial distance to the grounding line, r_l, the radius of the geothermal area, r_g, the radius to the ice divide at the boundary of the cauldron ice flow basin with the surrounding ice cap, r_d and the ice-surface elevation at the ice divide, z_d. A jökulhlaup is released when z_w reaches a critical level z_1 and terminated when z_w reaches z_2.

position at each time step is determined by solving a contact problem. At each node, the normal force exerted by the ice on the bedrock is compared with the water pressure at that location and the ice allowed to separate from the bed in case the water pressure is higher (see Gagliardini and others, 2013).

The lake is assumed to be hydraulically connected to the atmosphere through water passageways such as crevasses or moulins. The volume of water in the lake and surrounding waterways, V_w, is the sum of (i) the lake volume, taken to be the integral of the elevation of the bottom of the ice shelf, z_b, over the area of the lake, and (ii) the water volume in the passageways between the lake and the atmosphere, which we assume can be expressed as water level in the passageways, z_w, multiplied with their effective area, S, by analogy with the traditional way to express ground water storage in terms of a storage coefficient (Fetter, 2001). Therefore, variations in V_w, may be expressed as

$$\frac{dV_w}{dt} = \int_0^{r_l} \frac{dz_b}{dt} 2\pi r dr + S\frac{dz_w}{dt} = q_s + q_f + q_g - q_j, \quad (2)$$

where the flux components q_s, q_f, q_g and q_j on the right-hand side are inflow into the lake due to surface melting and rainfall on the surface, inflow of geothermal fluid, basal geothermal melting and rate of outflow from the lake during jökulhlaups, respectively. This equation is solved for z_w with explicit forward time stepping in such a way that the flux components, as well as simulated changes in the ice-shelf geometry, force changes in water pressure through adjustment of the piezometric height of the lake that induce further changes in the ice-shelf geometry through the dynamic boundary condition at the ice/water interface in a feedback loop. Each time step of the modelling involves an update of the mesh, calculation of the area where the glacier is grounded and an update of the piezometric height of the lake based on the previous geometry and the flux components. Changes in normal pressure at the ice/water interface due to variations in the piezometric height lead to stresses and strains in the ice, and the resulting ice motion drives changes in the volume of the subglacial water body that subsequently lead to changes in the piezometric height and grounding line position in the next time step. Because of the very different timescales for filling and emptying of the lake between and during jökulhlaups, variable-length time stepping was implemented with time steps switching between the order of hours between jökulhlaups and the order of minutes during jökulhlaups.

Surface mass balance over the ice flow basin, b_s, the rate of geothermal melting of ice, m_g and the rate of inflow of geothermal fluid from the geothermal system, q_f, are estimated from mass and energy conservation assuming long-term balance of total precipitation over the ice flow basin with area $A_i = \pi r_d^2$, bottom geothermal melting over an area $A_g = \pi r_g^2$ and outflow in jökulhlaups when averaged over many jökulhlaup cycles as in Jóhannesson and others (2007). The flux components q_s and q_g in Eqn (2) are assumed to be constant in time, ignoring the seasonal mass-balance cycle, which is not expected to be important for the emptying of the lake. The rate of jökulhlaup outflow, q_j, is assumed to rise linearly with time from zero to a constant discharge q_k over a time period t_r and fall linearly to zero over a time period t_f when the piezometric water level in the subglacial lake rises or falls to the thresholds z_1 and z_2, respectively (see Fig. 4). Table 1 gives the values used for model geometry and physical constants in the simulations.

Several model parameters are not well constrained by available observations or theory, in particular the parameters describing the geothermal melting, A_g (and consequently m_g), the timescales for the rise and fall of the jökulhlaup discharge, t_r and t_f, the effective area of the assumed hydraulic connection with the atmosphere, S, as well as the sliding parameters C and m. The numerical values of the parameters A_g, t_r, t_f and S as well as the grid resolution were varied by a

Table 1. Parameters defining an idealized, cylindrically symmetric model for the western Skaftá cauldron

Parameter	Value	Comment
A_i	20 km^2	Area of ice flow basin (Pálsson and others, 2006) (r_d = 2.52 km)
z_d	500 m	Ice divide elevation
A_g	π km^2	Area of geothermal melting (r_g = 1 km)
r_l	700 m	The initial radius to the grounding line
b_s	2.22 m w.e. a^{-1}	Surface mass balance
d_s	0.4 m w.e. a^{-1}	Sum of rain and (absolute value of the) surface ablation
m_g	17.8 m w.e. a^{-1}	Melting of ice at bottom of the ice shelf or glacier within radius r_g
q_s	0.25 m^3 s^{-1}	Discharge corresponding to rain and surface ablation
q_f	0.36 m^3 s^{-1}	Discharge corresponding to inflow of geothermal fluid
q_g	1.8 m^3 s^{-1}	Discharge corresponding to geothermal melting
q_k	100 m^3 s^{-1}	Discharge during a jökulhlaup (maximum value after initial rise and final fall)
z_1	400 m	Piezometric water level in the lake at the start of a jökulhlaup
z_2	320 m	Piezometric water level in the lake at the termination of a jökulhlaup
t_r	12 hours	Time period for the rise of discharge at the start of a jökulhlaup
t_f	12 hours	Time period for the fall of discharge at the end of a jökulhlaup
S	0.1 km^2	'Storage coefficient' (effective area) of an assumed hydraulic connection of the subglacial lake with the atmosphere
A	2.4×10^{-24} s^{-1} Pa^{-3}	Parameter in Glen's flow law ($\dot{e}_{ij} = A\tau_{ij}^n$, where $\dot{e}$ and τ are strain rate and deviatoric stress, respectively)
n	3	Exponent in Glen's flow law
C	2.3×10^{-21} s$^{1/3}$ m$^{-1/3}$ Pa	Parameter in Weertman's sliding law
m	3	Exponent in Weertman's sliding law

factor of 2–100 to test the sensitivity of the model, and no significant changes in simulation results occurred. For computational reasons, the adopted values of S are large compared with the expected magnitude of water passageways through bottom channels, englacial cavities and crevasses. Varying S by two orders of magnitude made little difference to model results, indicating that this parameter only affects the resulting hypsometric curve to a small degree.

The resulting hypsometric curve shows an approximately linear relation between ice-shelf elevation and lake water volume (Fig. 5, dashed curve), indicating that the subglacial water body maintains a similar shape as the ice shelf is lowered. The simulated hypsometric curve was scaled to fit the observed values for total outflow volume and surface lowering during the 2006 jökulhlaup, allowing the calculation of outflow discharge as a function of time based on the measured lowering of the ice shelf during the flood.

2.5. Floodwater temperature and energy available for subglacial melting

Continuous measurements of water temperature in Skaftá river were made at Fagrihvammur, 3 km downstream of the glacier margin (Fig. 1), during the September/October 2006 jökulhlaup, using a Starmon mini temperature recorder with an accuracy of ± 0.1°C. The measurements, as well as an evaluation of potential warming over the 3 km distance from the glacier margin to the measurement site, are described by Einarsson (2009). Discrete measurements of floodwater temperature at the glacier margin in jökulhlaups in Skaftá in August and October 2008 and October 2015 were made with a high-precision RBR thermometer, with an accuracy of ± 0.005°C. Measurements of water temperature in the subglacial lake of the western cauldron in June 2006 are described by Jóhannesson and others (2007).

The energy available for melting of ice along the subglacial flood path until a particular point in time after the floods starts may be used to calculate an upper bound on the volume of the flood path that can have been created by melting at that time

$$V_{\mathrm{melt}} = \frac{c_{\mathrm{w}}\rho_{\mathrm{w}}V_{\mathrm{l}}T_{\mathrm{l}} + g\rho_{\mathrm{w}}V_{\mathrm{l}}\Delta H - c_{\mathrm{w}}\rho_{\mathrm{w}}V_{\mathrm{s}}T_{\mathrm{s}}}{L\rho_{\mathrm{i}}}, \qquad (3)$$

where g is the acceleration of gravity and ρ_{w}, c_{w}, ρ_i and L are the density and the heat capacity of water, and the density and latent heat of fusion of ice, respectively (Table 2). T_{l} and T_{s} are the temperature of the floodwater in the lake and at the glacier snout. ΔH is the elevation difference between the water level in the subglacial lake and the glacier snout (815 m for the flood path from the western Skaftá cauldron, Einarsson, 2009). Finally V_{l} and V_{s} are the volumes of water released from the subglacial lake and at the glacier snout up to the time in question. The first term in the numerator on the right-hand side of the equation is the available thermal energy due to the initial heat of the water in the lake, the second term is the available potential energy and the third term is the thermal energy left in the water at the glacier snout. The kinetic energy in the water flow at the glacier snout is neglected as it is small compared with the other terms. This volume estimate is an upper bound as the potential energy component corresponds to flow all the way from the lake to the outlet and the thermal energy corresponding to the deviation of the subglacial floodwater temperature from the freezing point upstream from the snout is included in the estimate of the available energy.

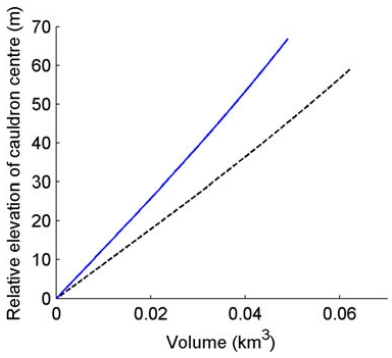

Fig. 5. Hypsometric curves for the subglacial lake below the western Skaftá cauldron showing lake volume as a function of the elevation of the cauldron centre. The result of the Elmer/Ice modelling (dashed curve) and a scaled curve that fits the observed flood volume vs. ice-shelf lowering in the September/October 2006 jökulhlaup (solid curve) are shown.

Table 2. Physical parameters used in melt volume calculations

Parameter	Value	Comment
g	9.82 m s^{-2}	Acceleration of gravity
ρ_{i}	910 kg m^{-3}	Density of ice
ρ_{w}	1000 kg m^{-3}	Density of water
L	3.34×10^5 J kg^{-1}	Latent heat of fusion
c_{w}	4.22×10^3 J kg^{-1} K^{-1}	Heat capacity of water

3. RESULTS

3.1. Proglacial discharge

A rapidly rising jökulhlaup from the western Skaftá cauldron emerged at the glacier margin on 27 September 2006, reaching a maximum discharge close to 100 m^3 s^{-1} in ~2 days. It had the typical form of small jökulhlaups from the western cauldron, with a relatively flat discharge maximum for ~6 days, and receded in ~4 days. The back-calculated flood discharge at the glacier terminus (Fig. 6, solid curve), after subtraction of the base flow, reached its maximum of ≈97 m^3 s^{-1} in the afternoon of 2 October. As the estimation of the time-varying base flow is uncertain, the true discharge maximum might have occurred in the interval 29 September to 2 October, but the maximum value of ≈100 m^3 s^{-1} is fairly accurate as the discharge peak was broad and flat.

As for other jökulhlaups from the Skaftá cauldrons, the rapid rise in flood discharge during the first 2 days cannot be described by classic jökulhlaup theory (Björnsson, 1977, 1992; Sigurðsson and Einarsson, 2005). Using model parameters based on the geometry of the flood path and channel roughness n_{m} (Manning's roughness) in the range 0.01–0.1 s m$^{-1/3}$, as reported for subglacial conditions by Cuffey and Paterson (2010), the classic theory implies that the discharge should increase by a factor of 2 in the range

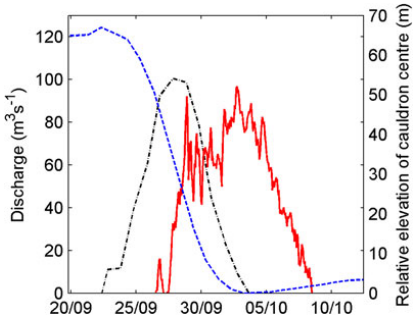

Fig. 6. Back-calculated discharge of jökulhlaup water (solid curve) at the glacier terminus during the jökulhlaup in September/October 2006 after subtracting base flow from the glacier and tributary rivers upstream of the Sveinstindur hydrometric station. The relative elevation of the cauldron centre, as measured with GPS, is also shown (dashed curve) as well as the calculated outflow from the subglacial lake (dash-dotted curve) derived from the lowering of the ice surface elevation using the hypsometric curve for the subglacial lake.

of 1–7 days for discharge between 20 and 80 $m^3 s^{-1}$. The discharge, however, increased from ~20 to ~40 $m^3 s^{-1}$ in approximately half a day and from ~40 to ~80 $m^3 s^{-1}$ in less than a day. The form of the discharge variation is also far from the nearly exponential concave shape typical for slowly rising jökulhlaups (Fig. 6).

3.2. The geometry of the cauldron, the subglacial lake and the adjacent flood path

Inward movement of the grounding line in the modelled lowering of the ice shelf (Fig. 7) is minimal, ~40 m and the water depth is reduced in approximately the same proportion everywhere during outflow. The lake shape for different stages is therefore similar, leading to the approximately linear hypsometric curve shown in Figure 5. This indicates that the shelf has a substantial internal strength and shear stress support at the sides. We find that the water pressure at the bottom of the ice shelf in the centre of the cauldron falls below the ice overburden (positive effective pressure at the top of the subglacial cavity) by 0.2–0.4 MPa during the main outflow phase. This imbalance is compensated by a bridging shear stress of 0.15–0.3 MPa at the margins of the ice shelf. The modelling, furthermore, shows considerable thickening of the ice shelf during subsidence, which also affects the time-dependent shape of the lake (Fig. 7). This thickening from 305 to 320 m is caused by increased ice flow towards the centre during subsidence. The ice flow is increased both because of increased surface slope of the cauldron and shear softening of the glacier ice. The shear softening is caused by higher shear stresses in the ice shelf as support from the water pressure in the lake is reduced. The linear shape of the hypsometric curve is, thus, a net result of complex ice dynamics where both lateral support and vertical extension play a role. The reciprocal of the slope of a straight line, fitted to the hypsometry (Fig. 5), is the 'effective' area of the lake, if it were being emptied in a piston-like manner. This area, 1 km^2, is smaller than the 1.5 km^2 initial area of the modelled lake and relatively constant during lowering. The lowering of the surface of the cauldron affects an area substantially larger than the subglacial lake so that the surface lowering at the lake edge is ~20% of the maximum lowering at the centre. The modelled surface lowering is more than 1 m at a radius of 1050 m, 1.5 times the initial radius of the lake.

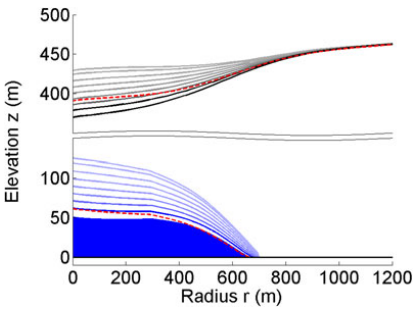

Fig. 7. Lake and surface geometry during a jökulhlaup modelled with Elmer/Ice. The geometry is drawn at daily intervals with darker colour as time progresses. The lake and surface geometries 1 month after the end of the jökulhlaup are also drawn (dashed curves).

The subtraction of the SAR and lidar DEMs from 1998 and 2010 indicates a subglacial water body with a smooth, approximately cylindrically symmetrical shape (Fig. 8). The area that subsided is ~2.5 km in diameter, with maximum depth of ~90 m near the centre of the cauldron. The elongated shapes that appear on the flanks of the central water cupola are due to surface crevasses represented in the 2010 lidar DEM that were formed or enhanced during the July 2010 jökulhlaup. These shapes are thus not surface topography expressions of variations in subglacial lake depth. The modelled lowering of the ice shelf indicates that the margins of the ice surface depression with comparatively little difference in elevation between 2010 and 1998 (Fig. 8) are formed by ice dynamics during the lowering of the ice shelf and by ice flow into the cauldron over the month that elapsed from the jökulhlaup in June 2010 to the lidar survey in July (Fig. 7). The true width of the subglacial lake before a jökulhlaup may thus be expected to be smaller than shown in Figure 8.

Melting over the subglacial flood path has created an elongated depression in the outlet area of the cauldron, visible as the extension to the southwest from the area of the western cauldron in Figure 1b. The depression is deeper shortly after a jökulhlaup (as in 2010) than shortly before a jökulhlaup (as in 1998) and has been observed to be bounded by thin belts of narrow crevasses on each side after jökulhlaups (O. Sigurðsson, personal communication, 2008), indicating subsidence of the glacier surface along the depression. The ice surface elevation difference indicates that an ice volume ~10 m high, a few hundred metres wide and ~3 km long, which takes the shape of a ridge in Figure 8, is melted as the depression is formed during the initial stage of a jökulhlaup. Due to smoothing caused by ice dynamics the true geometry of the subglacial volume could be narrower and higher.

3.3. The water level and the depth of the subglacial lake

The water level in the borehole was at 1488 m a.s.l. at the time of the instrument set-up in June 2006, which is ~5 m

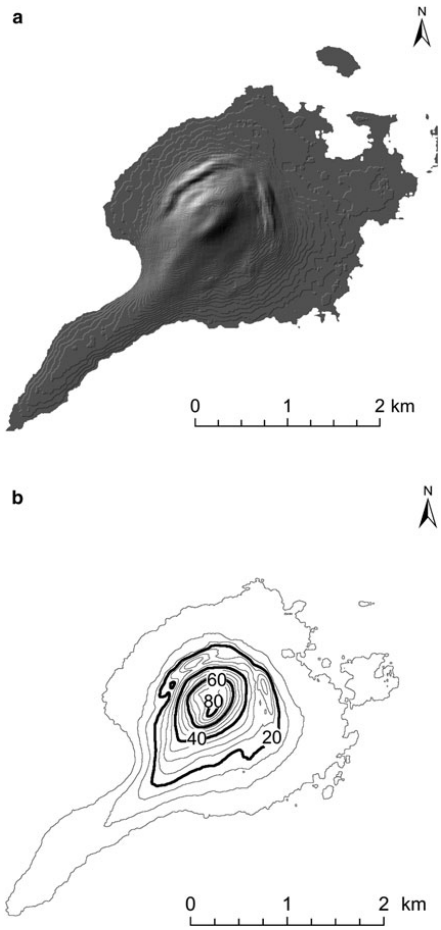

Fig. 8. (a) A hillshade of the difference between the adjusted 1998 SAR DEM and the 2010 lidar DEM. (b) A contour map of the inferred depth of the subglacial water body emptied in the 2010 flood, contour interval of 5 m. The data are smoothed with a 100 m × 100 m window.

higher than the level corresponding to flotation of the central part of the shelf. This deviation from floating balance means that an excess pressure of ~0.05 MPa was acting on the underside of the ice shelf near the centre (Einarsson, 2009). The ice shelf rose slowly by 12 m from early June to the triggering of the jökulhlaup. It then fell by 67 m in 11 days and by ~55 m in the 6 days of most rapid decline (Fig. 6, dashed curve).

Measurements of water depth and ice shelf lowering at the location of the June 2006 borehole show that the lake was ~125 m deep just before the jökulhlaup while the lowering of the ice shelf during the jökulhlaup was only 67 m, leaving ~60 m of water in the lake at the location of the borehole. Thus, the lake was not completely drained by the flood. The elevation of the centre of the western cauldron according to the 2010 lidar DEM (adjusted to account for the general lowering of the glacier in this area between 2006 and 2010) was ~16 m lower than after the jökulhlaup in 2006. This indicates that more water remained in the subglacial lake after the 2006 jökulhlaup than after the 2010 jökulhlaup.

3.4. Outflow from the subglacial lake

The outflow from the subglacial lake deduced from the GPS measurements of the lowering of the ice shelf is shown in Figure 6. The outflow reached a maximum of ~100 $m^3\ s^{-1}$ in ~4 days, at about the same time that appreciable flood discharge started at the terminus. The outflow then receded in ~4 days.

The travel time of the subglacial flood wave from the cauldron to the terminus is in the range 29–62 hours. This wide range arises both from an uncertainty in the timing of the start of outflow from the lake and from the terminus. There is a ±12 hour uncertainty of the timing of the start of outflow from the lake as the GPS recorder in the cauldron only recorded elevations once per day. The onset of outflow at the terminus is also not well determined, as the diurnal discharge variation at the outlet masked the start of discharge increase there. The mean speed of the front of the subglacial flood wave along the 40 km path from the cauldron is estimated at 0.2–0.4 m s^{-1}.

3.5. Transient volume of subglacial floodwater

Figure 9 shows the estimated volume of floodwater in the subglacial lake and the cumulative volume of the jökulhlaup discharge at the glacier margin during the September/October 2006 jökulhlaup, as well as the transient volume of water stored in the subglacial pathway. The volume of water in the subglacial pathway is estimated by subtracting the cumulative volume of flood discharge at the terminus from the cumulative volume of floodwater released from the subglacial lake. The subglacial water volume is considerable relative to the total flood volume of 5.3×10^{-2} km^3. It reached a maximum of ~3.3×10^{-2} km^3 on 30 September, 2 days after the outflow from the lake reached its maximum, and was already ~1.4×10^{-2} km^3 before any outflow started at the glacier margin. For flow speed equal to or larger than the mean propagation speed of the subglacial flood front and flood path length of 40 km, one finds that a flood path with a volume of less than half the inferred subglacial water volume is needed to carry the flood discharge at

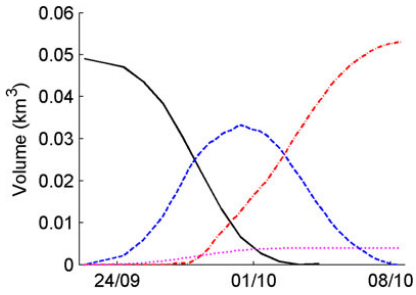

Fig. 9. Volume of floodwater in the subglacial lake (solid curve), cumulative volume of the flood discharge at the glacier terminus (dash-dotted curve), the estimated volume of water stored in the subglacial flow path (dashed curve) and calculated amount of melt due to friction in the flow and initial heat of the floodwater (dotted curve). Dates are day/month of 2006.

the time of maximum subglacial water storage. This will be elaborated below.

3.6. Floodwater temperature and thermodynamics

The measurements of floodwater temperature in Skaftá during the September/October 2006 jökulhlaup indicate that the outburst water was within 1°C from the melting point as it emerged from beneath the ice cap. The uncertainty of up to 1°C is caused by frictional heating and heat exchange with the atmosphere along the ~3 km long river path from the terminus to the thermometer location. Measurements of floodwater temperature at the glacier margin in jökulhlaups in Skaftá in August and October 2008 and October 2015 showed floodwater temperatures at the melting point within ± 0.01°C. The measurements were carried out at a discharge close to the maxima of 240 and 1290 $m^3\ s^{-1}$ for the August and October jökulhlaups in 2008, respectively, and close to the maximum of ~3000 $m^3\ s^{-1}$ for the 2015 jökulhlaup. The predicted outflow temperatures for these events, according to the heat transfer equation in the unsimplified jökulhlaup theory of Nye (1976) as formulated in Jóhannesson (2002), are 0.05–0.8°C and 1.0–2.5°C for the August and October jökulhlaups in 2008, respectively, and 1.8–3.4°C for the 2015 jökulhlaup. These calculations are based on the geometry of the flood path and channel roughness n_m (Manning's roughness) in the range 0.01–0.1 s $m^{-1/3}$, and also account for the initial heat stored in the lake water.

The vertical temperature profile through the 100 m deep subglacial lake in June 2006 (Jóhannesson and others, 2007) showed that the bulk of the water was close to 4.7°C, with a distinct ~10 m deep layer at 3.5°C at the bottom (both temperatures are higher than the temperature corresponding to maximum density of water at the pressures encountered in the lake). Temperature measurements at different depths in the subglacial lake below the eastern Skaftá cauldron over several months in 2007 showed little variation with time in the lake water temperature, which was close to 4.0°C at most depths (unpublished data from the Icelandic Meteorological Office). The lake water temperature in the western cauldron during the September/October 2006 jökulhlaup may thus be assumed to have been close to 4.5°C.

Most of the initial heat in the lake water is presumably lost during the first few kilometres of the flood path. This is indicated by the few hundred metres wide and up to ~10 m deep depression that stretches ~3 km southwestward from the western cauldron, along the assumed location of the flood path, that is more prominent shortly after jökulhlaups than shortly before the floods, as described above (Figs 1b and 8). The volume change of the depression between the 1998 DEM and the 2010 DEM is $\sim 1 \cdot 10^{-2}\ km^3$. Bearing in mind that the heat transfer in subglacial water flow may be assumed to be very rapid (Jóhannesson, 2002; Jarosch and Zwinger, 2015) and comparing this to the volume of ice melted by the heat content in 0.190 km^3 of 4.5°C warm water discharged out of the cauldron in the 2010 jökulhlaup, which is $1.2 \times 10^{-2}\ km^3$, it seems likely that most of the initial heat in the 2010 jökulhlaup floodwater was lost in the flow along this part of the path. These numbers should of course be considered to represent order of magnitudes estimates as the volume of the depression is determined from measurements of the glacier separated by many jökulhlaup cycles. We expected similar heat loss to have taken place in the 2006 jökulhlaup, and therefore the floodwater may be assumed to have been near the melting point for most of the length of the flood path.

4. DISCUSSION AND CONCLUSIONS

Our measurements of the lowering of the ice shelf in the western Skaftá cauldron during a jökulhlaup, along with discharge measurements of the proglacial flood discharge in Skaftá river, allow estimation of the transient subglacial storage of floodwater. The inferred subglacial storage and the measured discharge, along with information on floodwater temperatures in the subglacial reservoir and close to the glacier margin, may be used to draw conclusions about the formation of the subglacial flood path.

At the time of maximum subglacial storage, 4.3×10^{-2} km^3 of water had been released from the subglacial lake (Fig. 9). The initial heat contained in this volume of water with a temperature of ~4.5°C and heat formed by potential energy dissipation in the flow down the subglacial flood path (corresponding to a temperature rise of ~2.0°C) are sufficient to melt at most $\sim 3.4 \times 10^{-3}\ km^3$ of ice (Eqn (3)), if all available thermal energy is used in melting, and considering the potential energy corresponding to the entire elevation difference from the lake to the snout. This is <~10% of the volume of water in the subglacial pathway and subglacial storage along the path, which thus must have been formed mainly by mechanical processes. The ratio of the volume of ice that could have been melted at any particular point in time during the entire rising phase of the jökulhlaup to the subglacial water volume at the same time is also on the order of 10%. Melting therefore cannot have been the main process responsible for the formation of the initial subglacial flood path. Other processes, such as lifting of the ice, hydraulic fracturing as well as viscous and elastic deformation induced by water pressure higher than overburden pressure, must therefore be the main processes responsible for the propagation of the initial jökulhlaup flood wave and the formation of the subglacial path. This is in agreement with earlier findings of Björnsson (1992, 2002), Jóhannesson (2002), Flowers and others (2004) and Einarsson and others (2016) for rapidly rising jökulhlaups, and is in contrast to classic jökulhlaup theory (Nye, 1976) where the flood path is formed by a feedback mechanism between water flow and conduit enlargement. Similar transient water storage created by high subglacial water pressure and glacier lifting has been observed for other rapidly rising jökulhlaups at Gornersee, Switzerland (Huss and others, 2007; Werder and others, 2009), and at Hidden Creek Lake, Alaska (Bartholomaus and others, 2008, 2011). The substantial volume of floodwater that spreads subglacially during the initial phase of the jökulhlaup, $\sim 1.4 \times 10^{-2}\ km^3$, before any outflow has started at the terminus, also shows that outflow from the subglacial lake does not require direct throughflow of water extending from the lake to the terminus.

It may be assumed that essentially all the subglacial volume of the jökulhlaup path is formed during each individual flood. Preexisting channels, incised into the bedrock or conduits in the ice formed in prior jökulhlaups must be ice-filled since air- or water-filled subglacial cavities in the form of an incipient flood path with a substantial extension are unlikely to be sustained under the glacier between jökulhlaups. According to Nye's (1953) analysis of the

contraction of a subglacial cylindrical cavity with the creep parameter for temperate ice from Cuffey and Paterson (2010), the radius of an air-filled cavity under 400 m of ice will decrease to <10% of its initial value in less than a week. Low and broad air-filled cavities collapse even faster. Water-filled conduits with flowing water will contract and adjust to available water sources between jökulhlaups. This adjustment is not instantaneous but will take place over days to weeks, depending on the position within the glacier and the amplitude and rate of change of water input (Cuffey and Paterson, 2010). Finally, a substantial water body of stagnant water at the glacier bed is only stable in local depressions in the hydraulic potential (Björnsson, 1988), such as at the cauldrons between jökulhlaups, and such conditions are not present along the flood path of the Skaftá jökulhlaups (Magnússon, 2003).

Due to the strength of the overlying glacier, the part of the flood path that is initially formed by mechanical processes can be expected to be broad and flat and therefore the flow there will be in the form of a sheet. This part of the path is formed by lifting of the ice through elastic and viscous deformation and hydraulic fracturing induced by water pressure higher than the ice overburden pressure. It is, therefore, unlikely to have a horizontal width smaller than a few ice thicknesses.

Measurements of floodwater temperatures in Skaftá for discharges on the order of 240–3000 $m^3\ s^{-1}$ show that the jökulhlaup water is at or very close to the melting point when it emerges at the glacier terminus. Essentially all initial heat of the lake water and heat formed in the flood path by dissipation of potential energy has thus been lost from the floodwater. As pointed out by Björnsson (1992), Jóhannesson (2002) and Clarke (2003), this indicates much more effective heat transport from the floodwater to the surrounding ice walls of the subglacial flood path than is consistent with the heat transfer mechanism assumed in the classic unsimplified jökulhlaup theory of Nye (1976), and later developments of this theory by Spring and Hutter (1981, 1982) and Fowler (1999). A better physical understanding of subglacial water flow is clearly needed to explain this very efficient heat transfer (Jóhannesson, 2002; Werder and Funk, 2009; Jarosch and Zwinger, 2015).

Magnússon and others (2007) observed an increase in surface speed in an 8 km wide area on Skaftárjökull for a small jökulhlaup from the eastern cauldron in 1995, except for the uppermost 6 km of the flood path near the cauldron where no speed-up was observed. They suggested that the 1995 jökulhlaup was drained in a conduit along this uppermost part of the flood path and as a sheet farther down in agreement with the interpretation presented here for the 2006 jökulhlaup. Narrow flood paths with width <500 m extending from both cauldrons are indeed indicated by the elongated surface depressions near the cauldrons described earlier. Although melting driven by the initial heat of the floodwater can only create ~10% of the subglacial water storage, this melting can play an important role over a limited part of the flood path length. A plausible mechanism for the initiation of the flood therefore appears to be (i) melting of a conduit along the first ~3 km of the path, driven by rapid release of the initial heat of the lake water, and (ii) formation of a sheet-like flood path farther downglacier by lifting and ice deformation due to a propagating subglacial pressure wave (Jóhannesson, 2002; Einarsson and others, 2016). Such a sheet-like initial subglacial flood path can rapidly develop conduits to become a highly efficient waterway (Jóhannesson, 2002; Flowers and others, 2004; Einarsson and others, 2016) allowing faster rise of discharge than the conduit-melt–discharge feedback (Nye, 1976) (Fig. 6, solid curve). The formation of a pressure wave requires an efficient pressure connection between two locations of the flood path where subglacial water pressure near ice overburden at the upper location leads to pressure higher than ice overburden at the (lower) location farther down the path. In the case of the Skaftá cauldrons, the conduit formed by the release of the initial heat near the cauldron may provide this connection with a small potential gradient needed to drive the water flow. This situation may be an essential component in the formation of a subglacial pressure wave in jökulhlaups at this location. The propagating pressure wave would then not be formed at the source lake but some kilometres downstream of it, explaining the shift from conduit flow to sheet flow inferred for the 1995 jökulhlaup by Magnússon and others (2007).

We find that only part of the subglacial water storage is needed to carry the discharge of the flood, even for low estimates of the flow speed, particularly during the initial rise of the flood discharge. This may be interpreted as initial storage in subglacial reservoirs that do not contribute much to the transportation of floodwater. Such transient subglacial storage of floodwater has been documented for a rapidly rising jökulhlaup in 2004 from Gornersee in Switzerland (Huss and others, 2007; Werder and others, 2009). Up to half of the volume of this flood is reported to have been stored subglacially and they suggest that this storage is related to lateral spreading of the floodwater and uplift of the glacier. This is not a unique feature of rapidly rising jökulhlaups, as lateral spreading and glacier uplift has also been observed for slowly rising jökulhlaups from Grímsvötn and Gornersee, where a propagating subglacial pressure wave was not observed (Huss and others, 2007; Magnússon and others, 2007; Werder and others, 2009; Magnússon and others, 2011; Einarsson and others, 2016).

A rise in the ratio of subglacial volume needed to carry the discharge of the flood to the total volume of subglacial water may be inferred from our data. This indicates a development towards more efficient subglacial water flow and/or release of water from subglacial storage to the main flood path over the course of the 2006 jökulhlaup. This may be interpreted as a development towards effective conduit flow from ineffective initial sheet flow formed in the wake of a subglacial pressure wave.

Our estimate for the travel speed of the subglacial flood front in 2006 (0.2–0.4 $m\ s^{-1}$) is faster than the propagation speed of a small jökulhlaup from the eastern Skaftá cauldron in October 1995 (<0.06 $m\ s^{-1}$) estimated by Magnússon and others (2007, there is a typo in Magnússon's paper where this speed is given as 0.6 $m\ s^{-1}$). Magnússon and others' (2007) estimation is based on detection of ice surface speed-up due to the jökulhlaup by SAR satellite imagery before the flood front reached the ice margin. Similar propagation speeds as our estimate for the 2006 jökulhlaup have also been estimated for a small jökulhlaup from the western cauldron in August 2008 and a large jökulhlaup from the eastern cauldron in October 2008, 0.1–0.3 and 0.4–0.6 $m\ s^{-1}$, respectively (Einarsson and others, 2016). These travel speed estimates are considerably slower than the speed of the flood front of the rapidly rising jökulhlaup from Grímsvötn in November 1996 (1.3 $m\ s^{-1}$) (Björnsson, 2002)

but similar to the speed of a flood front of a rapidly rising jökulhlaup from Hidden Creek Lake, Alaska, in July 2006 (0.4 m s^{-1}) (Bartholomaus and others, 2011). The speed of the subglacial flood front for rapidly rising jökulhlaups therefore seems to vary between different locations due to differences in flood path geometry, and large subglacial floods appear to propagate faster than small floods at the same location.

There are indications that the speed of the subglacial water flow increases at later stages for jökulhlaups in Skaftá after the proglacial discharge has peaked. This development may also be interpreted as filling of lateral storage of floodwater during the initial phase of the flood that may later release subglacially stored water into the main flood path. Earthquake tremors, indicating boiling within the geothermal system below the subglacial lake, due to the pressure release accompanying the emptying of the lake, were observed during a jökulhlaup from the eastern cauldron in 2002. A time series for the concentration of suspended material in the jökulhlaup waters at the gauging station at Sveinstindur displayed a peak believed to result from the same boiling event. The timing of the earthquake tremors and the peak in the suspended sediments were used to estimate a speed for the subglacial water flow, $\sim 0.8 \pm 0.1$ m s^{-1} (O. Sigurðsson, personal communication, 2008). This is 2–4 times the speed estimated here for the initial phase of the 2006 jökulhlaup and 1.3–2 times the speed estimated for the 2008 October jökulhlaup.

The derived shape of the lake at a full stage (Fig. 8) resembles the theoretically predicted shape of subglacial lakes below a surface cauldron with a slope of the ice/water interface at the top of the lake that is opposite to the slope of the ice surface and an order of magnitude larger (Björnsson, 1975, 2002). The derived shape does not reflect the full depth and extent of the water body, as some water was left in the lake after the jökulhlaups in 2006 and 2010. For similar ice-shelf thickness in 2010 to that in 2006, ~40 m of water would have been left at the cauldron centre. The resolution of bedrock data is insufficient to determine whether this water is located in a bedrock depression or retained by the closing of the lake seal. The decline of the discharge after the flood peaks varies between jökulhlaups, and the final elevation of the ice shelf after jökulhlaups varies by tens of metres (unpublished data from the Icelandic Meteorological Office and the Institute of Earth Sciences at the University of Iceland). This indicates that the closing of the seal depends delicately on some (subglacial) conditions that vary from event to event. Termination of jökulhlaups before the water level drops below the bedrock threshold is also observed at Grímsvötn (Björnsson, 1974) and has been assumed to be caused by conduit closing because of ice deformation exceeding melting of conduit walls (Björnsson, 1974; Nye, 1976) or settling of a flat-based ice dam onto a smooth bedrock (Björnsson, 1974). Some jökulhlaups, for example at Gornersee, continue, however, until the source lake is empty (Werder and others, 2009).

The hypsometric curve for a subglacial lake during lowering in a jökulhlaup depends on the strength of the overlying ice shelf, which determines to what extent the shelf is carried by floating or shear forces. Our simulations show that the shelf has considerable shear strength, due to shear stresses induced by the subsidence that are caused by vertical shear straining over the entire shelf except at the centre, and the local force balance therefore deviates from floating equilibrium. The resulting hypsometric curve is nearly linear (Fig. 5) and not concave as it would be for a lake under an ice shelf mainly carried by floating. Our results show that ice-surface depressions caused by the emptying of subglacial lakes are considerably larger than the footprint of the corresponding water body at the glacier bed; in the case of the western Skaftá cauldron, modelled ice-surface subsidence >1 m is found over an area more than twice that of the subglacial lake. This result may be relevant for time-varying subglacial water bodies at other locations.

Our magnitude for the pressure difference and lateral shear stress, 0.2–0.4 and 0.15–0.3 MPa, respectively, may be crudely compared with the analytical results of the cauldron subsidence model of Evatt and Fowler (2007). Their model predicts ~0.15 and ~0.2 MPa for the pressure difference and shear stress, respectively, when the model parameters have been adapted to the spatial scale of the western Skaftá cauldron, assuming ice flow parameters for temperate ice and a similar outflow magnitude as for the 2006 jökulhlaup. The model of Evatt and Fowler is based on 2-D geometry, rather than cylindrical geometry, and the water outflow is calculated by Nye's (1976) theory for slowly rising jökulhlaups, whereas we employ an outflow variation corresponding to a rapidly rising flood. Considering these differences in assumptions and the formulation of the models, there is overall agreement between the models on the dynamics of the cauldron subsidence.

Many of the most well-known rapidly rising jökulhlaups, such as the jökulhlaups from the Katla volcano (Tómasson, 1996) and the 1996 Grímsvötn jökulhlaup, are dramatic and up to more than three orders of magnitude larger than the jökulhlaup described in this paper. The relatively small size of the rapidly rising jökulhlaups from the Skaftá cauldrons therefore indicates that the total water volume (i.e. flood size) is not the key factor determining the rapidity of flood release. Considering that some large and small jökulhlaups in Iceland in modern times were rapidly rising (Björnsson, 2002; Jóhannesson, 2002; Sigurðsson and Einarsson, 2005; Einarsson and others, 2016), the type of large jökulhlaups at the end of the last glaciation in Iceland and elsewhere must be considered an open question. A fundamental understanding of the conditions that determine the development of subglacial floods, in particular whether they develop rapidly by lifting of the overlying ice or over a longer time through a feedback between discharge and ice melting in a conduit, is therefore required for an improved understanding of prehistoric jökulhlaups. Theoretical studies of the palaeohydraulics of jökulhlaups from Lake Missoula, Montana, USA (Clarke and others, 1984), and Lake Agassiz, North America (Clarke and others, 2004), are based on the assumption that these floods were of the slowly rising type and controlled by the melt-discharge-feedback in a conduit. The possibility of a sheet-like flood from Lake Agassiz is deemed highly unlikely by Clarke and others (2005) as the inflow into the lake was not rapid and as it is not likely that the critical conditions for ice-dam lifting would be reached over large areas of a dam resting on an irregular bed and variously attacked by iceberg calving. Our example of a rapidly rising flood with an initial sheet-like flood path from the slowly filling subglacial lake below the western Skaftá cauldron shows that rapid inflow is not an essential condition for the release of such floods. Our interpretation also indicates that a flood path that starts as a conduit near the source lake can develop as

a sheet farther downstream if a propagating subglacial pressure wave is formed.

ACKNOWLEDGEMENTS

The Icelandic Research Fund, the Landsvirkjun (National Power Company of Iceland) Research Fund, the Icelandic Road Administration, the Kvískerja fund and the Iceland Glaciological Society provided financial and field support, which made this study possible. A map of the subglacial topography along the route of jökulhlaups from the Skaftá cauldrons and the inferred paths of the jökulhlaups shown in Figure 1 was made available by Helgi Björnsson and Finnur Pálsson at the Institute of Earth Sciences of the University of Iceland. Halldór Geirsson at the Icelandic Meteorological Office provided GPS base data from Grímsvötn and Skrokkalda. We thank Olivier Gagliardini for assistance with the Elmer/Ice model calculations. The Icelandic Coast Guard provided helicopter transportation to the western cauldron in November 2006. This material is based upon work supported in part by the National Aeronautics and Space Administration through the NASA Astrobiology Institute under Cooperative Agreement NNA04CC08A issued through the Office of Space Science. Thomas Zwinger was supported by the Nordic Centre of Excellence, 'eScience Tools for Investigating Climate Change at High Northern Latitudes' (eSTICC) funded by NordForsk. We thank Vilhjálmur S. Kjartansson, Gunnar Sigurðsson, Hlynur Skagfjörð Pálsson and Mary Miller for assistance during field operations. We thank Gwenn Flowers and two anonymous reviewers of an earlier version of the manuscript and Geoffrey W. Evatt and an anonymous reviewer of this manuscript for detailed and constructive comments that helped us improve the paper and Ken Moxham for help with the English language. This publication is contribution No. 4 of the Nordic Centre of Excellence SVALI, 'Stability and Variations of Arctic Land Ice', funded by the Nordic Top-level Research Initiative (TRI).

REFERENCES

Bartholomaus TC, Anderson RS and Anderson SP (2008) Response of glacier basal motion to transient water storage. *Nat. Geosci.*, **1**(1), 33–37 (doi: 10.1038/ngeo.2007.52)

Bartholomaus TC, Anderson RS and Anderson SP (2011) Growth and collapse of the distributed subglacial hydrologic system of Kennicott Glacier, Alaska, USA, and its effects on basal motion. *J. Glaciol.*, **57**(206), 985–1002 (doi: 10.3189/002214311798843269)

Bell RE (2008) The role of subglacial water in ice-sheet mass balance. *Nat. Geosci.*, **1**(5), 297–304 (doi: 10.1038/ngeo186)

Björnsson H (1974) Explanation of jökulhlaups from Grímsvötn, Vatnajökull, Iceland. *Jökull*, **24**, 1–26

Björnsson H (1975) Subglacial water reservoirs, jökulhlaups and volcanic eruptions. *Jökull*, **25**, 1–11

Björnsson H (1977) The cause of jökulhlaups in the Skaftá river, Vatnajökull. *Jökull*, **27**, 71–78

Björnsson H (1988) *Hydrology of ice caps in volcanic regions*. Societas Scientarium Islandica, University of Iceland, Reykjavík, Iceland

Björnsson H (1992) Jökulhlaups in Iceland: prediction, characteristics and simulation. *Ann. Glaciol.*, **16**, 95–106

Björnsson H (2002) Subglacial lakes and jökulhlaups in Iceland. *Global Planet. Change*, **35**, 255–271

Björnsson H (2010) Understanding jökulhlaups: from tale to theory. *J. Glaciol.*, **56**(200), 1002–1010

Clarke GKC (2003) Hydraulics of subglacial outburst floods: new insights from the Spring-Hutter formulation. *J. Glaciol.*, **49**(165), 299–313

Clarke GKC, Mathews WH and Pack RT (1984) Outburst floods from glacial Lake Missoula. *Quat. Res.*, **22**(3), 289–299

Clarke GKC, Leverington DW, Teller JT and Dyke AS (2004) Paleohydraulics of the last outburst flood from glacial Lake Agassis and the 8200 BP cold event. *Quat. Sci. Rev.*, **23**, 389–407 (doi: 10.1016/j.quascirev.2003.06.004)

Clarke GKC, Leverington DW, Teller JT, Dyke AS and Marshall SJ (2005) Fresh arguments against the Shaw megaflood hypothesis. A reply to comments by David Sharpe on 'Paleohydraulics of the last outburst flood from glacial Lake Agassiz and the 8200 BP cold event'. *Quat. Sci. Rev.*, **24**, 1533–1541 (doi: 10.1016/j.quascirev.2004.12.003)

Cuffey KM and Paterson WSB (2010) *The physics of glaciers*, 4th edn. Elsevier, Oxford

Doyle SH and 15 others (2015) Amplified melt and flow of the Greenland ice sheet driven by late-summer cyclonic rainfall. *Nat. Geosci.*, **8**, 647–653 (doi: 10.1038/ngeo2482)

Einarsson B (2009) *Jökulhlaups in Skaftá: A study of a jökulhlaup from the Western Skaftá cauldron in the Vatnajökull ice cap, Iceland*. (MS thesis, University of Iceland, also available as technical report VI 2009–006 from the Icelandic Meteorological Office)

Einarsson B and 5 others (2016) A spectrum of jökulhlaup dynamics revealed by GPS measurements of glacier surface motion. *Ann. Glaciol.*, **57**(72), 47–61 (doi: 10.1017/aog.2016.8)

Evatt GW and Fowler AC (2007) Cauldron subsidence and subglacial floods. *Ann. Glaciol.*, **45**, 163–168 (doi: 10.3189/172756407782282561)

Fetter CW (2001) *Applied Hydrogeology. International edn*. 4th edn. Pearson Education, New Jersey

Flowers GE, Björnsson H, Pálsson F and Clarke GKC (2004) A coupled sheet–conduit mechanism for jökulhlaup propagation. *Geophys. Res. Lett.*, **31**(5), L05401 (doi: 10.1029/2003GL019088)

Fowler AC (1999) Breaking the seal at Grímsvötn, Iceland. *J. Glaciol.*, **45**(151), 506–516

Fricker HA, Scambos T, Bindschadler R and Padman L (2007) An active subglacial water system in West Antarctica mapped from space. *Science*, **315**(5818), 1544–1548 (doi: 10.1126/science.1136897)

Fudge TJ, Harper JT, Humphrey NF and Pfeffer WT (2009) Rapid glacier sliding, reverse ice motion and subglacial water pressure during an autumn rainstorm. *Ann. Glaciol.*, **50**(52), 101–108

Gagliardini O and 14 others (2013) Capabilities and performance of Elmer/Ice, a new-generation ice sheet model. *Geosci. Model Dev.*, **6**(4), 1299–1318

Huss M, Bauder A, Werder M, Funk M and Hock R (2007) Glacier-dammed lake outburst events of Gornersee, Switzerland. *J. Glaciol.*, **53**(181), 189–200

Iken A and Bindschadler RA (1986) Combined measurements of subglacial water pressure and surface velocity of Findelengletscher, Switzerland: conclusions about drainage system and sliding mechanism. *J. Glaciol.*, **32**(110), 101–119

Jarosch AH and Zwinger T (2015) *Explicit numerical modeling of heat transfer in glacial channels*. American Geophysical Union, Fall Meeting 2015, abstract #C54B-05

Jóhannesson T (2002) Propagation of a subglacial flood wave during the initiation of a jökulhlaup. *Hydrol. Sci. J.*, **47**(3), 417–434

Jóhannesson T, Thorsteinsson Th, Stefánsson A, Gaidos E and Einarsson B (2007) Circulation and thermodynamics in a subglacial geothermal lake under the Western Skaftá cauldron of the Vatnajökull ice cap, Iceland. *Geophys. Res. Lett.*, **34**(19), L19502

Jóhannesson T and 7 others (2013) Ice-volume changes, bias estimation of mass-balance measurements and changes in subglacial lakes derived by lidar mapping of the surface of Icelandic glaciers. *Ann. Glaciol.*, **54**(63), 63–74 (doi: 10.3189/2012AoG63A422)

Jónsdóttir JF, Kristjánsdóttir GB and Zóphóníasson S (2001) *Skaftá við Sveinstind, vhm 166 Rennslislykill nr. 5 [Skaftá by*

Sveinstindur, vhm 166 Discharge water elevation relationship number 5]. National Energy Authority, Reykjavík, Report OS-2001/001

Jónsson GÞ and Þórarinsdóttir T (2011) *Hlaup í Múlakvísl 8.–10. júlí 2011 [Outburst flood in Múlakvísl 8–10 July 2011]*. Icelandic Meteorological Office, Reykjavík, GThJ-TTh/2011-01

Jónsson S (2007) *Flóðrakning með takmörkuðum gögnum [Flood routing with limited input data]*. (MS-thesis, University of Iceland)

Magnússon E (2003) *Airborne SAR data from S-Iceland: analyses, DEM improvements and glaciological application*. (MS-thesis, University of Iceland)

Magnússon E, Rott H, Björnsson H and Pálsson F (2007) The impact of jökulhlaups on basal sliding observed by SAR interferometry on Vatnajökull, Iceland. *J. Glaciol.*, **53**(181), 232–240

Magnússon E and 8 others (2011) Localized uplift of Vatnajökull, Iceland: subglacial water accumulation deduced from InSAR and GPS observations. *J. Glaciol.*, **57**(203), 475–484

Nye JF (1953) The flow law of ice from measurements in glacier tunnels, laboratory experiments and the Jungfraufirn borehole experiment. *Proc. R. Soc. London, Ser. A*, **219**(1139), 477–489

Nye JF (1976) Water flow in glaciers: Jökulhlaups, tunnels and veins. *J. Glaciol.*, **17**(76), 181–207

Pálsson F, Björnsson H, Haraldsson HH and Magnússon E (2006) *Vatnajökull: Mass balance, meltwater drainage and surface velocity of the glacial year 2004–2005*. Institute of Earth Sciences, University of Iceland, Report RH-06-2006

Rignot E and Kanagaratnam P (2006) Changes in the velocity structure of the Greenland Ice Sheet. *Science*, **311**(5763), 986–990

Roberts MJ (2005) Jökulhlaups: a reassessment of floodwater flow through glaciers *Rev. Geophys.*, **43**, RG1002 (doi: 10.1029/2003RG000147)

Sigurðsson O and Einarsson B (2005) *Jökulhlaupaannáll 1989–2004 [Catalogue of jökulhlaups in Iceland 1989–2004]*. National Energy Authority, Reykjavík, Report OS-2005-031

Spring U and Hutter K (1981) Numerical studies of jökulhlaups. *Cold Reg. Sci. Technol.*, **4**(3), 227–244

Spring U and Hutter K (1982) Conduit flow of a fluid through its solid phase and its application to intraglacial channel flow. *Int. J. Eng. Sci.*, **20**(2), 327–363

Stearns LA, Smith BL and Hamilton GS (2008) Subglacial floods cause rapid increase in flow speed of a major East Antarctic outlet glacier. *Nat. Geosci.*, **1**, 827–831 (doi: 10.1038/ngeo0356)

Sugiyama S, Bauder A, Huss M, Riesen P and Funk M (2008) Triggering and drainage mechanisms of the 2004 glacier-dammed lake outburst in Gornergletscher, Switzerland. *J. Geophys. Res.*, **113**, F04019 (doi: 10.1029/2007JF000920)

Thórarinsson S (1974) *Vötnin stríð. Saga Skeiðarárhlaupa og Grímsvatnagosa. [The swift flowing rivers. The history of Grímsvötn jökulhlaups and eruptions]*. Bókaútgáfa Menningarsjóðs, Reykjavík. 254 pp

Thorsteinsson Th and 8 others (2007) A hot water drill with built-in sterilization: design, testing and performance. *Jökull*, **57**, 71–82

Tómasson H (1996) The jökulhlaup from Katla in 1918. *Ann. Glaciol.*, **22**, 249–254

Werder MA and Funk M (2009) Dye tracing a jökulhlaup: II. Testing a jökulhlaup model against flow speeds inferred from measurements. *J. Glaciol.*, **55**(193), 899–908

Werder MA, Loye A and Funk M (2009) Dye tracing a jökulhlaup: I. Subglacial water transit speed and water-storage mechanism. *J. Glaciol.*, **55**(193), 889–898

Zóphóníasson S (2002) *Rennsli í Skaftárhlaupum 1955–2002 [Discharge in jökulhlaups in Skaftá 1955–2002]*. National Energy Authority, Reykjavík, Report SZ-2002/01

MS received 9 December 2016 and accepted in revised form 26 May 2017; first published online 6 July 2017

Paper III

Hydrology and dynamics of two Icelandic outlet glaciers revealed by discharge and GPS measurements.

Einarsson B and Jóhannesson T (2018)

To be submitted to the Journal of Glaciology

Hydrology and dynamics of two Icelandic outlet glaciers revealed by discharge and GPS measurements

Bergur Einarsson[1] and Tómas Jóhannesson[1]

[1]*Icelandic Meteorological Office, Reykjavík, Iceland*

Correspondence: Bergur Einarsson <bergur@vedur.is>

ABSTRACT. Continuous GPS measurements on two broad and gently sloping temperate ice-cap outlets in Iceland show motion events of increased velocity (i) during the early melt season, (ii) contemporaneous with events of increased surface melt or rain and (iii) during the emptying of supraglacial slush ponds. They also show periods of slower movement than late winter velocities prior to early-melt-season motion events and in the wake of motion events during the height of the melt season. We interpret these events, with the aid of runoff modelling on the glacier and estimates of longitudinal stress-gradient coupling lengths, as being induced by hydrological forcing on basal slip. Lack of response in movement to certain runoff pulses and the characteristics of the diurnal variation in measured proglacial discharge indicate a development in the ablation zone of a fast, efficient subglacial hydraulic system early in the summer. The passing of a jökulhlaup and high subglacial groundwater flow do not disturb this development.

INTRODUCTION

Broad ice-cap outlet glaciers with surface slope less than 0.1 are common in Iceland. Such outlets discharge ice from more than half of each of the four main ice caps in Iceland: Vatnajökull, Hofsjökull, Langjökull and Mýrdalsjökull. These four ice caps account for ∼95% of the area of the 10% glacier cover of Iceland (Björnsson, 2017; Sigurðsson and others, 2017). Understanding the hydrology and the dynamics of their

outlets is important, as glacial rivers partly fed by them provide ∼65% of the electric power production in Iceland (Þorgeirsdóttir and others, 2015) and are crossed by bridges, power lines and other infrastructure.

Changes in climate are predicted to cause large changes in runoff from these glaciers (Flowers and others, 2005; Jóhannesson and others, 2007; Jónsdóttir, 2008; Einarsson and Jónsson, 2010). Flowers and others (2005) show that the predicted thinning and retreat of Vatnajökull can be expected to alter the subglacial hydraulic catchment structure, resulting in discharge switching between rivers. Knowledge of possible effects of runoff changes on the dynamics of the glacier and possible feedbacks of the dynamics on runoff is therefore important as well. In a larger context, studies of the interaction of glacier hydrology and glacier dynamics are important for future projections of sea level rise caused by glacier mass loss (Radić and Hock, 2014).

The connection between the hydrology of glaciers and their motion has been studied in detail for temperate valley glaciers such as Findelengletscher, Switzerland (Iken and Bindschadler, 1986; Iken and Truffer, 1997), Storglaciären, Sweden (Hooke and others, 1989; Jansson, 1995), Black Rapids and Fels Glaciers, Alaska (Raymond and others, 1995), Glacier d'Arolla, Switzerland (Nienow and others, 1998, 2005; Mair and others, 2001, 2002a, 2002b; Swift and others, 2005), Bench Glacier, Alaska (Harper and others, 2005; Fudge and others, 2009), and Kennicott Glacier, Alaska (Bartholomaus and others, 2008, 2011). The interaction of glacier hydrology and dynamics has also been studied for the large ice sheets of Greenland (e.g. Zwally and others, 2002; Rignot and Kanagaratnam, 2006; Bartholomew and others, 2010, 2011, 2012; Schoof, 2010; Doyle and others, 2015) and Antarctica (see Bell, 2008 for a review). These studies have shown a complex relationship between water input to the glacier drainage system and glacier motion where increased water input exceeding the transport capacity of the subglacial hydraulic system is generally observed to cause increased basal slip. This connection is complicated by the adjustment of the hydraulic system to increased inflow by greater connectivity and volumetric capacity of cavities (e.g. Iken and Truffer, 1997) and the formation of an efficient conduit network (Mair and others, 2001).

The same general results have been observed in studies in Iceland on Skeiðarárjökull (Magnússon and others, 2011) and Breiðamerkurjökull (Van Boeckel, 2015). Other phenomena, such as the effect of a surge on the subglacial hydraulic system (Björnsson, 1998) and a slowdown caused by persistent conduit drainage from a subglacial lake (Magnússon and others, 2010), have been observed on Skeiðarárjökull. Both Skeiðarárjökull and Breiðamerkurjökull are valley-glacier-like outlets of Vatnajökull ice cap, terminating close to sea level and underlain by relatively impermeable bedrock below the sediments at the glacier bed (Sigurðsson and others, 2006).

Less is known about the hydraulic system of the broad and gently sloping ice cap outlets draining to the west and north from Vatnajökull and from Hofsjökull, Langjökull and Mýrdalsjökull ice caps, except for the extreme cases of jökulhlaups (Magnússon and others, 2007; Einarsson and others, 2016, 2017) and research on the sensitivity of the ice-flow velocity to surface meltwater flux and of the properties of the glacier bed beneath Hofsjökull (Minchew and others, 2016). These glaciers terminate in the Icelandic highlands and some of them are underlain by highly permeable groundwater aquifers (Sigurðsson 1990; Sigurðsson and others, 2006). Their hydrology has been studied by several authors (Björnsson, 1988a; Flowers and others, 2003; Magnússon, 2003) and variation in the basal hydrological system can be expected to be important for their dynamics, as basal slip has been shown to be a substantial contributor to the ice flow of Hofsjökull (Minchew and others, 2015).

These glaciers, with an area of hundreds of square kilometres and ice thickness of hundreds of metres, are an order of magnitude larger and substantially thicker than many of the most studied valley glaciers in the Alps, Scandinavia and North America (e.g. Mair and others, 2001) but an order of magnitude smaller and thinner than most of the outlet-glacier catchments studied on the Greenland ice sheet (e.g. Bartholomew and others, 2011; Lindbäck and others, 2014). They nevertheless resemble many of the land-terminating ice sheet outlets in southwest Greenland and might be an analogue for wetter and warmer future of polar glaciers (Björnsson, 2017).

To gain understanding of the hydraulics of such ice cap outlets and their interaction with the ice motion and the underlying groundwater system, we analysed available discharge data from two glacial rivers and ice-surface velocities from continuous GPS measurements on the glacier feeding them. The selected rivers are Austari-Jökulsá and Skaftá, draining northern Hofsjökull and the Skaftárjökull outlet glacier in western Vatnajökull, respectively (Fig. 1). We also modelled surface melt and other hydrological surface processes on the two glaciers using the distributed physically-based model WaSiM (Schulla, 2017) to estimate runoff input to the subglacial hydraulic system.

This paper presents observations of discharge and ice motion and discusses the development of an efficient subglacial conduit system at both locations, based on an analysis of diurnal variations in discharge and differences in the response of the glacier motion to runoff events. The paper also presents measurements and analysis of transient events of increased motion due to the onset of melting at the beginning of summer, drainage of surface slush ponds and other runoff events. Observations of surface velocities slower than late winter velocities, small post-event effects of jökulhlaups on the development of the subglacial hydraulic system and the effects of groundwater flow on glacier hydraulics are also presented and discussed.

FIELD SITES AND DATA

There are a number of hydrometric stations in each of the two selected rivers, Austari-Jökulsá and Skaftá. Data from the most upstream station in each river are best suited for research on glacial discharge as they are least affected by runoff from proglacial areas. The location of the stations is in both cases dictated by hydropower interests rather than the interest of glaciological research. The stations are, therefore, not located at the glacier margin but ∼20 km and ∼25 km downstream of the glacier in the case of Austari-Jökulsá and Skaftá, respectively.

Both rivers are fed by relatively flat highland watersheds, with elevation ranging between 600–1950 m a.s.l., partly covered with broad and gently sloping ice-cap outlets. The climate of Iceland is maritime with cool summers and mild winters (Einarsson, 1984). The mean winter (1 October to 30 April) temperatures for the period 2001–2010 in the watershed of the highest hydrometric stations in Austari-Jökulsá and Skaftá are around −6°C, and the mean summer (1 May to 30 September) temperatures are around 4°C, according to a dataset of gridded daily temperatures for Iceland (Crochet and Jóhannesson, 2011).

Austari-Jökulsá river and northern Hofsjökull

In Austari-Jökulsá, the hydrometric station closest to the glacier is at Austurbugur (Fig. 1) where measurements were initiated in 2007 (Icelandic Meteorological Office, 2017a). The total watershed of the measurement site is 259 km^2, of which 103 km^2 (40%) is glacier-covered.

Annual mass-balance measurements are available for a minimum of 14 mass-balance stakes every year since 1988 at Sátujökull, a neighbouring outlet glacier from northern Hofsjökull (Thorsteinsson and others, 2017). The resulting mean winter mass balance for the period 1988–2015 is 1.5 $m_{w.e.}\,a^{-1}$ and the corresponding summer balance is −2.0 $m_{w.e.}\,a^{-1}$, with estimated uncertainty at ±0.15$m_{w.e.}\,a^{-1}$.

Geodetic mass balance for Sátujökull is also available for the periods 1986–1999, 1999–2004, 2004–2008, 2008–2013 and 2013–2015 (Jóhannesson and others, 2013; Thorsteinsson and others, 2017) and has been used to correct a bias in the traditional mass-balance measurements (Thorsteinsson and others, 2017). Sátujökull feeds the river Vestari-Jökulsá, which is the next river west of Austari-Jökulsá, and mass-balance processes and hydraulics of the glacier are expected to be similar for both rivers and their glacier-covered watersheds.

A continuous GPS station was run high in the ablation area of Sátujökull at ∼1250 m a.s.l. for the summers of 2011–2013 (Figs 1 and 2). The station was installed on the glacier during the annual mass balance spring expedition and taken down in the autumn expedition each year, providing data from 1 to 5 May and ending between 17 September and 9 October. The station is denoted as SATJ.

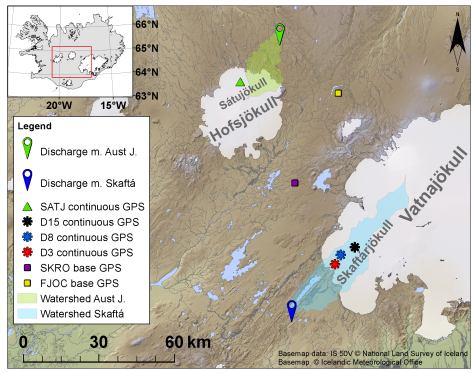

Figure 1. Location of Hofsjökull and Vatnajökull ice caps. Locations of hydrometric stations, continuous GPS measurements and GPS base stations. The watersheds of the highest up-river hydrometric stations in Austari-Jökulsá and Skaftá rivers are indicated with coloured shadings.

Skaftá river and Skaftárjökull

In Skaftá, the hydrometric station at Sveinstindur is closest to the glacier (Fig. 1). The glacier is Skaftárjökull, an outlet glacier from Vatnajökull ice cap. The area of the watershed draining to the station is 637 km^2, of which 390 km^2 (61%) is glacier-covered. The water divides on the glacier can be affected by changes in its surface geometry due to surges (Björnsson and others, 2003) but are expected to be stable during our study

Figure 2. The GPS station, SATJ, in May 2011. The GPS instruments was installed on top of the glacier surface on a quadropod. The station is located high in the ablation area of the broad and gently sloping Sátujökull at ∼1250 m a.s.l. The glacier terminates in the relatively flat highland north of Hofsjökull ice cap.

period as the glacier has not surged since 1994 (Björnsson, 2017). Measurements at Sveinstindur were initiated in 1986 (Icelandic Meteorological Office, 2017b).

Mass-balance measurements from the nearby outlet glacier Tungnaárjökull are available since 1992 from the joint mass-balance survey of the Glaciology group at the Institute of Earth Sciences, University of Iceland, and the National Power Company, Landsvirkjun. Tungnaárjökull has a mean winter mass balance of $1.5\,\mathrm{m_{w.e.}\,a^{-1}}$ and summer balance of $-2.6\,\mathrm{m_{w.e.}\,a^{-1}}$ with estimated uncertainty at $\pm 0.15\mathrm{m_{w.e.}\,a^{-1}}$, for the period 1992–2015. Estimates of the energy balance in the ablation area of Tungnárjökull for the 2013 melt season, based on data from an automatic weather station (AWS) at ∼1075 m a.s.l., are available from the Glaciology group at the Institute of Earth Sciences, University of Iceland.

Three continuous GPS stations were run as part of a jökulhlaup research project at 3 km, 8 km and 15 km from the glacier margin on Skaftárjökull during the summer of 2008 (Einarsson and others, 2016). The stations are denoted as D3, D8 and D15 based on their distance from the glacier margin. They are located in the ablation area at ∼870, ∼1020 and ∼1170 m a.s.l., respectively. D15 and D3 were set up on 19 April while D8 was set up on 30 June. All stations ran past mid-September but data are sporadic after that time due to power problems. D3 and D15 were redeployed at their original location in 2013 on 6 and 8 June and ran until 13 and 29 September, respectively. During the GPS occupation periods, jökulhlaups affected ice-flow velocities for roughly two weeks in 2008. As part of a separate jökulhlaup research project, GPS stations were in sporadic operation for 40 and 68 days during winter at D3 and D15, respectively, from December 2014 to March 2015. Data from these stations are used here to estimate winter velocities for comparison with summer velocities measured in 2008 and 2013.

METHODS

Hydrometric measurements of discharge in glacial rivers

The discharge in Austari-Jökulsá at Austurbugur and Skaftá at Sveinstindur was measured by monitoring the water level in the river by a pressure transducer located upriver from a stable natural controlling cross section. The water level is then converted to discharge using a water-level–discharge rating curve that is constructed from discrete water-level and discharge measurements (Icelandic Meteorological Office, 2017a,b). The hydrometric data were quality-checked and corrected for biases as needed at the end of each hydrological year. Data missing because of instrument breakdown, ice formation or other causes were estimated using meteorological data from nearby weather stations or discharge from nearby rivers that have similar discharge

characteristics. The uncertainty of discharge measurements at Sveinstindur is estimated at ±2% (Jónsdóttir and others, 2001) and is expected to be similar for the measurements at Austurbugur, which are done in the same way and with similar instruments. For further details on hydrological measurements in glacier rivers in Iceland see Einarsson (2012), and on instrumentation see Icelandic Meteorological Office (2017a,b).

Diurnal variations in discharge

Characteristics of the diurnal variation in discharge were studied by normalizing the variation within each day by z-scores (standard score computed by subtracting the mean and dividing by the standard deviation; Kreyszig, 1999). The normalized daily hydrographs were then stacked for study of phase and shape, analogous to the approach of Raymond and others (1995), both for weekly and monthly periods. The daily range of discharge and timing of extrema were determined directly from hourly time series. A more sophisticated approach for estimating the characteristics of the diurnal variation was also tested. The phase and amplitude of an analytic function with the observed shape of the diurnal variation along with daily mean discharge and a linear trend of discharge within the day were fitted to the hourly discharge data for each day using nonlinear least-squares. This approach gave results similar to simple direct estimation from the hourly data and was abandoned as the increased complexity did not lead to significant improvement in the results.

Days when the discharge from the glacier is low are not expected to have a substantial glacier-melt-originated diurnal variation. All days with mean glacial discharge lower than ∼10% of the mean glacial discharge (the mean for days with a value higher than zero) are therefore filtered out. Days when the diurnal variation is distorted by other changes in discharge (e.g. rain events) are also filtered out. This was done by eliminating days where the discharge difference between two consecutive days is more than $10\,\mathrm{m^3\,s^{-1}}$ (∼40% of mean summer discharge) for Austari-Jökulsá and $20\,\mathrm{m^3\,s^{-1}}$ (∼20% of mean summer discharge) for Skaftá.

Estimation of input to the hydraulic system of the glaciers

Distributed surface mass-balance model

Surface melt, M, on Sátujökull and Skaftárjökull was estimated using degree–day modelling (e.g. Braithwaite, 1985). The modelling was done with the glacier module of the hydrological model WaSiM (Schulla, 2017). Separate degree–day factors are used for snow (DDF_{snow}), firn (DDF_{firn}), and ice (DDF_{ice}). Daily melt is calculated over a distributed grid as

$$M_{\mathrm{jk}} = \begin{cases} DDF_{\mathrm{snow/firn/ice}}(T_{\mathrm{jk}} - T_m) & \text{if } T_{\mathrm{jk}} > T_m \\ 0 & \text{if } T_{\mathrm{jk}} \leq T_m \end{cases} \quad (1)$$

where T_{m} is the threshold temperature for melt, and T_{jk} is daily-mean temperature at grid point (j,k) in a dataset of daily temperatures with a horizontal spacing of 1 km for the whole of Iceland (Crochet and Jóhannesson, 2011). The temperature dataset has been updated to include the years 2011–2016.

Snow accumulation is modelled on the same grid as the melt, based on interpolation of gridded precipitation from reanalysis with the numerical weather prediction model Harmonie with a horizontal grid-point spacing of 2.5 km (Nawri and others, 2017). This modelling was also done with the glacier module of the hydrological model WaSiM. Precipitation is divided into solid snow and liquid rain by a linear transition over a 2°C interval centered at temperature, $T_{\mathrm{s/r}}$ (Schulla, 2017). Solid and liquid precipitation values were scaled with a constant scaling parameter, S_{pre}, to account for possible biases in the reanalysis weather data compared to accumulation measurements. Liquid precipitation is added to runoff from melt.

In the melt modelling, a liquid storage, equal to 10% of the water equivalent of the solid snowpack, is filled each spring before runoff is released (Schulla, 2017). This is done to account for refreezing and water storage due to capillary forces in the snowpack. The stored water is then released in proportion to the thinning of the snowpack. The value of 10% is based on a guideline number from Schulla (2017) as this parameter is not well constrained by optimization with reference to mass-balance data. Doubling or halving this value results in a 1–3 day shift in the estimated start of runoff release from the snowpack.

Following Crochet (2012), a parameter set was selected from a large sample of randomly generated values for each parameter. The selection was performed in three rounds of progressively narrower range for each parameter, based on the results from the previous round. Each round had 500 parameter combinations. The selection was carried out by minimizing the sum of squared residuals from a comparison with 234 winter and summer balance values from the stakes on Sátujökull. Modelled mass balance at each stake is represented by piecewise-bilinear interpolation of results from the four grid nodes around the stake location. The selected parameter set was further validated by comparison with the available geodetic mass-balance measurements for Sátujökull and was found to be in the top 5% with respect to performance. The selected degree–day factors are consistent with previously published values (Jóhannesson and others, 1995; Jóhannesson, 1997; Hock, 2003; Guðmundsson and others, 2009; Wake and Marshall, 2015). The same holds for the rain/snow temperature threshold, compared with previous glacier and hydrological modelling in Iceland (Jóhannesson and others,

1995; Jóhannesson, 1997; T. Þórarinsdóttir, personal communication). The optimized parameter values are given in Table 1.

Table 1. Parameters used in melt calculations.

Parameter	Value	Comment
DDF_{snow}	$4.57{\cdot}10^{-3}\,\mathrm{m_{w.e.}}\,^{\circ}\mathrm{C}^{-1}\,\mathrm{d}^{-1}$	Degree-day factor for snow
DDF_{firn}	$6.47{\cdot}10^{-3}\,\mathrm{m_{w.e.}}\,^{\circ}\mathrm{C}^{-1}\,\mathrm{d}^{-1}$	Degree-day factor for firn
DDF_{ice}	$7.45{\cdot}10^{-3}\,\mathrm{m_{w.e.}}\,^{\circ}\mathrm{C}^{-1}\,\mathrm{d}^{-1}$	Degree-day factor for ice
T_{m}	$0.3\,^{\circ}\mathrm{C}$	Threshold temperature for melt
$T_{\mathrm{s/r}}$	$1.3\,^{\circ}\mathrm{C}$	Transition temperature for snow–rain
S_{pre}	0.88	Precipitation scaling factor

The parameter set selected for Sátujökull was also used on Skaftárjökull. Conditions are expected to be similar on these two glaciers as they are both relatively gently sloping and wide ice cap outlets in the central highland of Iceland, and with a similar elevation range and dust deposition. Our modelling is, furthermore, intended to estimate timing and relative amplitude of runoff rather than detailed mass-balance and ice volume changes, for which a separate parameter optimization for Skaftárjökull would have been desirable.

Estimation of meltwater input at each GPS site

Glacier flow at each of the GPS instrument sites is affected by changes in basal drag over a substantial distance up- and down-glacier through longitudinal stress-gradient coupling (Kamb and Echelmeyer, 1986; Mair and others, 2001). Observed changes in surface velocities must therefore be viewed in connection with runoff arriving at the bed over an appropriate distance along a flowline that intersects the location of the instrument. Input to the subglacial hydraulic system at each site is thus estimated from runoff along a line of grid points parallel to the direction of the maximum ice surface slope. Our approach is an approximation and again only intended to estimate the timing and relative amplitude of runoff.

Runoff from grid point i is given a weight, w_{i}, with an influence transfer function $w_{\mathrm{i}} = exp(-(\Delta x_{\mathrm{i}})/l)$ based on Kamb and Echelmeyer's (1986) analysis of longitudinal stress gradients in ice flow. Δx_{i} is the distance of grid point i from the location of the GPS, along an x-axis pointing in the downslope direction. l is the longitudinal coupling length at each site given by:

$$l = \sqrt{4nf\bar{u}_0 h\bar{\eta}/\tau_0} \tag{2}$$

where n is the ice flow-law exponent, f is channel shape factor, $\bar{u}_0$ is the vertically averaged ice-flow velocity, h is the local ice thickness and $\bar{\eta}$ is the effective longitudinal viscosity. τ_0 is the average basal shear stress in the area and given by $\tau_0 = \rho_i g \alpha_0 h_0$, where ρ_i is the density of ice, g is the acceleration of gravity and α_0 and h_0 are the average surface slope and thickness of the glacier in the area, respectively. $\bar{\eta}$ is estimated by an approximation for wide channels from Kamb and Echelmeyer (1986):

$$\bar{\eta} = \frac{0.6}{\tau_B A^{2/3}} \left| \frac{d\bar{u}}{dx} \right|^{-1/3} \tan^{-1} \left(\tau_B A^{1/3} \left| \frac{d\bar{u}}{dx} \right|^{-1/3} \right) , \tag{3}$$

written here in terms of the creep parameter, A, in $\mathrm{s}^{-1}\,\mathrm{Pa}^{-3}$. τ_B is the local basal shear stress, approximated by τ_0.

Measurements of the longitudinal strain rate, $\frac{d\bar{u}}{dx}$, are not available at any of the locations but $\frac{d\bar{u}}{dx}$ can be crudely estimated by several methods. Differences in measured summer velocities at different mass balance stakes can be used on Sátujökull, and differences in measured summer velocities at the GPS sites can be used on Skaftárjökull. Longitudinal strain rate can, furthermore, be expected to be roughly equal to horizontal strain rate assuming that the glacier is in mass-balance equilibrium. Estimates of horizontal strain rate from the average mass balance and ice thickness at each site can therefore also be used. Assuming that the horizontal glacier flow is cylindrically symmetrical provides yet another estimate through an assumption of mass conservation because the transverse strain rate is then defined by the geometry and the mean flow velocity and is equal to the longitudinal strain rate near the equilibrium line.

These different approaches for estimating the longitudinal strain rate provide several order-of-magnitude estimates for each location. This introduces uncertainty which is accounted for by calculating a range for the coupling length at each site. The maximum coupling length results from minimum strain rate and vice versa. As the longitudinal stain rate enters the formula for coupling length, Eqns (2) and (3), as a square root of a cube root, a wide range of strain rate results in a much narrower range for the coupling length. The maximum and minimum coupling lengths are used to calculate two different estimates enveloping the runoff affecting each GPS site. The resulting longitudinal coupling lengths are on the order of 2–7 ice thicknesses at each location. These results are intermediate values between the expected values for valley glaciers and ice sheets which are 1–3 and 4–10 ice thicknesses, respectively (Kamb and Echelmeyer, 1986), as can be expected for broad ice-cap outlets. These results are consistent with the conclusion of Mair and others (2001) that averaging of basal drag over an area on the order of 4 to 5 ice thicknesses was needed to explain major motion events that they observed. Parameters and longitudinal coupling lengths used in our analysis are given in Table 2.

This approach ignores how glacier motion is affected by transfer of variations in subglacial water pressure over length scales longer than the longitudinal ice-flow coupling lengths. Such dynamical effects would be associated with the transfer of water pressure within the subglacial drainage system induced by runoff changes rather than with stress coupling in the ice and they depend on the state of the drainage system over large areas at each point in time. The longitudinal coupling caused by the ice flow is used here as first approximation that captures the effect of runoff events that overwhelm the subglacial hydraulic system locally during spring and summer. Possible effects of subglacial pressure variations over longer length scales are given further consideration in the results and discussion sections.

Ice surface velocities based on continuous GPS measurements

The GPS instruments on both Sátujökull and Skaftárjökull were installed on top of the glacier surface on quadropods (Fig. 2). Trimble NetRS and Trimble 5700 dual-frequency instruments recording at 15 s intervals were used. The GPS data were processed kinematically with the GAMIT-Track utility (Herring and others, 2010) using a set-up for long baselines. The data were processed with respect to a base station at Fjórðungsalda (FJOC) for Sátujökull, and Skrokkalda (SKRO) for Skaftárjökull, with baselines of ∼40 km and ∼35 km, respectively. The resulting locations are filtered with a 24-hour Gaussian filter and hourly values extracted. Hourly horizontal velocities were then extracted from location values 24 hours apart. Finally, daily median values were calculated from the hourly velocities. Standard deviation of the velocities for 7–10 day periods with approximately constant glacier motion was found to be 0.1–0.2 cm d^{-1}. This may be used as an indication of the uncertainty in the velocities.

RESULTS

Diurnal variation in river discharge due to glacial runoff

Diurnal variation in discharge due to glacial runoff typically becomes noticeable in late May in Skaftá and mid-June in Austari-Jökulsá (Fig. 3). There is considerable variability between years in the timing of this onset. It can be noticed as early as the beginning of May or as late as mid-June in Skaftá and as early as the beginning of June and as late as early July for Austari-Jökulsá (Fig. 3).

The development of the diurnal variation of discharge during the course of summer is also different between years. A higher maximum amplitude, both absolute and relative (compared to daily mean discharge), is reached in warm years (e.g. 2004, 2008, 2010 and 2014) or when winter snow cover on the glacier is thin (e.g. 1999, 2000, 2009 and 2013) (Fig. 3). The maximum is also earlier in the summer in such years. The summers

Table 2. Parameters and resulting longitudinal coupling lengths.

Parameter	Value	Comment
h_{SATJ}	300 m	Ice thickness at the SATJ GPS site (Björnsson, 1988b)
α_{SATJ}	0.035	Ice surface slope at SATJ
$\frac{d\bar{u}}{dx}_{\mathrm{SATJmax}}$	$0.01\,\mathrm{a}^{-1}$	Maximum estimate of longitudinal strain rate at SATJ
$\frac{d\bar{u}}{dx}_{\mathrm{SATJmin}}$	$0.001\,\mathrm{a}^{-1}$	Minimum estimate of longitudinal strain rate at SATJ
l_{SATJmin}	1000 m	Minimum longitudinal coupling length at SATJ
l_{SATJmax}	1700 m	Maximum longitudinal coupling length at SATJ
h_{D3}	320 m	Ice thickness at the D3 GPS site, data from the Glaciology group at the Institute of Earth Sciences, University of Iceland
α_{D3}	0.052	Ice surface slope at D3
$\frac{d\bar{u}}{dx}_{\mathrm{D3max}}$	$0.01\,\mathrm{a}^{-1}$	Maximum estimate of longitudinal strain rate at D3
$\frac{d\bar{u}}{dx}_{\mathrm{D3min}}$	$0.004\,\mathrm{a}^{-1}$	Minimum estimate of longitudinal strain rate at D3
l_{D3min}	620 m	Minimum longitudinal coupling length at D3
l_{D3max}	740 m	Maximum longitudinal coupling length at D3
h_{D8}	440 m	Ice thickness at the D8 GPS site, data from the Glaciology group at the Institute of Earth Sciences, University of Iceland
α_{D8}	0.02	Ice surface slope at D8
$\frac{d\bar{u}}{dx}_{\mathrm{D8max}}$	$0.005\,\mathrm{a}^{-1}$	Maximum estimate of longitudinal strain rate at D8
$\frac{d\bar{u}}{dx}_{\mathrm{D8min}}$	$0.001\,\mathrm{a}^{-1}$	Minimum estimate of longitudinal strain rate at D8
l_{D8min}	1600 m	Minimum longitudinal coupling length at D8
l_{D8max}	2400 m	Maximum longitudinal coupling length at D8
h_{D15}	600 m	Ice thickness at the D15 GPS site, data from the Glaciology group at the Institute of Earth Sciences, University of Iceland
α_{D15}	0.016	Ice surface slope at D15
$\frac{d\bar{u}}{dx}_{\mathrm{D15max}}$	$0.0001\,\mathrm{a}^{-1}$	Maximum estimate of longitudinal strain rate at D15
$\frac{d\bar{u}}{dx}_{\mathrm{D15min}}$	$0.002\,\mathrm{a}^{-1}$	Minimum estimate of longitudinal strain rate at D15
l_{D15min}	2200 m	Minimum longitudinal coupling length at D15
l_{D15max}	4000 m	Maximum longitudinal coupling length at D15
g	$9.82\,\mathrm{m\,s}^{-2}$	Acceleration of gravity
ρ_{i}	$910\,\mathrm{kg\,m}^{-3}$	Density of ice
A	$2.4{\cdot}10^{-24}\,\mathrm{s}^{-1}\,\mathrm{Pa}^{-3}$	Parameter in Glen's flow law ($\dot{\epsilon}_{\mathrm{ij}} = A\tau_{\mathrm{ij}}^{n}$, where $\dot{\epsilon}$ and τ are strain rate and deviatoric stress, respectively), appropriate for temperate ice
n	3	Exponent in Glen's flow law
f	1	Channel shape factor, appropriate for wide channels

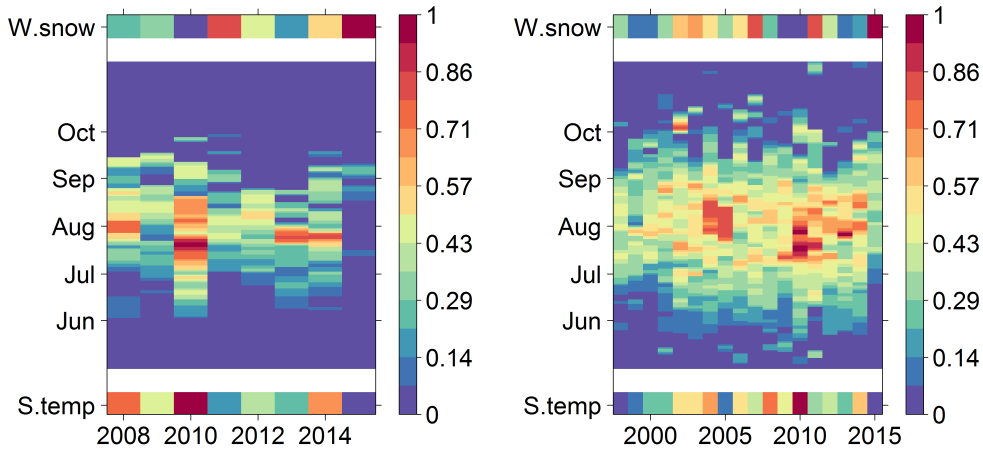

Figure 3. Magnitude of the diurnal variation of measured discharge in Austari-Jökulsá at Austurbugur (left) and in Skaftá at Sveinstindur (right), shown relative to the magnitude of the highest observed discharge. Relative values of annual winter snow accumulation and mean summer temperature are shown at the top and the bottom of the graphs, respectively.

of 2010 and 2015 are end members of this spectrum. The summer of 2010 was warm, and winter accumulation was low, while the summer of 2015 was cold and winter accumulation high. Summer melt in 2010 was also amplified by decreased albedo of the snow surface due to volcanic tephra from the Eyjafjallajökull volcanic eruption (Thorsteinsson and others, 2017).

The diurnal variation during July and August in both rivers has a similar shape (Fig. 4). A sharp maximum is reached through a steep increase in discharge for ∼10 hours. A minimum is then reached from a longer recession-like lowering in discharge for ∼14 hours. The diurnal variation is therefore asymmetric both in the shape and timing of the extrema within the day. The growth of the discharge in the two rivers is similar but the recession in Skaftá river is noticeably slower. Skaftá river has, therefore, a wider maximum and narrower minimum than Austari-Jökulsá river.

The timing of the diurnal maximum in Austari-Jökulsá by the hydrometric station at Austurbugur is typically between hours 21 and 23 for days with regular diurnal variation, except for the first half of June when it is often around hour 24. In Skaftá by the hydrometric station at Sveinstindur, the diurnal maximum typically takes place around hour 23 in mid-July and in August but between hours 24 and 01 in June and

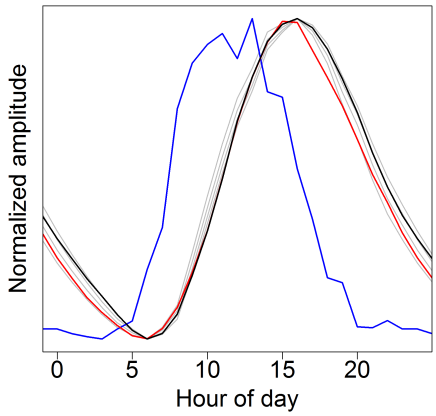

Figure 4. Median shape of diurnal variations in July and August discharge in Austari-Jökulsá at Austurbugur (red) and in Skaftá at Sveinstindur (black). Median scaled diurnal variation in energy balance observed at an AWS at Tungnaárjökull in the summer of 2013 is also shown (blue). Results of routing melt calculated from the energy balance though a linear reservoir with recession constant of 5–8 hours are shown in grey.

in the beginning of July. This corresponds to diurnal maxima at the glacier margin between hours 16 and 19 at both locations, based on estimated travel times of the diurnal maximum between Austurbugur and Eyfirðingavað in Austari-Jökulsá and available estimates for Skaftá (Kristinsson, 2005). This is a delay of 3–6 hours for the maxima at the glacier margin, compared with the local time of maximum solar elevation.

Minimum in discharge within the day in Austari-Jökulsá at Austurbugur is around hours 11 to 13, which corresponds to hours 06 to 08 at the glacier margin. In Skaftá at Sveinstindur, the minimum is around hours 13 to 15, corresponding to hours 05 to 07 at the glacier margin. No clear changes are seen at either location in the timing of the minimum during the course of the summer.

The shape of the diurnal variation in Skaftá and the timing of extrema at the glacier margin during July and August can be reproduced by routing a diurnal variation in the production of melt through a linear reservoir with recession constant of 5–8 hours (grey lines in Fig. 4). The melt production is estimated from hourly energy balance measurements at an AWS at 1076 m a.s.l. on nearby Tungnárjökull (data provided by the Glaciology group at the Institute of Earth Sciences, University of Iceland).

Diurnal glacial discharge variations have been observed and analysed before and after nine jökulhlaups in Skaftá. The relative magnitude of the diurnal variations compared with the mean discharge, the timing of

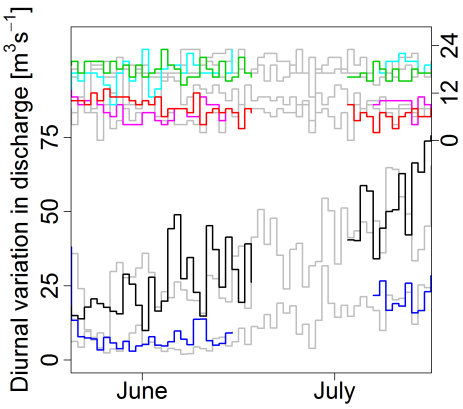

Figure 5. Two examples of the development of the diurnal discharge variations in Skaftá at Sveinstindur during periods interrupted by jökulhlaups, from 2010 (black) and 2015 (blue). Timing (hour) of maximum and minimum is presented by the right y-axis, from 2010 (maximum green, minimum red) and 2015 (maximum cyan, minimum magenta). Data during the jökulhlaup events are not drawn, leading to gaps in the curves. Similar data from 2011 and 1996, which have overall discharge characteristics similar to 2010 and 2015, are shown in the background (grey).

maximum and minimum discharge and the shape of the discharge variation is not observed to be different from the seasonal development in other years (Fig. 5). The passing of a jökulhlaup and formation of a subglacial flood path does not, therefore, seem to have a substantial effect on the development of the subglacial hydrological system as reflected by the diurnal discharge variation.

Glacial hydrology and glacier dynamics

Substantial variability is observed in daily mean velocities at the four GPS sites during the melt season. Each summer, 1–4 speed-up events were identified with daily maximum velocities 2–4 times the mean at each site. A number of smaller peaks and days with velocities as low as 20% of the mean are observed (Figs 6, 7 and 8). The data from 2011 on Sátujökull resemble the data from 2012 and 2013, and are omitted in Figure 8 for simplicity. Winter velocities at SATJ are estimated from 10 days of measurements from 15 to 25 May 2011 during a cold spring when no melt took place at the glacier according to our runoff modelling.

The instruments located at SATJ on Sátujökull (Fig. 8) and D15 on Skaftárjökull in 2008 (Fig. 6) were installed before melting started within the hypothesized area that affects their locations through longitudinal

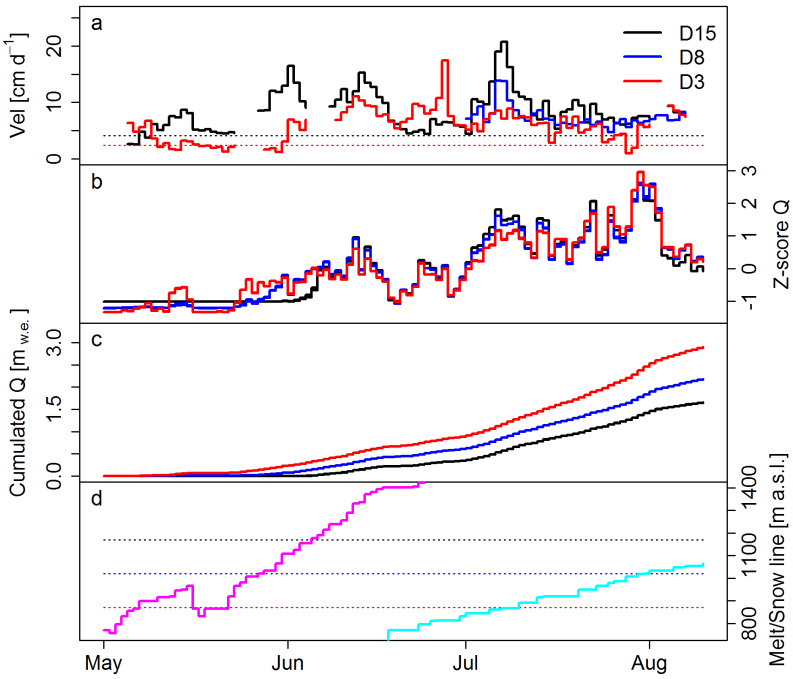

Figure 6. (a) Daily horizontal ice surface velocities on Skaftárjökull during the summer of 2008 at 3 km (D3, red), 8 km (D8, blue) and 15 km (D15, black) from the glacier margin. Observed winter velocities at D3 and D15 from 2014/2015 are shown with dotted lines. (b, c) Scaled and cumulative modelled runoff from the area longitudinally stress-gradient coupled to the GPS sites (the same colour coding). Two estimates are drawn for each of the runoff series based on maximum and minimum estimates of longitudinal coupling lengths, but the difference is not usually noticeable at this scale. (d) The progression of the highest elevation on the glacier with melt (magenta) and the elevation of the snow line (cyan). The elevation of the GPS instruments is shown with dotted lines for reference.

stress coupling. In all cases, a peak with a maximum of approximately twice the earlier velocity is observed as soon as runoff from the snowpack starts in each area. These peaks are 8–14 days in duration and reach the highest velocity towards the end (Figs 6a and 8a).

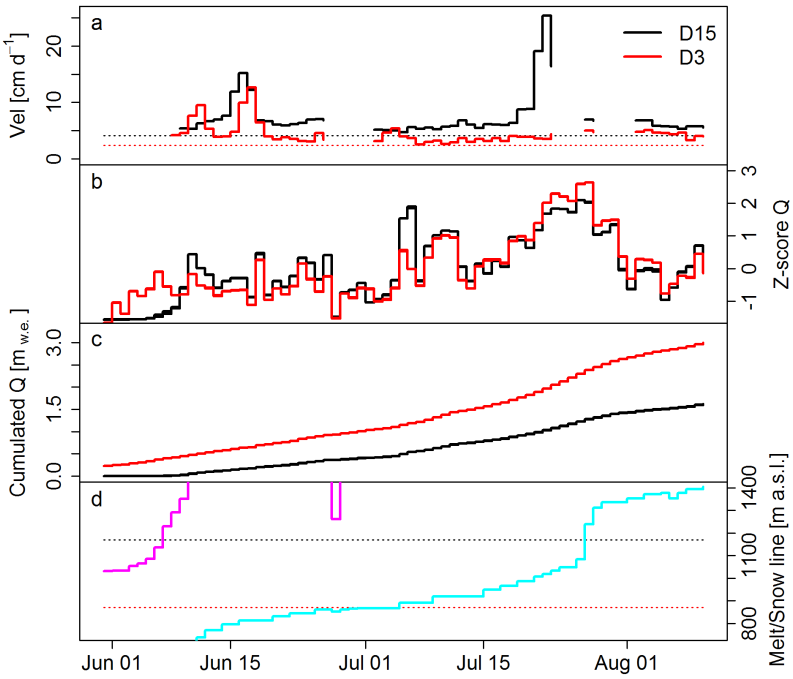

Figure 7. (a) Daily horizontal ice surface velocities on Skaftárjökull during the summer of 2013 at 3 km (D3, red) and 15 km (D15, black) from the glacier margin. Observed winter velocities at D3 and D15 from 2014/2015 are shown with dotted lines. (b, c) Scaled and cumulative modelled runoff from the area longitudinally stress-gradient coupled to the GPS sites (the same colour coding). Two estimates are drawn for each of the runoff series based on maximum and minimum estimates of longitudinal coupling lengths, but the difference is not usually noticeable at this scale. (d) The progression of the highest elevation on the glacier with melt (magenta) and the elevation of the snow line (cyan). The elevation of the GPS instruments is shown with dotted lines for reference.

A number of motion events follow the initial events in periods with rain or a sharp increase in surface melt, for example at D8 and D15 in the beginning of July 2008 (Fig. 6a,b) and two events in July on Sátujökull in 2013 (Fig. 8a,b). Other events are observed in periods without any discharge increase or rain events. Two velocity peaks at D3 in the middle of June 2013, an event between 21 and 23 July 2013 at D15 and an event

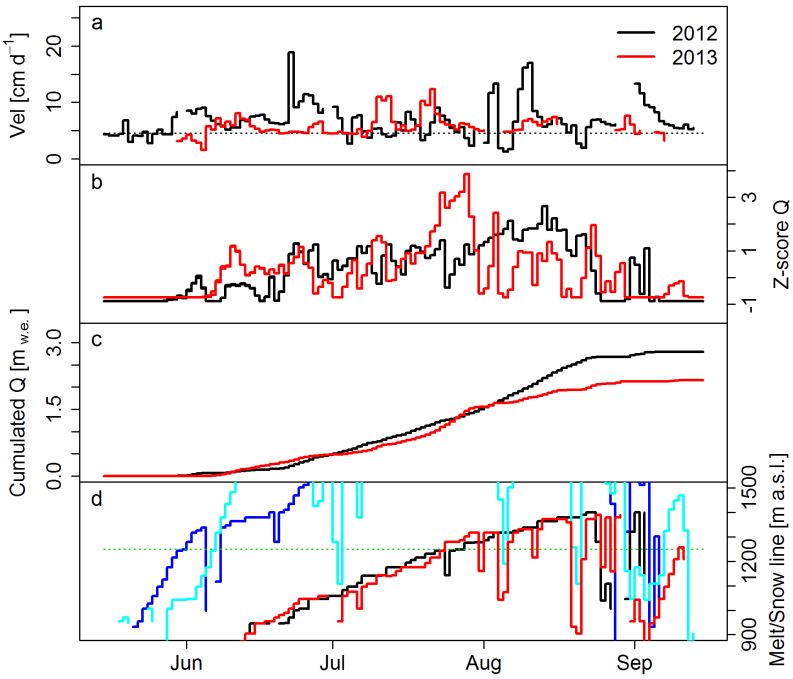

Figure 8. (a) Daily horizontal ice surface velocities at SATJ, high in the ablation area on Sátujökull, during the summers of 2012 (black) and 2013 (red). Observed late winter velocity from 2011 is shown with a dotted line. (b, c) Scaled and cumulative modelled runoff from the area longitudinally stress-gradient coupled to the GPS site (the same colour coding). Two estimates are drawn for each of the runoff series based on maximum and minimum estimates of longitudinal coupling lengths, but the difference is not usually noticeable at this scale. (d) The progression of the highest elevation on the glacier with melt in 2012 (blue) and 2013 (cyan) and the elevation of the snow line in 2012 (black) and 2013 (red). The elevation of the GPS instrument is shown with a dotted line for reference (green).

between 18 and 23 July 2013 at SATJ are examples of such events (Figs 7a,b and 8a,b). These events all take place in the two-week period before the modelled elevation of the snow line passes the elevation of the GPS site.

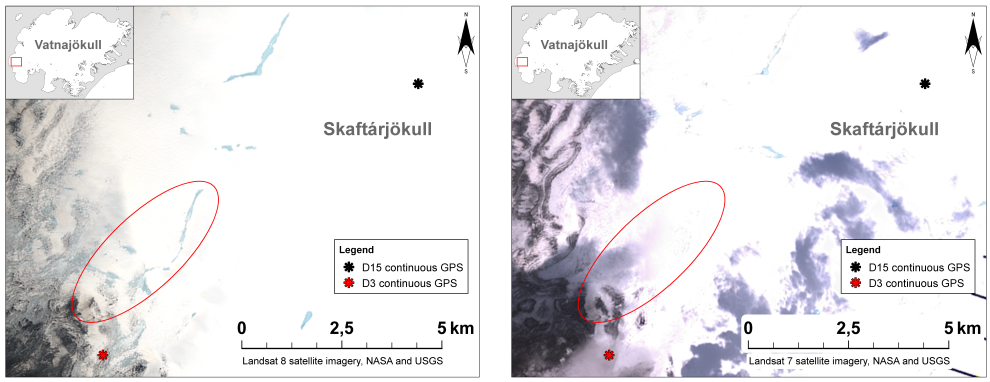

Figure 9. Optical satellite images of the ablation zone on Skaftárjökull showing emptying of supraglacial slush ponds between 6 June 2013 (left) and 14 June 2013 (right). A red ellipse surrounds the area where the main changes are observed. The images are from Landsat 8 and 7, respectively, of NASA and the US Geological Survey (USGS).

Slush ponds are often observed on field trips on Hofsjökull and Vatnajökull. They tend to form in the ablation zone during the melt season in the area above the receding snow line. Their depth is equal to the thickness of the remaining winter snow layer. Such ponds have often been observed to drain over a period of a few days, sometimes by one pond draining to another and so on until the water finds its way to the englacial hydraulic system through crevasses or moulins.

Cloud-free Landsat satellite images are available a few days before, during or a few days after some of these events. Slush ponds with an area on the order of hectares are observed in the vicinity of the GPS sites in all cases. Satellite images from Landsat 8 on 6 June 2013 and Landsat 7 on 14 June 2013, which encompass the observed motion event on 10 and 11 June at D3, show drainage of ponds in the area longitudinally coupled to D3 (Fig. 9). Drainage is also observed in two cases in 2013 between images that encompass a part of motion events. The images from (i) Landsat 8 on 22 July and Landsat 7 on 23 July coincide with the observed motion event between 18 and 23 July at SATJ (Fig. 8a) and (ii) Landsat 7 on 23 July and Landsat 8 on 24 July coincide with the observed motion event between 21 and 23 July at D15 (Fig. 7a). Cloud-free images are unfortunately not available in the two weeks preceding these events. We suggest that the drainage events are the reason for the contemporaneous motion events (see discussion section).

An event of increased velocity at D15 between 9 May and 15 May 2008 takes place about 2 weeks before any runoff has started in the area hypothesized to be longitudinally stress-gradient coupled to the GPS site (Fig. 6a). The start of melting lower on the glacier in the area near D3 is rather slow in 2008, with a small

initial peak between 9 May and 15 May, but then melting shuts down again before continuous melting starts about a week later (Fig. 6b). Melt is therefore ongoing down-glacier from D15 during the event. The highest predicted elevation of melting is ∼250 m lower than D15 during the event, corresponding to a distance ∼10 km down-glacier. Similarly, a 1 day velocity increase is observed at SATJ in 2012 on 19 May (Fig. 8a). Melt is ongoing ∼350 m lower on the glacier, at ∼6 km distance down-glacier, at that time. These events take place before the hydrologically induced spring speed-up but still seem to be connected to the onset of melt far down-glacier.

Observed substantial runoff peaks do not all cause motion events on Skaftárjökull. Such cases can be seen for example for D3, D8 and D15 in late July 2008 and at D3 and D15 in early July 2013 (Figs 6a,b and 7a,b). A runoff of ∼2.4 $m_{w.e.}$, ∼1.7 $m_{w.e.}$ and ∼1.4 $m_{w.e.}$ has been discharged through the subglacial system at D3, D8 and D15 at this time in July 2008, respectively (Fig. 6c). Runoff of ∼1.2 $m_{w.e.}$ and ∼0.6 $m_{w.e.}$ has been discharged through the system at D3 and D15 in early July 2013 (Fig. 7c).

A distinct difference in relative velocity response to a runoff increase is observed at D3 compared to D8 and D15 in early July 2008 (Fig. 6a,b). This melt event is similar in relative magnitude at all locations but causes a motion event only at D8 and D15 but not at D3. A substantial runoff of ∼1.1 $m_{w.e.}$ has taken place at D3 at the time while ∼0.8 $m_{w.e.}$ and ∼0.5 $m_{w.e.}$ have been discharged through the system at D8 and D15, respectively, which are higher on the glacier (Fig. 1). A motion event is observed for all major runoff pulses at the SATJ site on Sátujökull (Fig. 8a,b).

Motion events with velocities slower than winter velocities are observed in a number of cases. Days with velocities of half to two-thirds of the preceding winter velocities are observed shortly before the initial velocity increase of the melt season at Sátujökull in 2012 and 2013 and at D3 in 2008 (Figs 6a and 8a). The slowdown event at D3 in 2008 has a duration of about half a month. The duration of such slowdown events is shorter on Sátujökull, 1 day in 2013 and 2 separate days in 2012 with 3 days of velocities similar to late winter values in between. The velocity for the first 2 days of observations at D15 in early May 2008 (Fig. 6a) is, furthermore, suspected to be lower than late winter values, based on comparison to velocities later in May during periods with no melt on the whole glacier (Fig. 6a,b).

Days with velocities lower than winter velocities are observed in late July at D3 in 2008 (Fig. 6a) and in July and August on Sátujökull in 2012 (Fig. 8a). These midsummer slowdown events are observed to take place in a sequence of successively lower minima in between velocity peaks both at D3 and SATJ.

DISCUSSION

Fast subglacial hydraulic system and diurnal variation in discharge

Incoming shortwave radiation is the dominant component in the energy available for melt on Icelandic glaciers (Björnsson and Pálsson, 2008), with a substantial diurnal variation and a flat minimum during night time (Fig. 4). This variability creates diurnal variation in the melt production on the glacier and in the glacial runoff, as has been widely observed in discharge measurements in glacial rivers (e.g. Raymond and others, 1995; Swift and others, 2005; Cuffey and Paterson, 2010).

The effect of the subglacial hydraulic system on this well-known runoff variability can be used to infer some properties of the subglacial system. The shape and timing of the extrema of the diurnal variation in the proglacial discharge in July and August are well captured by routing the diurnal melt through a single linear reservoir with a recession constant on the order of hours (Fig. 4). This indicates that the diurnal variation in water input to the glacier is carried as a wave through an effective channelized fast hydrological system as has been suggested in earlier studies (Raymond and others, 1995; Swift and others, 2005; Cuffey and Paterson, 2010). This type of hydraulic system is therefore present under parts of Sátujökull and Skaftárjökull when well-developed diurnal variations are observed in their proglacial discharge.

Slow hydraulic system and spring events

A substantial velocity increase is observed at the onset of the melt season in all cases when a GPS instrument is in place before runoff starts from the snowpack on the glacier. Such early-melt-season speed-up events have been reported for many glaciers (Iken and others, 1983; Iken and Bindschadler, 1986; Willis, 1995; Mair and others, 2001, 2002a; Bartholomew and others, 2010, 2011) and are referred to as spring events. They are associated with increased basal slip due to high subglacial water pressure caused by melt water arriving at the glacier bed and flooding an inefficient distributed hydraulic system at the end of the winter (e.g. Mair and others, 2001).

Rearrangement of the subglacial hydraulic system

Our measurements indicate an inefficient, slow hydraulic system under the ablation area of the glacier at the beginning of the melt season and an efficient, fast system later in the season. The hydraulic systems of Sátujökull and Skaftárjökull must therefore change from distributed subglacial cavity systems (Kamb, 1987) with slow, inefficient drainage (e.g. Raymond and others, 1995; Cuffey and Paterson, 2010) to an arborescent conduit system (Röthlisberger, 1972) with efficient, fast drainage (e.g. Raymond and others, 1995; Cuffey

and Paterson, 2010) as the melt season progresses. Such changes have been inferred with several different methods on many glaciers (e.g. Raymond and others, 1995; Nienow and others, 1998; Mair and others, 2001; 2002b; Schuler, 2002; Bartholomaus and others, 2008; Sundal and others, 2011; van Boeckel, 2015) and have, furthermore, been reproduced by modelling (Hewitt and others, 2012; Hewitt, 2013; Werder and others, 2013).

The observed shifting of the discharge maximum to a timing up to 2 hours earlier in the day during the first few weeks of the melt season also indicates rearrangement and increased efficiency of the subglacial hydraulic system (Raymond and others, 1995; Swift and others, 2005). The earlier onset and relatively larger diurnal discharge variations in warm years with thin snow cover (Fig. 3) is consistent with this interpretation. Melt is high in such years, which should lead to faster development of a subglacial conduit system (Cuffey and Paterson, 2010).

The 8–14 day extent of the spring events indicates the duration of this transformation at each location. This duration is within the range of adjustment times of subglacial conduits to increased melt reported by Cuffey and Paterson (2010) as a few days to one or two weeks. A sharp increase in runoff can exceed the capacity of the drainage system later in the melt season after the spring event and the initial formation of conduits (Cuffey and Paterson, 2010). The events at D8 and D15 in the beginning of July 2008 (Fig. 6a,b) and the two events in July on Sátujökull in 2013 (Fig. 8a,b) are examples of such events.

The observed velocity increase at D3 during the early July 2008 motion event is relatively much smaller than at D8 and D15 although the relative magnitude of the corresponding runoff event is similar at all locations. An efficient subglacial conduit system, therefore, seems to have already formed at D3 at this time while the drainage system at D8 and D15 was still inefficient and with slow discharge rates. Later in 2008, in the last week of July, a similar runoff event took place without an increase in ice motion at any of the three sites (Fig. 6a,b). An efficient subglacial conduit system seems to have been formed at all the sites before this event as more melt had been discharged through the glacier at D8 and D15 at this time than in early July (Fig. 6c).

Different runoff amounts are needed to develop a conduit system at each location depending on the local hydrological potential (Cuffey and Paterson, 2010). The variability in runoff, the timing of conduit formation and other local conditions might also play a role. It is therefore not unexpected that a conduit system seems to be in place at D15 in 2013 after only $\sim$0.6 $m_{w.e.}$ of cumulative discharge have been conducted through the subglacial hydraulic system while the system is still inefficient at D8 in early July 2008 after a discharge of $\sim$0.8 $m_{w.e.}$(Figs 6c and 7c).

The observations clearly show an up-glacier progression in the development of the fast discharging conduit system at Skaftárjökull, as expected, when melt and the snow line advance up-glacier through the course of the melt season. Nienow and others (1998), Mair and others (2002b) and Bartholomew and others (2010, 2011) report similar up-glacier progression for Glacier d'Arolla in Switzerland and for a transect on the western margin of the Greenland ice sheet.

The up-glacier progression of an efficient conduit system has been associated with the emergence of the low-albedo impermeable ice surface from underneath the winter snowpack (Nienow and others, 1998). The progression is, therefore, proposed to follow the movement of the snow line up-glacier (Nienow and others, 1998). This is not consistent with our interpretation of an efficient, fast system already being formed at D15 during the runoff event in late July 2008, as the snow line is still at ∼150 m below D15 (or ∼7 km farther down-glacier) at that time (Fig. 6d). Similarly, an efficient subglacial hydraulic system appears to have been formed at D15 before the passing of the snow line because the runoff event in early July 2013 was not associated with a speed-up event (Fig. 7a,b,d). The development of an efficient drainage system farther up-glacier than the snow line at the time has been inferred at Glacier d'Arolla in 1995 (Mair and others, 2002b) and on Bench Glacier in 2003 (Harper and others, 2005). The snowpack on Skaftárjökull at D15 is present well into the melt season (Figs 6d and 7d). There is thus time for the development of efficient percolation of surface snowmelt to the base of the snowpack and for an efficient supraglacial drainage system within a saturated layer at the snow/ice interface to develop like described by Mair and others(2002b) as a precondition for subglacial channel development above the snow line. Water flow observed in a saturated layer with thickness on the order of 0.1 m at the bottom of a snow pit at D8 in June 2009 supports a development of this kind.

The passing of jökulhlaups at Skaftárjökull seems to have little permanent effect on the subglacial hydraulic system as reflected by the development of diurnal variations (Fig. 5). The jökulhlaups are inferred to start with an initial widespread sheet-like flood (Björnsson, 2002; Magnússon and others, 2007; Einarsson and others, 2016, 2017) that is quickly contracted into a few main conduits due to differences in subglacial melt caused by heterogeneities in the sheet thickness and flow velocities (Walder, 1982; Flowers and others, 2004). The remnant of the jökulhlaup flood path will therefore be a few large conduits from the source lake to the terminus. These relict jökulhlaup conduits only cover a small area of the glacier bed and may not be located near the many places where water from the surface is discharged to the bed. The passing of a jökulhlaup is therefore not expected to have a significant lasting effect on the arrangement and connectivity of the subglacial hydraulic system.

Development of the subglacial hydraulic system and subglacial groundwater flow

A sufficiently transmissive groundwater system has been found to suppress the formation of conduits almost entirely in model calculations (Flowers, 2008). Both Sátujökull and Skaftárjökull are underlain by highly permeable bedrock (Sigurðsson and others, 2006), and groundwater flow from western Vatnajökull and northern Hofsjökull is substantial (Sigurðsson, 1990). Model calculations indicate that up to 80% of water reaching the glacier bed at Skaftárjökull might be transported from the glacier as groundwater (Flowers and others, 2003). The observed motion events on both Sátujökull and Skaftárjökull show that the subglacial groundwater system does not manage to fully accommodate and dampen short-term runoff variation, and the groundwater flow is, therefore, apparently not able to accommodate the whole transient summer increase in runoff.

These results are not unexpected considering available indications about the subglacial water pressure field for these glaciers. Hydrological conditions on western Vatnajökull have been observed to be consistent with subglacial water pressure close (within ∼5% for specific cases) to the ice overburden pressure on a regional scale (Björnsson, 1988a). A high water table in the englacial hydraulic system is needed to sustain subglacial water pressure close to the ice overburden. The subglacial bedrock and sediments and a substantial part of the glacier itself must therefore be water-saturated. Groundwater flow in unconfined aquifers underneath the glacier will then be driven by the potential formed by this water table. This is in accordance with earlier modelling results that the subglacial groundwater flow direction is similar to the direction of water flow at the glacier bed (Flowers and others, 2003). The hydrological potential driving the subglacial groundwater flow is, furthermore, capped by the overburden pressure of the glacier as higher subglacial water pressure would cause flotation of the glacier.

In order to drive a typical runoff rate during the height of the melt season of $7.5{\cdot}10^{-2}\,\mathrm{m_{w.e.}\,d^{-1}}$ as Darcian groundwater flow, a change in the hydraulic head corresponding to ∼100 m rise in the englacial water level is needed. This order-of-magnitude estimate assumes that the increased runoff is transferred a distance of ∼5 km from the ablation area to outside the glacier, consistent with Flowers and others' (2003) modelling of water exchange with the subglacial aquifer that indicates recharge beneath most of the glacier ablation area and expulsion near the glacier margin and in the periglacial area. Transmissivity values for this estimation are from Sævarsdóttir (2002a,b) and include both water flow through the bedrock matrix and along fissures. This magnitude of the rise in the englacial water table is not possible without widespread flotation of the glacier since basal water pressure is only a few tens of metres below ice overburden pressure before the summer season.

Changes in the subglacial hydraulic system are thus the only possible way of accommodating and discharging summer runoff.

Our GPS measurements can unfortunately not be used to study whether lifting of the glacier is associated with the observed motion events. Vertical movements are masked by lowering of the instruments that sit on the glacier surface but not on stakes drilled into the ice. Our melt calculations are too crude to be used for a reliable correction of this effect. We cannot, therefore, determine whether lifting plays a role in the development of the subglacial hydraulic system at Sátujökull and Skaftárjökull, as has been observed on other glaciers (Iken and others, 1983; Mair and others, 2002a; Bartholomew and others, 2010; Magnússon and others, 2011). The extreme case of jökulhlaups is an exception as we have observed widespread lifting to be important for the flood path formation at Skaftárjökull in such floods (Einarsson and others, 2016, 2017).

Slowdown and pre-melt-season motion events

A slowdown event, relative to the preceding winter velocities, is observed before the spring event in all cases where the GPS instruments are set up sufficiently early, indicating a lowering in basal slip due to increased basal drag. An earlier set-up of GPS stations would be preferable as our measurements often only capture a few days of late winter velocities or only days with velocities lower than late winter velocities from other years, for example at D15 in 2008 and SATJ in 2013. Slowdown events before the melt season sets in are nevertheless, apparently, a persistent phenomenon in the dynamics of both glaciers. Minchew and others (2016) observed a similar decrease in velocities below winter values in the earlier half of June 2012 in parts of Hofsjökull that had experienced little or no surface melt up to that point in time. Substantial surface melt and spring speed-up had taken place in lower areas at that time.

A plausible explanation for these events might be a pressure increase in hydraulically connected bed areas due to onset of melt down-glacier from the area that is slowing down when large parts of the bed are still hydraulically unconnected. Runoff from the snowpack had started lower down on the glaciers in all cases according to our modelling. The elevation difference between the areas with modelled runoff and the GPS sites is ∼100–300 m (Figs 6a,d and 8a,d), corresponding to a horizontal distance of ∼2–12 km.

The water pressure in unconnected parts of the glacier bed may decrease with increasing pressure in adjacent connected areas of the bed (Mair and others, 2001; Lappegard, 2006; Lefeuvre and others, 2018). The pressure signal could also to some extent propagate up-glacier into largely unconnected areas in narrow widely separated channels maintained trough the winter season by runoff due to normal geothermal melting and energy dissipated by the flow of the ice. Harper and others (2005) report such up-glacier propagation of

high water pressure over a distance on the order of kilometres into areas where melt has not yet started on Bench Glacier during spring.

The pre-melt events with increased velocity are harder to explain but they could also be caused by up-glacier propagation of pressure perturbations where basal drag in connected areas dominates in the overall force balance. A pressure drop in the unconnected areas due to increased basal slip (Iken and Truffer, 1997) could then subsequently counteract this development and cause increased basal drag in the unconnected areas to become dominant. Such a course of events might explain the observed increase in velocity that is followed by a slowdown at SATJ in 2012 (Fig. 8a).

The slowdown events later in the melt season are similar to late-summer slowdown that has been observed on outlet glaciers from the Greenland ice sheet (Bartholomew and others, 2010) and found in model simulations by Hewitt (2013). These events occur during decreasing runoff at the height of the melt season in the wake of increased motion due to an earlier increase in runoff. A well-developed, efficient conduit system can, therefore, be assumed to have formed and to be effectively draining water from large areas of the glacier bed at low water pressure (Fountain and Walder, 1998; Cuffey and Paterson, 2010) causing increased basal drag and lowered basal slip (Mair and others, 2001).

Other transient motion events

Transient motion of glaciers due to the flooding of the hydraulic system as a consequence of the emptying of supraglacial (Das and others, 2008) and marginal lakes (Bartholomaus and others, 2008, 2011) and jökulhlaups (Magnússon and others, 2007; Einarsson and others, 2016) has been reported by several authors. The emptying of supraglacial slush ponds appears to have a noticeable effect at Sátujökull and Skaftárjökull although the water volume released in these events is orders of magnitudes smaller than in the above-mentioned examples. This emptying often takes place as a series of emptying of one pond into the next and so on until the discharge from a number of ponds finds its way into the glacier through crevasses or moulins. The motion response induced by emptying of one pond might also lead to hydrofracturing and crack formation causing the emptying of other ponds as reported for supraglacial lakes in Greenland (Stevens and others, 2015).

The motion event associated with emptying of slush ponds is of limited extent, as these events are only observed when the snow line is in the vicinity of the GPS site concerned and increased ice motion is not observed at other GPS sites farther up- or down-glacier at Skaftárjökull. The better-developed hydraulic system farther down-glacier of the snow line seems, therefore, to be able to accommodate the increased discharge without exceeding its capacity. Motion events of this type are, furthermore, short-lived, with a maximum duration of

a few days. This type of events is therefore not likely to be important for the development of the subglacial hydraulic system, but they do add to the complexity and variability of the system.

CONCLUSIONS

The formation of a fast high-capacity subglacial conduit system during the melt season is inferred, in the presence of substantial subglacial groundwater flow, at both Sátujökull and Skaftárjökull. The rearrangement of the subglacial hydraulic system from a slow distributed system during winter to a fast system is indicated by the facts that (i) the diurnal variation in discharge during the melt season is well described by a simple linear reservoir with a short recession constant and (ii) there is little dynamic response in ice motion to runoff events during the height of the melt season.

Hydrologically induced events of both increased and decreased basal slip are observed. Events of decreased basal slip are suggested to be caused by (i) up-glacier propagation of high subglacial water pressure in hydraulically connected areas of the glacier bed in spring, associated with a lowering of basal pressure in adjacent areas, and (ii) low subglacial water pressure over large areas due to efficient drainage of water in mid-summer. Most events of increased basal slip are triggered by runoff input larger than the highly variable capacity of the subglacial hydraulic system at the time. The effect of a pressure signal in the subglacial hydraulic system may extend beyond the area connected to the pressure disturbance through longitudinal stress-gradient coupling.

The relationship between runoff and glacier dynamics on the two glaciers is complex and dependent on the seasonal development of the subglacial hydraulic system as has been observed for other glaciers, ranging from small alpine glaciers (Mair and others, 2001) to the Greenland ice sheet (Bartholomew and others, 2010; Sundal and others, 2011). The effect of surface runoff on basal motion of Sátujökull and Skaftárjökull appears to depend on (i) hydrologically induced pressure variations in the connected part of the subglacial system (and opposite pressure variations in the unconnected part of the system (Lappegard, 2006; Lefeuvre and others, 2018)), (ii) the spatial development of the connected system (which is affected by previous discharge through the system (Lefeuvre, 2016)) and (iii) the interconnection, arrangement and nature of the connected system (which affects the pressure variations caused by runoff changes (Cuffey and Paterson, 2010)).

ACKNOWLEDGEMENTS

This publication is contribution number 90 of the Nordic Centre of Excellence SVALI, 'Stability and Variations of Arctic Land Ice', funded by the Nordic Top-level Research Initiative (TRI). The Icelandic

Research Fund, the Landsvirkjun (National Power Company of Iceland) Research Fund, the Icelandic Road Administration and the Iceland Glaciological Society provided additional financial and field support for GPS measurements on Skaftárjökull, which made this study possible. We thank Benedikt G. Ófeigsson, Vilhjálmur S. Kjartansson, Þorsteinn Þorsteinsson, Matthew J. Roberts and Eyjólfur Magnússon for assistance with the GPS measurements and their processing. Information on the subglacial topography below the GPS sites at Skaftárjökull and mass balance and energy balance data from Tungnaárjökull were made available by Finnur Pálsson and Louise Steffensen Schmidt at the Institute of Earth Sciences, University of Iceland. We thank Gwenn E. Flowers and Helgi Björnsson for constructive comments that helped us improve the paper. We thank Pierre-Marie Lefeuvre for fruitful discussion on subglacial hydrology and quantification of diurnal variations in glacier discharge, and Ken Moxham for help with the English language.

REFERENCES

Bartholomaus TC, Anderson RS and Anderson SP (2008) Response of glacier basal motion to transient water storage. *Nat. Geosci.*, **1**(1), 33–37 (doi: 10.1038/ngeo.2007.52)

Bartholomaus TC, Anderson RS and Anderson SP (2011) Growth and collapse of the distributed subglacial hydrologic system of Kennicott Glacier, Alaska, USA, and its effects on basal motion. *J. Glaciol.*, **57**(206), 985–1002 (doi: 10.3189/002214311798843269)

Bartholomew I, Nienow P, Mair D, Hubbard A, King MA and Sole A (2010) Seasonal evolution of subglacial drainage and acceleration in a Greenland outlet glacier. *Nat. Geosci.*, **3** 408–411

Bartholomew ID, Nienow P, Sole A, Mair D, Cowton T, King MA and Palmer S (2011) Seasonal variations in Greenland ice sheet motion: Inland extent and behaviour at higher elevations. *Earth Planet Sc. Lett.*, **307**, 271–278

Bartholomew ID, Nienow P, Sole A, Mair D, Cowton T and King MA (2012) Short-term variability in Greenland ice sheet motion forced by time-varying meltwater drainage: Implications for the relationship between subglacial drainage system behavior and ice velocity. *J. Geophys. Res.*, **117**, F03002 (doi:10.1029/2011JF002220)

Bell RE (2008) The role of subglacial water in ice-sheet mass balance. *Nat. Geosci.*, **1**(5), 297–304 (doi:10.1038/ngeo186)

Björnsson H (1988a) *Hydrology of ice caps in volcanic regions.* Societas Scientarium Islandica, University of Iceland, Reykjavík, Iceland

Björnsson H (1988b) *Hofsjökull, ice thickness, Map 1:200 000.* Reykjavík, Science institute, University of Iceland

Björnsson H (1998) Hydrological characteristics of the drainage system beneath a surging glacier. *Nature*, **395**, 771–774 (doi:10.1038/27384)

Björnsson H (2002) Subglacial lakes and jökulhlaups in Iceland. *Glob. Planet. Change*, **35**, 255–271 (doi:10.1016/S0921-8181(02)00130-3)

Björnsson H (2017) *The Glaciers of Iceland. A historical, cultural and scientific overview.* Atlantis press. (doi:10.2991/978-94-6239-207-6)

Björnsson H, Pálsson F, Sigurðsson O and Flowers GE (2003) Surges of glaciers in Iceland. *Ann. Glaciol.*, **36**, 82–90 (doi:10.3189/172756403781816365)

Björnsson H and Pálsson F (2008) Icelandic glaciers. *Jökull*, **58**, 365–386

Braithwaite RJ (1985) Calculation of degree–days for glacier-climate research. *Z. Gletscherkd. Glazialgeol.*, **20**(1984), 1–8

Crochet P (2012) *A semi-automatic multi-objective calibration of the WaSiM hydrological model.* Reykjavík, Icel. Meteorol. Office, Technical Report PC/2012-01

Crochet P and Jóhannesson T (2011) A data set of gridded daily temperature in Iceland, 1949–2010. *Jökull*, **61**, 1–17

Cuffey KM and Paterson WSB (2010) *The physics of glaciers. Fourth Edition.* Oxford, Elsevier

Das SB, Joughin I, Behn MD, Howat IM, King MA, Lizarralde D and Bhatia MP (2008) Fracture propagation to the base of the Greenland ice sheet during supraglacial lake drainage. *Science*, **320**, 778–781 (doi:10.1126/science.1153360)

Doyle SH, Hubbard A, van de Wal RSW, Box JE, van As D, Scharrer K, Meierbachtol TW, Smeets PCJP, Harper JT, Johansson E, Mottram RH, Mikkelsen AB, Wilhelms F, Patton H, Christoffersen P and Hubbard B (2015) Amplified melt and flow of the Greenland ice sheet driven by late-summer cyclonic rainfall. *Nat. Geosci.*, **8**, 647–653 (doi:10.1038/ngeo2482)

Einarsson B (2012) *Available discharge time-series from glacier-covered catchments in Iceland.* Reykjavík, Icel. Meteorol. Office, Technical Report BE/2012-01

Einarsson B and Jónsson S (2010) *The effect of climate change on runoff from two watersheds in Iceland.* Reykjavík, Icel. Meteorol. Office, Report 2010-16

Einarsson B, Magnússon E, Roberts MJ, Pálsson F, Thorsteinsson Th and Jóhannesson T (2016) A spectrum of jökulhlaup dynamics revealed by GPS measurements of glacier surface motion. *Ann. Glaciol.*, **57**, 47–61 (doi:10.1017/aog.2016.8)

Einarsson B, Jóhannesson T, Thorsteinsson Th, Gaidos E and Zwinger T (2017) Subglacial flood path development during a rapidly rising jökulhlaup from the western Skaftá cauldron, Vatnajökull, Iceland. *J. Glaciol.*, **63**(240), 670–682 (doi:10.1017/jog.2017.33)

Einarsson MA (1984) *Climate of Iceland. In:* van Loon H, *ed., Climates of the Oceans.* Amsterdam, Elsevier, 673–697

Flowers GE (2008) Subglacial modulation of the hydrograph from glacierized basins. *Hydrol. Process.*, **22**, 3903–3918 (doi:10.1002/hyp.7095)

Flowers GE, Björnsson H and Pálsson F (2003) New insights into the subglacial and periglacial hydrology of Vatnajökull, Iceland, from a distributed physical model. *J. Glaciol.*, **49**(165), 257–270 (doi:10.3189/172756503781830827)

Flowers GE, Björnsson H, Pálsson F and Clarke GKC (2004) A coupled sheet–conduit mechanism for jökulhlaup propagation. *Geophys. Res. Lett.*, **31**(5), L05401 (doi:10.1029/2003GL019088)

Flowers GE, Marshall SJ, Björnsson H and Clarke GKC (2005) Sensitivity of Vatnajökull ice cap hydrology and dynamics to climate warming over the next 2 centuries. *J. Geophys. Res.*, **110**, F02011 (doi:10.1029/2004JF000200)

Fountain AG and Walder JS (1998) Water flow through temperate glaciers. *Rev. Geophys.*, **36**(3), 299–328

Fudge TJ, Harper JT, Humphrey NF and Pfeffer WT (2009) Rapid glacier sliding, reverse ice motion and subglacial water pressure during an autumn rainstorm. *Ann. Glaciol.*, **50**(52), 101–108

Guðmundsson S, Björnsson H, Pálsson F and Harladsson HH (2009) Comparison of energy balance and degree–day models of summer ablation on the Langjökull ice cap, SW-Iceland. *Jökull*, **59**, 1–18

Harper JT, Humphrey NF, Pfeffer WT, Fudge T and O'Neel S (2005) Evolution of subglacial water pressure along a glacier's length. *Ann. Glaciol.*, **40**, 31–36

Herring TA, King RW and McClusky SC (2010) *Introduction to GAMIT/GLOBK. Release 10.4.* Massachusetts Institute of Technology, Cambridge, MA. www-gpsg.mit.edu/∼simon/gtgk

Hewitt IJ (2013) Seasonal changes in ice sheet motion due to melt water lubrication. *Earth Planet. Sci. Lett.*, **371–372**, 16–25 (doi:10.1016/j.epsl.2013.04.022)

Hewitt IJ, Schoof C and Werder MA (2012) Flotation and open water flow in a model for subglacial drainage. Part II: Channel flow. *J. Fluid Mech.*, **702**, 157–187 (doi:10.1017/jfm.2012.166)

Hock R (2003) Temperature index melt modelling in mountain areas. *J. Hydro.*, **282**, 104–115

Hooke RLeB, Calla P, Holmlund P, Nilsson M and Stroeven A (1989) A 3 year record of seasonal variations in surface velocity, Storglaciären, Sweden. *J. Glaciol.*, **35**(120), 235–247

Icel. Meteorol. Office (2017a) *Rennslisskýrsla vatnsárið 2015/2016, V228, Austari-Jökulsá, Austurbugur [Discharge report for the water year 2015/2016, V299, Austari-Jökulsá; Austurbugur].* Reykjavík, Icel. Meteorol. Office [In Icelandic]

Icel. Meteorol. Office (2017b) *Rennslisskýrsla vatnsárið 2015/2016, V299, Skaftá; Sveinstindur [Discharge report for the water year 2015/2016, V299, Skaftá; Sveinstindur].* Reykjavík, Icel. Meteorol. Office [In Icelandic]

Iken A, Röthlisberger H, Flotron A and Haeberli W (1983) The uplift of Unteraargletscher at the beginning of the melt season – a consequence of water storage at the bed? *J. Glaciol.*, **29**(101), 28–47

Iken A and Bindschadler RA (1986) Combined measurements of subglacial water pressure and surface velocity of Findelengletscher, Switzerland: Conclusions about drainage system and sliding mechanism. *J. Glaciol.*, **32**(110), 101–119

Iken A and Truffer M (1997) The relationship between subglacial water pressure and velocity of Findelengletscher, Switzerland, during its advance and retreat. *J. Glaciol.*, **43**(144), 328–338

Jansson P (1995) Water pressure and basal sliding on Storglaciären, northern Sweden. *J. Glaciol.*, **41**(138), 232–240

Jóhannesson T (1997) The response of two Icelandic glaciers to climate warming computed with a degree–day glacier mass-balance model coupled to a dynamic glacier model. *J. Glaciol.*, **43**(143), 321–327

Jóhannesson T, Sigurdsson O, Laumann T and Kennett M (1995) Degree–day glacier mass-balance modelling with applications to glaciers in Iceland, Norway and Greenland. *J. Glaciol.*, **41**(138), 345–358

Jóhannesson T, Aðalgeirsdóttir G, Björnsson H, Crochet P, Elíasson, EB, Guðmundsson S, Jónsdóttir JF, Ólafsson H, Pálsson F, Rögnvaldsson Ó, Sigurðsson O, Snorrason Á, Blöndal Sveinsson ÓG and Thorsteinsson Th (2007). *Effect of climate change on hydrology and hydro-resources in Iceland.* Reykjavík, National Energy Authority – Hydrological Service. Report OS-2007/011, ISBN: 978-9979-68-224-0

Jóhannesson T, Björnsson H, Magnússon E, Guðmundsson S, Pálsson F, Sigurðsson O, Thorsteinsson Th, and Berthier E (2013) Ice-volume changes, bias estimation of mass-balance measurements and changes in

subglacial lakes derived by lidar mapping of the surface of Icelandic glaciers. *Ann. Glaciol.*, **54**(63), 63–74 (doi: 10.3189/2012AoG63A422)

Jónsdóttir JF (2008) A runoff map based on numerically simulated precipitation and a projection of future runoff in Iceland. *Hydrolog. Sci. J.*, **53**(1), 100–111

Jónsdóttir JF, Kristjánsdóttir GB and Zóphóníasson S (2001) *Skaftá við Sveinstind, vhm 166 Rennslislykill nr. 5 [Skaftá by Sveinstindur, vhm 166 Discharge water elevation relationship number 5].* National Energy Authority, Reykjavík, Report OS-2001/001

Kamb B (1987) Glacier surge mechanism based on linked cavity configuration of the basal water conduit system. *J. Geophys. Res.*, **B92**, 9083–9100

Kamb B and Echelmeyer K (1986) Stress coupling in glacier flow: I. Longitudinal averaging of the influence of ice thickness and surface slope. *J. Glaciol.*, **31**(111), 267–284

Kreyszig E (1999) *Advanced engineering mathematics, 8th edn.* Wiley, New York

Kristinsson B (2005) *Rennslismælingar í vestari kvísl Skaftár við vhm 470 og samanburður við rennsli Skaftár hjá Sveinstindi, vhm 166, árin 1997–2004. [Discharge measurements in the western branch of Skaftá by vhm 470 and comparison with discharge in Skaftá at Sveinstindur, vhm 166, for the years 1997–2004].* National Energy Authority, Report BK-2005-01 [In Icelandic]

Lappegard G (2006) *Basal hydraulics of hard-bedded glacier: Observations and theory related to Engabreen Norway.* Dr.Scient. Thesis. Department of Geosciences, Faculty of Mathematics and Natural Sciences, University of Oslo

Lefeuvre PM (2016) *Subglacial processes and subglacial hydrology.* Ph.D. dissertation. Department of Geosciences, Faculty of Mathematics and Natural Sciences, University of Oslo

Lefeuvre PM, Zwinger T, Jackson M, Gagliardini O, Lappegard G and Hagen JO (2018) Stress redistribution explains anti-correlated subglacial pressure variations. *Front. Earth Sci.*, **5:110** (doi:10.3389/-feart.2017.00110)

Lindbäck K, Pettersson R, Doyle SH, Helanow C, Jansson P, Kristensen SS, Stenseng L, Forsberg R and Hubbard AL (2014) High-resolution ice thickness and bed topography of a land-terminating section of the Greenland ice sheet. *Earth Syst. Sci. Data*, **6**, 331–338 (doi:10.5194/essd-6-331-2014)

Magnússon E (2003) *Airborne SAR data from S-Iceland: analyses, DEM improvements and glaciological application.* MS-thesis, University of Iceland

Magnússon E, Rott H, Björnsson H and Pálsson F (2007) The impact of jökulhlaups on basal sliding observed by SAR interferometry on Vatnajökull, Iceland. *J. Glaciol.*, **53**(181), 232–240

Magnússon E, Björnsson H, Rott H and Pálsson F (2010) Reduced glacier sliding caused by persistent drainage from a subglacial lake. *The Cryosphere*, **4**, 13–20

Magnússon E, Björnsson H, Rott H, Roberts MJ, Pálsson F, Guðmundsson S, Bennett RA, Geirsson H and Sturkell E (2011) Localized uplift of Vatnajökull, Iceland: subglacial water accumulation deduced from InSAR and GPS observations. *J. Glaciol.*, **57**(203), 475–484 (doi:10.3189/002214311796905703)

Mair D, Nienow P, Willis I and Sharp M (2001) Spatial patterns of glacier motion during a high-velocity event: Haut Glacier d'Arolla, Switzerland. *J. Glaciol.*, **47**(156), 9–20

Mair DWF, Sharp MJ and Willis IC (2002a) Evidence for basal cavity opening from analysis of surface uplift during a high-velocity event: Haut Glacier d'Arolla, Switzerland. *J. Glaciol.,* **48**(161), 208–216

Mair D, Nienow P, Sharp M, Wohlleben T and Willis I (2002b) Influence of subglacial drainage system evolution on glacier surface motion: Haut Glacier d'Arolla, Switzerland. *J. Geophys. Res.*, **107**(B8), (doi:10.1029/2001JB000514)

Minchew B, Simons M, Hensley S, Björnsson H and Pálsson F (2015) Early melt season velocity fields of Langjökull and Hofsjökull, central Iceland. *J. Glaciol.,* **61**(226), 253–266 (doi:10.3189/2015JoG14J023)

Minchew B, Simons M, Björnsson H, Pálsson F, Morlighem M, Seroussi H, Larour E and Hensley S (2016) Plastic bed beneath Hofsjokull ice cap, central Iceland, and the sensitivity of ice flow to surface meltwater flux. *J. Glaciol.*, **62**(231), 147–158 (doi:10.1017/jog.2016.26)

Nawri N, Pálmason B, Petersen GN, Björnsson H and Þorsteinsson S (2017) *The ICRA atmospheric reanalysis project for Iceland.* Reykjavík, Icel. Meteorol. Office, Report 2017-005

Nienow PW, Sharp MJ and Willis IC (1998) Seasonal changes in the morphology of the subglacial drainage system, Haut Glacier d'Arolla, Switzerland. *Earth Surf. Proc. Land.* **23**, 825–843

Nienow PW, Hubbard AL, Hubbard BP, Chandler DM, Mair DWF, Sharp MJ and Willis IC (2005) Hydrological controls on diurnal ice flow variability in valley glaciers. *J. Geophys. Res.*, **110**, F04002 (doi:10.1029/2003JF000112)

Radić V and Hock R (2014) Glaciers in the Earth's hydrological cycle: Assessments of glacier mass and runoff changes on global and regional scales. *Surv. Geophys.*, **35**(3), 813–837 (doi:10.1007/s10712-013-9262-y)

Raymond CF, Benedict RJ, Harrison WD, Echelmeyer KA and Strum M (1995) Hydrological discharges and motion of Fels and Black Rapids Glaciers, Alaska, U.S.A.: implications for the structure of their drainage systems. *J. Glaciol.*, **41**(138), 290–304

Rignot E and Kanagaratnam P (2006) Changes in the velocity structure of the Greenland ice sheet. *Science*, **311**(5763), 986–990 (doi:10.1126/science.1121381)

Röthlisberger H (1972) Water pressure in intra- and subglacial channels. *J. Glaciol.*, **11**(62), 177–203

Schoof C (2010) Ice-sheet acceleration driven by melt supply variability. *Nature*, **468** (doi:10.1038/-nature09618)

Schuler T (2002) *Investigation of water drainage through an alpine glacier by tracer experiments and numerical modeling.* Ph.D disseration. Swiss Federal Institute of Technology Zürich

Schulla J (2017) *Model Description WaSiM (Water balance Simulation Model), completely revised version of 2012 with 2013 to 2017 extensions.* Retrieved from wasim.ch/downloads/doku/wasim/wasim_2017_en.pdf

Sigurðsson F (1990) Groundwater from glacial areas in Iceland. *Jökull*, **40**, 119–146

Sigurðsson F, Jónsdóttir JF, Halldórsdóttir SG and Jóhannsson Þ (2006) *Vatnafarsleg flokkun vatnsfalla á Íslandi [Hydrological classification of rivers in Iceland].* Reykjavík, National Energy Authority - Hydrological Service. Technical Report FS/JFJ/SGH/THJ-2006/001 [In Icelandic]

Sigurðsson O, Williams RS Jr and Víkingsson S (2017) *Map of the glaciers of Iceland, Map 1:500 000.* Reykjavík, Icel. Meteorol. Office

Stevens LA, Behn MD, McGuire JJ, Das SB, Joughin I, Herring T, Shean DE and King MA (2008) Greenland supraglacial lake drainages triggered by hydrologically induced basal slip. *Nature*, **522**, 73–76

Sundal AV, Shepherd A, Nienow P, Hanna E, Palmer S and Huybrechts P (2011) Melt-induced speed-up of Greenland ice sheet offset by efficient subglacial drainage. *Nature*, **469**, 521–524 (doi:10.1038/-nature09740)

Swift DA, Nienow PW, Hoey TB and Mair DWF (2005) Seasonal evolution of runoff from Haut Glacier d'Arolla, Switzerland and implications for glacial geomorphic processes. *J. Hydrol.*, **309**, 133–148 (doi:10.1016/j.jhydrol.2004.11.016)

Sævarsdóttir RH (2002a) *Berglektarkort af Skaftársvæðinu [Map of bedrock hydraulic conductivity in the Skaftá area].* Reykjavík, National Energy Authority, Report OS-2002/035 [In Icelandic]

Sævarsdóttir RH (2002b) *Sprungulektarkort af Skaftársvæðinu [Map of hydraulic conductivity along fissures in the Skaftá area].* Reykjavík, National Energy Authority, Report OS-2002/039 [In Icelandic]

Thorsteinsson Th, Jóhannesson T, Sigurðsson O and Einarsson B (2017) *Afkomumælingar á Hofsjökli 1988–2013 [Mass balance measurements on Hofsjökull 1988–2013].* Reykjavík, Icel. Meteorol. Office, Report 2017-015 [In Icelandic]

Van Boeckel T (2015) *Relating subglacial water flow to surface velocity variations of Breiðamerkurjökull, Iceland.* MS-thesis, University of Iceland

Wake LM and Marshall SJ (2015) Assessment of current methods of positive degree–day calculation using in situ observations from glaciated regions. *J. Glaciol.*, **61**(226), 329–344

Walder JS (1982) Stability of sheet flow of water beneath temperate glaciers and implications for glacier surging. *J. Glaciol.*, **28**(99), 273–293

Werder MA, Hewitt IJ, Schoof C and Flowers GE (2013) Modeling chanelized and distributed subglacial drainage in two dimensions. *J. Geophys. Res.*, **118**, 1–19 (doi:10.1002/jgrf.20146)

Willis IC (1995) Intra-annual variations in glacier motion: a review. *Prog. Phys. Geog.*, **19**(1), 61–106

Zwally HJ, Abdalati W, Herring T, Larson K, Saba J and Steffen K (2002) Surface melt-induced acceleration of Greenland ice-sheet flow. *Science*, **297**, 218–222

Þorgeirsdóttir EB, Einarsson K, Thoroddsen S, Georgsdóttir L, Ketilsson J and Guðmundsdóttir M (2015) *Virkjunarkostir til umfjöllunar í 3. áfanga rammaáætlunar [Power production options for discussion in the 3rd stage of the master plan for nature protection and energy utilization].* Reykjavík, National Energy Authority, Report OS-2015/14 [In Icelandic]